Journal of Medicinal Chemistry

pubs.acs.org/jmc

Article

Exploration of Alternative Scaffolds for $P2Y_{14}$ Receptor Antagonists Containing a Biaryl Core

Young-Hwan Jung,[⊥] Jinha Yu,[⊥] Zhiwei Wen, Veronica Salmaso, Tadeusz P. Karcz, Ngan B. Phung, Zhoumou Chen, Sierra Duca, John M. Bennett, Steven Dudas, Daniela Salvemini, Zhan-Guo Gao, Donald N. Cook, and Kenneth A. Jacobson*

Cite This: https://dx.doi.org/10.1021/acs.jmedchem.0c00745

Read Online

ACCESS | Metrics & More | Article Recommendations | Supporting Information

ABSTRACT: Various heteroaryl and bicyclo-aliphatic analogues of zwitterionic biaryl $P2Y_{14}$ receptor ($P2Y_{14}R$) antagonists were synthesized, and affinity was measured in $P2Y_{14}R$-expressing Chinese hamster ovary cells by flow cytometry. Given this series' low water solubility, various polyethylene glycol derivatives of the distally binding piperidin-4-yl moiety of moderate affinity were synthesized. Rotation of previously identified 1,2,3-triazole attached to the central *m*-benzoic acid core (**25**) provided moderate affinity but not indole and benzimidazole substitution of the aryl-triazole. The corresponding $P2Y_{14}R$ region is predicted by homology modeling as a deep, sterically limited hydrophobic pocket, with the outward pointing piperidine moiety being the most flexible. Bicyclic-substituted piperidine ring derivatives of naphthalene antagonist **1**, e.g., quinuclidine **17** (MRS4608, $IC_{50} \approx 20$ nM at $hP2Y_{14}R/mP2Y_{14}R$), or of triazole **2**, preserved affinity. Potent antagonists **1**, **7a**, **17**, and **23** (10 mg/kg) protected in an ovalbumin/*Aspergillus* mouse asthma model, and PEG conjugate **12** reduced chronic pain. Thus, we expanded $P2Y_{14}R$ antagonist structure−activity relationship, introducing diverse physical−chemical properties.

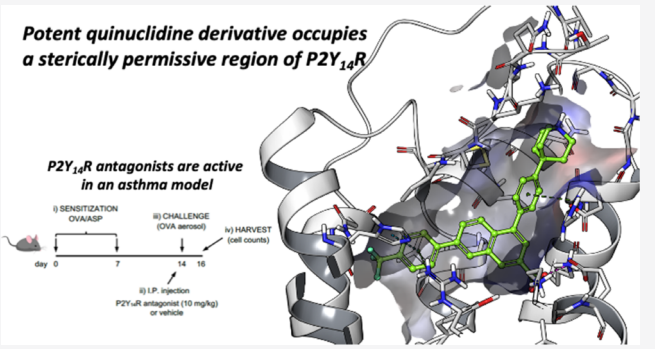

INTRODUCTION

The $P2Y_{14}$ receptor ($P2Y_{14}R$, previously termed GPR105) is activated by uridine-5′-diphosphoglucose (UDPG) and is expressed in human immune cells, including mast cells and neutrophils.[1] As with other P2 receptors that sense extracellular nucleotides as danger signals,[2] UDPG released by stressed cells serves as a damage-associated molecular pattern (DAMP) to activate the innate immune system via the $P2Y_{14}R$. Thus, modulation by ligands and regulation of the $P2Y_{14}R$ are considered a target for the treatment of inflammation, diabetes, cardiac progenitor cell therapy, pain, and pulmonary diseases, such as cystic fibrosis and asthma.[1−12] In renal intercalated cells, $P2Y_{14}R$ activation by endogenous UDPG leads to neutrophil recruitment and elevated inflammation, which is reduced by a $P2Y_{14}R$ antagonist.[4,5] Furthermore, in the eye, the $P2Y_{14}R$ gene is expressed at the highest levels in the trabecular meshwork, suggesting that this receptor might have a role in the regulation of outflow resistance in the context of glaucoma treatment.[13]

The original non-nucleotide lead, **1** (4-[4-(4-piperidinyl)-phenyl]-7-[4-(trifluoromethyl)phenyl]-2-naphthalenecarboxylic acid, PPTN, Chart 1), in our structure−activity relationship (SAR) studies of $P2Y_{14}R$ antagonists appeared in a patent and later publications by Black and co-workers and Belley et al. on $P2Y_{14}R$ antagonists.[14−16] Examined across the entire P2YR family of eight G protein-coupled receptors (GPCRs), **1** was characterized as a highly potent (K_i < 1 nM) and selective $P2Y_{14}R$ antagonist in functional assays and in reduction of UDPG-induced chemotaxis of human neutrophils.[17,18] However, **1** showed poor aqueous solubility and bioavailability, suggesting that a prodrug approach is needed.[16]

Our approach to exploring $P2Y_{14}R$ antagonist SAR is based on insights gained from modeling of the receptor binding. Although lacking an X-ray structure, the $P2Y_{14}R$ can be modeled on the closely related human (h) $P2Y_{12}R$ structure (45% sequence identity), within the Gi-coupled P2YR subfamily.[19,20] We initially probed the piperidine moiety (yellow region of **1**, Chart 1) in this series of naphthalenes and found it to have flexibility of substitution of the secondary amine, which we proposed is directed toward the extracellular space when receptor-bound. This secondary amine was

Received: May 3, 2020

Chart 1. Structures of Two Keys, Previously Reported $P2Y_{14}R$ Antagonists Comparing Analogous Regions That Were Structurally Modified in This Study

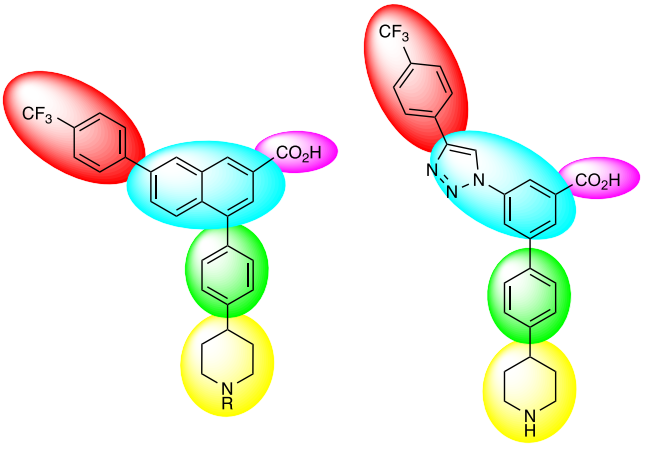

suitable for chain extension, including creating a site for fluorophore attachment through a click reaction of an azide-functionalized fluorophore with an extended alkyne.[19] A resulting fluorescent antagonist of high affinity (MRS4174 **36**, K_i = 0.08 nM in a $hP2Y_{14}R$ functional assay, structure in the Supporting Information) containing an Alexa Fluor 488 (AF488) fluorophore is now our standard tool for drug screening at this receptor using flow cytometry of whole cells expressing the receptor.

Although a naphthalene moiety is found in many important bioactive molecules,[21] we previously focused on replacing this moiety of **1** with a bioisostere to improve the physicochemical properties of the series.[22] Thus, we introduced the biaryl (phenyl-triazole) ring system (**2**, blue region) as a bioisosteric substitute for naphthalene. In a subsequent $P2Y_{14}R$ SAR study,[23] we preserved the red (with hydrophobic substituents favored) and blue regions and varied the green and yellow regions with other aryl groups containing hydrophilic substituents, including furan and thiophene substitution of the phenyl ring. The selection of aryl and extended groups was guided by molecular modeling, using both docking in a $P2Y_{12}R$-based homology model and molecular dynamics (MD) simulation.[22,23] From that study, a 2,5-disubstituted thienyl group emerged as a favored bioisosteric replacement for this *p*-substituted phenyl ring (green region). However, the substitution with nitrogen heteroatoms within either of the *p*-substituted phenyl moieties (green and red regions) greatly reduced binding affinity. Moreover, the purple region of **1** and **2** was found empirically to be best kept as a carboxylate, consistent with a predicted interaction of this anionic group with three amino acid residues in the receptor. An attempt to substitute this carboxylate with the bioisostere tetrazole[24] resulted in a 7- to 30-fold affinity reduction of potent $P2Y_{14}R$ antagonists.[23] Thus, the reported biaryl scaffolds in $P2Y_{14}R$ antagonists in **1** and **2** appeared to be of limited ability to be further modified to enhance $P2Y_{14}R$ affinity.

In this study, we have re-examined each of the regions of **1** and **2**, with the intention of identifying alternative scaffolds for $P2Y_{14}R$ antagonists. Both empirical SAR probing of alternative scaffolds and the computational modeling of the new antagonists with both the human (h) and mouse (m) $P2Y_{14}R$ are included here. One important objective is to identify new $P2Y_{14}R$ antagonists that could be useful for in vivo studies. We have quantified modest improvements in aqueous solubility, and we demonstrate the efficacy of selected analogues in mouse models of asthma and chronic neuropathic pain.

RESULTS

Selection of Target Structures. We have re-examined substitution in all regions of the previously reported key naphthalene **1** and triazole **2** derivatives as $P2Y_{14}R$ antagonist scaffolds. The new target structures selected are shown in Tables 1A and 1B. Initially, we probed minor modifications (**3** and **4**), and terminal *N*-alkyl and acyl extensions (**5**−**14**) of the piperidine moiety of **1**, including amide-linked polyethylene glycol (PEG) chains (**11**−**14**), were introduced to enhance water solubility (Table 1A). In general, covalently bound PEG is known to reduce aggregation in aqueous solutions of hydrophobic or highly H-bonding drug substances and biologics with a low liability of toxicity.[25] Simple alkyl or acyl extensions of the piperidine nitrogen in the form of tertiary amines or amides were reported by Kiselev et al.[19] with significant retention of $P2Y_{14}R$ affinity, and their SAR is expanded here. Synthetic procedures for simple acyl derivatives **8** and **9** were recently reported.[12] Several of the alkyl-extended analogues in Table 1A were tested previously using a functional assay[19] and are re-assayed here using our standard whole cell fluorescence binding assay.

Bicyclic analogues of the piperidine moiety of either **1** or **2** were included (**17**−**21**), with the aim to conformationally constrain the compounds and empirically test if the constrained conformation may be the receptor-preferred one. By analogy, we previously applied the approach of conformationally constraining a ring moiety, i.e., ribose, to increase the potency and selectivity of purinergic nucleoside and nucleotide ligands.[26] The absence of an experimental $P2Y_{14}R$ structure is limiting the predictive power of modeling, so binding affinity of conformationally constrained ligands could indirectly provide structural information on the preferred binding mode of the compounds. Adding carbon bridges to the piperidine ring of **2** was also intended to reduce hydrophobicity, paradoxically, and increase solubility[27] while retaining $P2Y_{14}R$ affinity. The compact 3D-shaped conformation of a bridged piperidine might improve the solubility by increasing the fraction of the solvent-exposed polar surface area. Also, this region in the receptor binding site is predicted to be less sterically crowded than deeper in the site, so three-dimensionality, e.g., in the form of a bicyclic quinuclidine, might be tolerated. The alkene derivative **3** was desired both as a precursor for introduction of a fused cyclopropane ring and for radiolabeling by catalytic reduction. We also re-examined substitution of the carboxylic acids of **1** and **2**, which appeared to be already optimized based on the earlier studies. Thus, two uncharged substitutions of this carboxylate of **2** were included in this study (**15** and **16**).

We probed the effect on $P2Y_{14}R$ affinity of other scaffold modifications and compared them to known reference compounds **2**, **22**, and **23** (Table 1B). Modifications included a rotation of the 1,2,3-triazole ring of the blue region of **2** by a single position to form **24**−**26** and its replacement with an amide group (**27**−**29**). Synthetic procedures for rotated triazole **25** and its $P2Y_{14}R$ affinity were recently reported.[12] Rotation of the triazole was predicted by modeling to maintain a geometry of the polycyclic scaffold of **2**. Among the amide derivatives synthesized, a three-dimensional cubane replace-

https://dx.doi.org/10.1021/acs.jmedchem.0c00745
J. Med. Chem. XXXX, XXX, XXX−XXX

Table 1A. hP2Y$_{14}$R Inhibitory Potency of Piperidine Variations of Naphthalene and Phenyl-Triazole Derivatives[e]

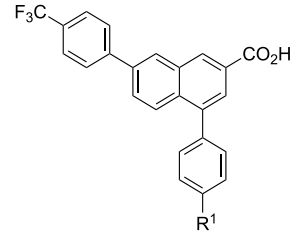

1, 3, 5 – 14, 17, 21

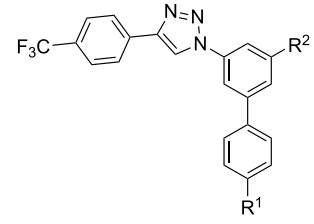

2, 4, 15, 16, 18 – 20

Compound	R^1 = , other changes	cLogP[d]	IC$_{50}$ (μM)[a]
1[b]		6.18	0.0060±0.0001
2[b]		4.64	0.0317±0.0080
3		6.09	0.018±0.002
4		3.95	0.233±0.026
5		7.00	0.195±0.120
6a		6.55	0.139±0.019
6b		7.96	0.133±0.111
7a		7.54	0.0763±0.0244
7b		8.80	0.131±0.011
8[b]		6.47	0.0276±0.0043
9[b]		6.74	0.0418±0.0018
10		7.41	2.44±1.54

Compound	R^1 = , other changes	cLogP[d]	IC$_{50}$ (μM)[a]
11		5.52	1.41±0.56
12		2.46	0.963±0.417
13		5.27	0.979±0.331
14		5.84	2.83±1.15
15		4.39	c
16		5.34	42.1±8.4
17		6.32	0.0200±0.0044
18		4.96	0.105±0.010
19		4.58	0.359±0.069
20		4.57	0.639±0.136
21		2.72	0.0383±0.0022

[a]IC$_{50}$ values were determined by flow cytometry of hP2Y$_{14}$R-CHO cells using fluorescent antagonist tracer **36** and expressed as mean ± SEM (n = 3–5). [b]IC$_{50}$ values were from Junker et al.,[22] Yu et al.,[23] and Mufti et al.[12] [c]No inhibition by the compound discerned at the highest concentration; therefore, IC$_{50}$ > 100 μM. [d]cLogP calculated using ALOGPS 2.1 program (www.vcclab.org/lab/alogps/).[24] [e]R^2 = CO$_2$H, unless noted.

https://dx.doi.org/10.1021/acs.jmedchem.0c00745
J. Med. Chem. XXXX, XXX, XXX−XXX

Table 1B. hP2Y$_{14}$R Inhibitory Potency of Alternative Scaffolds Containing a Biaryl Core

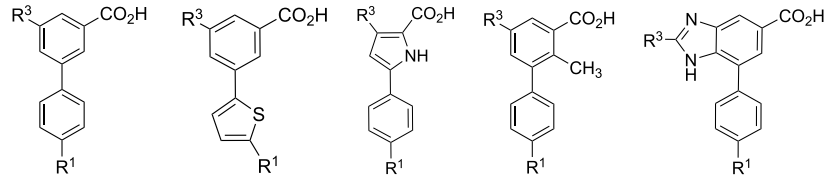

22, 24, 25, 27 – 32 **23, 26** **33** **34** **35**

Compound	R^3 =	R^1 =	cLogP[d]	IC_{50} (μM)[a]
22[b]	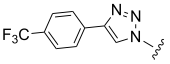	$CONH_2$	3.63	0.269±0.121
23[b]	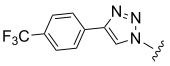	$CONH(CH_2)_3NH_2$	0.84	0.169±0.042
24	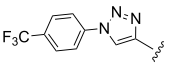	$CONH_2$	3.65	1.68±0.38
25[b]	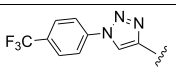	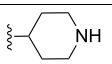	4.64	0.644±0.175
26	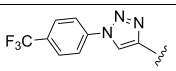	$CONH(CH_2)_3NH_2$	0.85	2.60±0.56
27	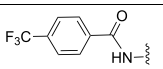	$CONH_2$	3.50	3.05±0.21
28	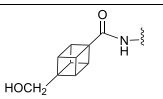	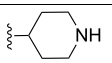	1.14	c
29	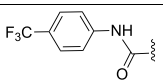	$CONH_2$	3.52	6.04±0.81
30	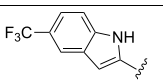	$CONH_2$	4.31	2.44±0.43
31	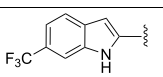	$CONH_2$	4.30	2.03±0.34
32	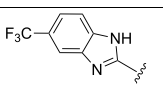	$CONH_2$	3.77	24.4±3.3
33	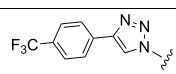	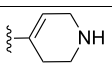	3.92	c
34	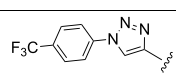	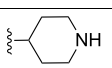	4.66	11.1±1.6
35	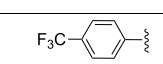	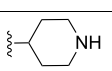	4.82	c

[a]IC_{50} values were determined by flow cytometry of hP2Y$_{14}$R-CHO cells using fluorescent antagonist tracer **36** and expressed as mean ± SEM (n = 3−5). [b]IC_{50} values were from Junker et al.,[22] Yu et al.,[23] and Mufti et al.[12] [c]No inhibition by the compound discerned at the highest concentration; therefore, IC_{50} > 100 μM. [d]cLogP calculated using ALOGPS 2.1 program (www.vcclab.org/lab/alogps/).[24]

ment of the 4-trifluoromethyl-phenyl ring was introduced in **28**, based on a published report that cubane can serve as a benzene ring bioisostere.[28,29] We also fused two aryl rings of **2** to form various heterocycles (**30**−**32**), e.g., to form benzimidazoles and an indole from the fusion of the 4-trifluoromethyl-phenyl ring (red, Chart 1) with the 1,2,3-triazole. The SAR of the central phenyl ring of **2** was not previously explored; here, we introduce various heterocyclic substitutions, i.e., a pyrrole (**33**), and methylation of the phenyl ring (**34**). Benzimidazole derivative **35** was an additional variation of ring fusion, by combining ring equivalents of the central 1,3,5-trisubstituted phenyl ring and the 1,2,3-triazole.

https://dx.doi.org/10.1021/acs.jmedchem.0c00745
J. Med. Chem. XXXX, XXX, XXX−XXX

Scheme 1. (A–D) Synthesis of Piperidine-Modified Analogues of 1 and 2[a]

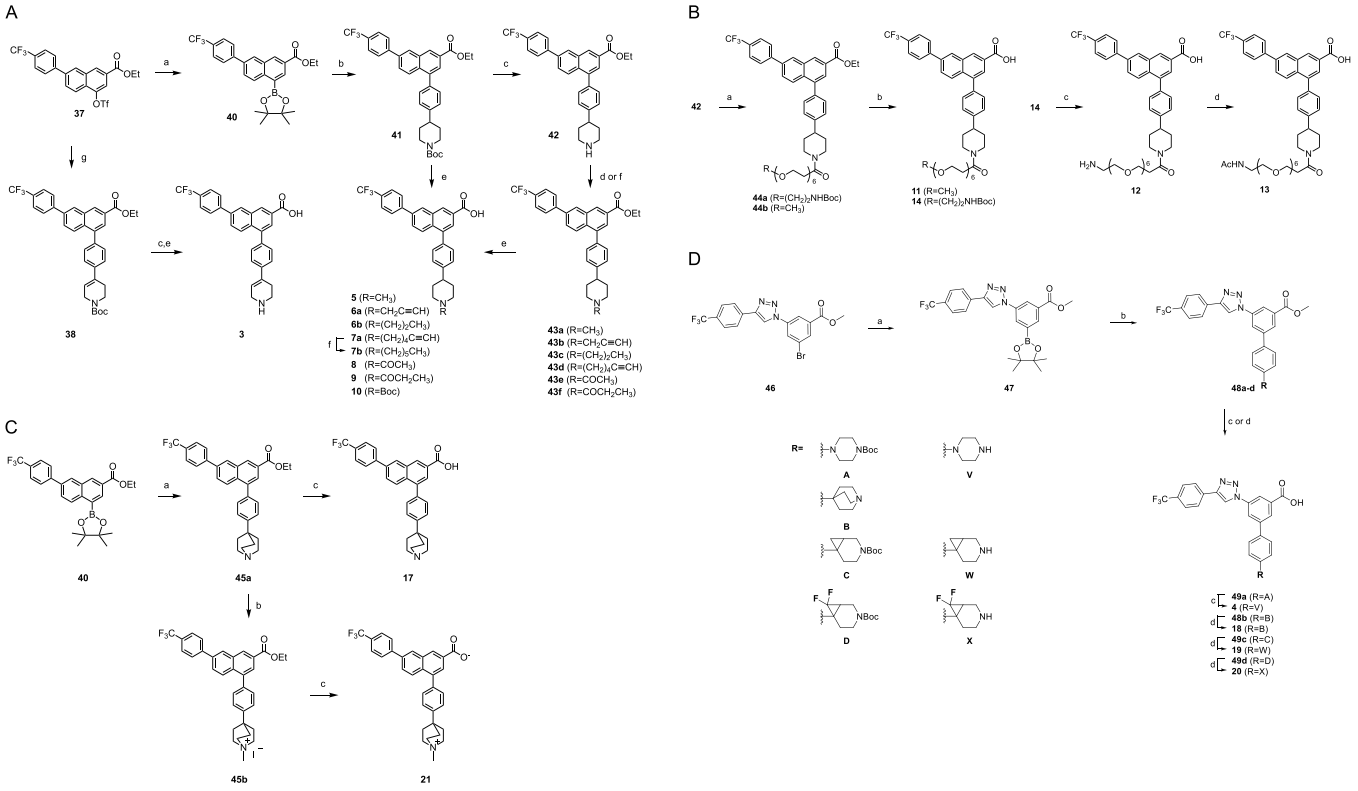

[a](A) Reagents and conditions: (a) B_2pin_2, $PdCl_2(dppf)$, KOAc, dioxane, 85 °C, 4 h, 61%; (b) *tert*-butyl 4-(4-bromophenyl)piperidine-1-carboxylate, $Pd(PPh_3)_4$, K_2CO_3, DMF, 80 °C, 5 h, 59%; (c) TFA/THF = 1:1, rt, 1 h, 90–93%; (d) CH_3I or $HC{\equiv}CCH_2Br$ or $CH_3(CH_2)_2I$, K_2CO_3, CH_3CN, rt or 50 °C, 15 h, 55% (**43a**) or 65% (**43b**) or 68% (**43c**); 6-bromohexyne-1, K_2CO_3, DMF, rt, 15 h, 70% for **43d**; Ac_2O, Et_3N, CH_3CN, rt, 0.5 h, 49% for **43e**; propionic acid, HATU, DIPEA, DMF, rt, 2 h, 54% for **43f**; (e) KOH, MeOH, H_2O, 50 °C, 48–88%; (f) H_2, Rh/C, MeOH/EtOAc (1:1), 100 psi, 92%; (g) *tert*-butyl 4-(4-(4,4,5,5-tetramethyl-1,3,2-dioxaborolan-2-yl)phenyl)-3,6-dihydropyridine-1(2*H*)-carboxylate, $PdCl_2(PPh_3)_2$, Na_2CO_3, 1,4-dioxane/water (10:1), 80 °C, 12 h, 48%. (B) Reagents and conditions: (a) Boc-NH-PEG_6-CH_2CH_2COOH or mPEG_5-CH_2CH_2COOH, HATU, DIPEA, DMF, rt, 1 h, 94% (**44a**) or 93% (**44b**); (b) KOH, MeOH, H_2O, 50 °C, 15 h, 65% (**11**) or 79% (**14**); (c) TFA/THF = 1:1, rt, 1 h, 91%; (d) Ac_2O, pyr, rt, 1 h, 59%. (C) Reagents and conditions: (a) 4-(4-bromophenyl)quinuclidine **96**, $Pd(PPh_3)_4$, K_2CO_3, DMF, 80 °C, 3 h, 88%; (b) CH_3I, K_2CO_3, CH_3CN/MeOH (1:1), 37 °C, 1 h, 55%; (c) KOH, MeOH, H_2O, 50 °C, 12 h, 53% (**17**) or 71% (**21**). (D) Reagents and conditions: (a) B_2pin_2, $PdCl_2(dppf)$, KOAc, dioxane, 70 °C, 15 h, 87%; (b) *tert*-butyl 4-(4-bromophenyl)piperazine-1-carboxylate, **96**, **99**, or **101**, $Pd(PPh_3)_4$, K_2CO_3, DMF, 80 °C, 3 h, 32–41%; (c) KOH, MeOH, H_2O, 50 °C, 59–94%; (d) TFA/THF = 2:1, rt, 0.5 h, 35–79%.

Chemical Synthesis. The synthesis of the novel heteroaryl, piperidinyl, and bicyclo-aliphatic analogues (**3**, **4**, **6**, **7b**, **10–21**, **24**, and **26–35**) is shown in Schemes 1–4. The synthesis of the piperidin-4-yl derivatives of the potent naphthalene antagonist **1** in which the secondary amine was alkylated or acylated with small groups (**5–10**) or acylated with water-solubilizing PEG groups (**11–14**) is shown in Scheme 1A,B. An amide linkage, rather than an alkylated piperidine group, was chosen for the PEG conjugates due to the relatively high $P2Y_{14}R$ affinity of simple acyl derivatives **8** and **9**. First, a key intermediate, e.g., aryl dioxaborolane **40**, was subjected to a Pd-catalyzed Suzuki coupling with either a bromoaryl or aryl triflate precursor, e.g., **37**.[23] This affixed the *p*-substituted phenyl ring to the central naphthalene or phenyl ring of reference antagonist **1** or **2**, respectively. For most of the analogues, removal of the Boc-piperidine protection, e.g., of **41**, and saponification of the ethyl ester, e.g., of **42**, were performed sequentially. However, when N-acylation with a PEG group was desired, this group was installed first on secondary amine **42** before saponification. The $(PEG)_6$ conjugates **11–14** were more water soluble than parent **1**, as expected. For example, PEG derivative **12** was found to be completely soluble in water at a concentration of 150 mM.

The bromoaryl intermediates **96–101** for the synthesis of bridged piperidine products **17–21** were prepared as described in the Supporting Information (Scheme S1). Phenylquinuclidine derivative **17** related to **1** was prepared by a Suzuki coupling, as shown in Scheme 1C from intermediate **40**, protected as an ethyl ester. Other bridged piperidine derivatives of **2** were prepared from bromo intermediate **46**,[23] as shown in Scheme 1D. The attempted substitution of the carboxylic acid of the central phenyl ring with closely related uncharged groups was performed, as described in Scheme S2.

Rotation of the triazole ring of reference compound **2** and thienyl analogue **23** by one position was accomplished, as shown in Scheme 2, to provide **25** and **26**, respectively. The carboxylic group of commercial 1,3,5-trisubstituted benzene derivative **53** was first protected as the methyl ester **54** followed by substitution of iodo of the central phenyl ring with TMS-acetylene to yield **55**. Compound **55** was reacted with TBAF for deprotection of TMS to afford **56** having an alkyne group. Subsequently, **56** was reacted with 1-azido-4-

https://dx.doi.org/10.1021/acs.jmedchem.0c00745
J. Med. Chem. XXXX, XXX, XXX–XXX

Scheme 2. Synthesis of Reverse Triazole Analogues of 2[a]

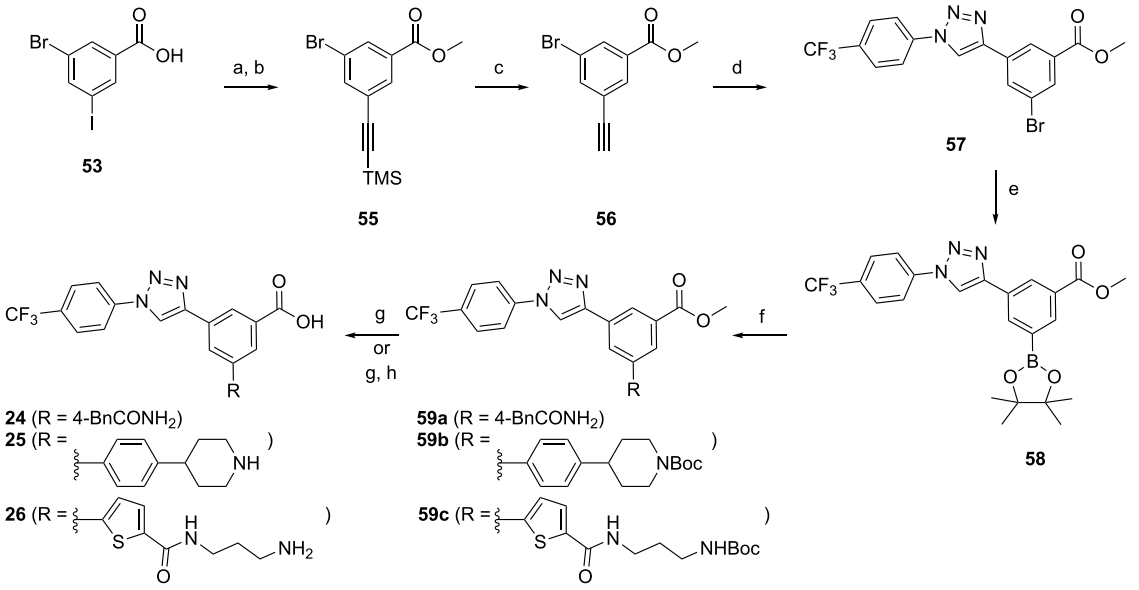

[a]Reagents and conditions: (a) $SOCl_2$, MeOH, rt, 15 h, 96%; (b) TMS-acetylene, $PdCl_2(PPh_3)_2$, CuI, Et_3N, DMF, rt, 5 h, 92%; (c) TBAF, THF, rt, 0.5 h, 94%; (d) 1-azido-4-(trifluoromethyl)benzene, $CuSO_4{\cdot}5H_2O$, Na ascorbate, THF/H_2O, rt, 1 h, 46%; (e) $B_2(pin)_2$, KOAc, $PdCl_2(dppf)$, dioxane, 70 °C, 15 h, 76%; (f) *tert*-butyl 4-(4-bromophenyl)piperidine-1-carboxylate, $Pd(PPh)_4$, K_2CO_3, DMF, 85 °C, 2 h for **59b** (39%) or 4-$BrPhCONH_2$ or *tert*-butyl (3-(5-bromothiophene-2-carboxamido)propyl) carbamate, $PdCl_2(dppf)_2$, $NaCO_3$, DME, 50 °C, 46% (**59a**) or 52% (**59c**); (g) KOH, MeOH, H_2O, 50 °C, 15 h, 60−99%; (h) TFA/THF = 1:1, rt, 1 h, 61% (**25**) or 45% (**26**).

(trifluoromethyl)benzene in the presence of copper sulfate to afford rotated triazole **57**, which was then reacted with bis(pinacolato)diboron (B_2pin_2) to yield **58**. Suzuki reactions of **58** with 4-$BrPhCONH_2$, *tert*-butyl 4-(4-bromophenyl)-piperidine-1-carboxylate, or *tert*-butyl (3-(5-bromothiophene-2-carboxamido)propyl) carbamate yielded **59a−59c**, respectively, and were followed by hydrolysis of the methyl ester to provide **24** and **60b** and **60c**, respectively. Removal of the *N*-Boc protecting groups of **60b** and **60c** afforded rotated triazole analogues **25** and **26**, respectively.

Amides in place of the triazole ring were prepared, as shown in Scheme 3A. A Suzuki reaction established the biaryl group of **63** prior to the amide formation using HATU. Amide analogues of reference compound **2** and a primary carboxamide **22**, i.e., **27** and **28**, respectively, were included. A cubane amide was introduced in compound **28**. The direction of the amide linking group in primary carboxamide analogue **29** was reversed for comparison to **27** (Scheme 3B). The carboxylic group of commercial precursor **61a** was protected as the methyl ester **61b**, which was coupled with dioxaborolane group **62**, followed by Suzuki reactions with 4-$BrPhCONH_2$ or *tert*-butyl 4-(4-bromophenyl)piperidine-1-carboxylate to afford **63a** and **63b**, respectively. Subsequently, **63a** and **63b** were coupled with *p*-$CF_3PhCOOH$ or 4-$(HOCH_2)$cubane-1-COOH to yield **64a** and **64b**, respectively, which were then deprotected by one of the two methods to yield **27** and **28**, respectively. For the synthesis of **29** in which the direction of the amide linking group was reversed compared with **27**, esterification of **66** was conducted to afford **67**, which was coupled with *p*-trifluoromethylaniline **69**,[30] followed by a Suzuki reaction with 4-aminocarbonylphenylboronic acid pinacol ester **70**, which was hydrolyzed to yield **29**.

Fused rings derived from the *p*-trifluoromethylphenyl group were prepared in **30−32**, as shown in Scheme 3C,D. The Sonogashira reactions of **56** with trifluoromethyl-substituted 2-iodo-anilines were performed to prepare **71a** and **71b**, which were cyclized to indoles **72a** and **72b**, respectively. Compounds **72a** and **72b** were subjected to a Suzuki reaction to afford **73a** and **73b**, respectively, which were hydrolyzed to yield **30** and **31**, respectively. To synthesize **32**, intermediate **66b** was first cyclized to a benzimidazole **74**. Compound **74** was coupled with 4-aminocarbonylphenylboronic acid pinacol ester through a Suzuki reaction, and the product **75** was then hydrolyzed to afford **32**.

Modification of the central phenyl ring of **2** was accomplished, as shown in Scheme 4A (pyrrole analogue **33**, which was also substituted with an alkene in the piperidine ring), Scheme 4B (aryl-methyl analogue **34**), and Scheme 4C (benzimidazole **35**). For preparation of **33**, the pyrrole scaffold of **78** was formed from **77**, which was synthesized with commercial **76** and *p*-toluenesulfonic anhydride (Ts_2O). Subsequently, a Suzuki reaction was conducted with *tert*-butyl 4-(4,4,5,5-tetramethyl-1,3,2-dioxaborolan-2-yl)-3,6-dihydropyridine-1(2*H*)-carboxylate to afford **79** followed by conversion of the amine functionality into an azide **80**. The azide was subjected to a click reaction with 4-ethynyl-*α*,*α*,*α*-trifluorotoluene to afford triazole **81**, which was then deprotected to yield **33**. For the synthesis of **34**, the iodo group of **83** was substituted with TMS-acetylene to afford **84**, which was reacted with TBAF for deprotection of TMS to yield **85**. This was followed by the click reaction with 1-azido-4-(trifluoromethyl)benzene to afford **86**. A Suzuki reaction of **86** with *tert*-butyl 4-(4-(4,4,5,5-tetramethyl-1,3,2-dioxaborolan-2-yl)phenyl)piperidine-1-carboxylate yielded **87**, which was then deprotected at the *N*-Boc group **88** and hydrolyzed to afford **34**. To prepare **35**, compound **89** was cyclized to benzimidazole **90**, which was coupled with *tert*-butyl 4-(4-(4,4,5,5-tetramethyl-1,3,2-dioxaborolan-2-yl)phenyl)-piperidine-1-carboxylate through a Suzuki reaction to synthesize **91** followed by deprotection to afford **35**.

https://dx.doi.org/10.1021/acs.jmedchem.0c00745
J. Med. Chem. XXXX, XXX, XXX−XXX

Scheme 3. (A–D) Synthesis of Analogues of 2 in Which the Triazole Moiety Has Been Replaced with an Amide or Fused with the Terminal 4-Trifluoromethylaryl Ring[a]

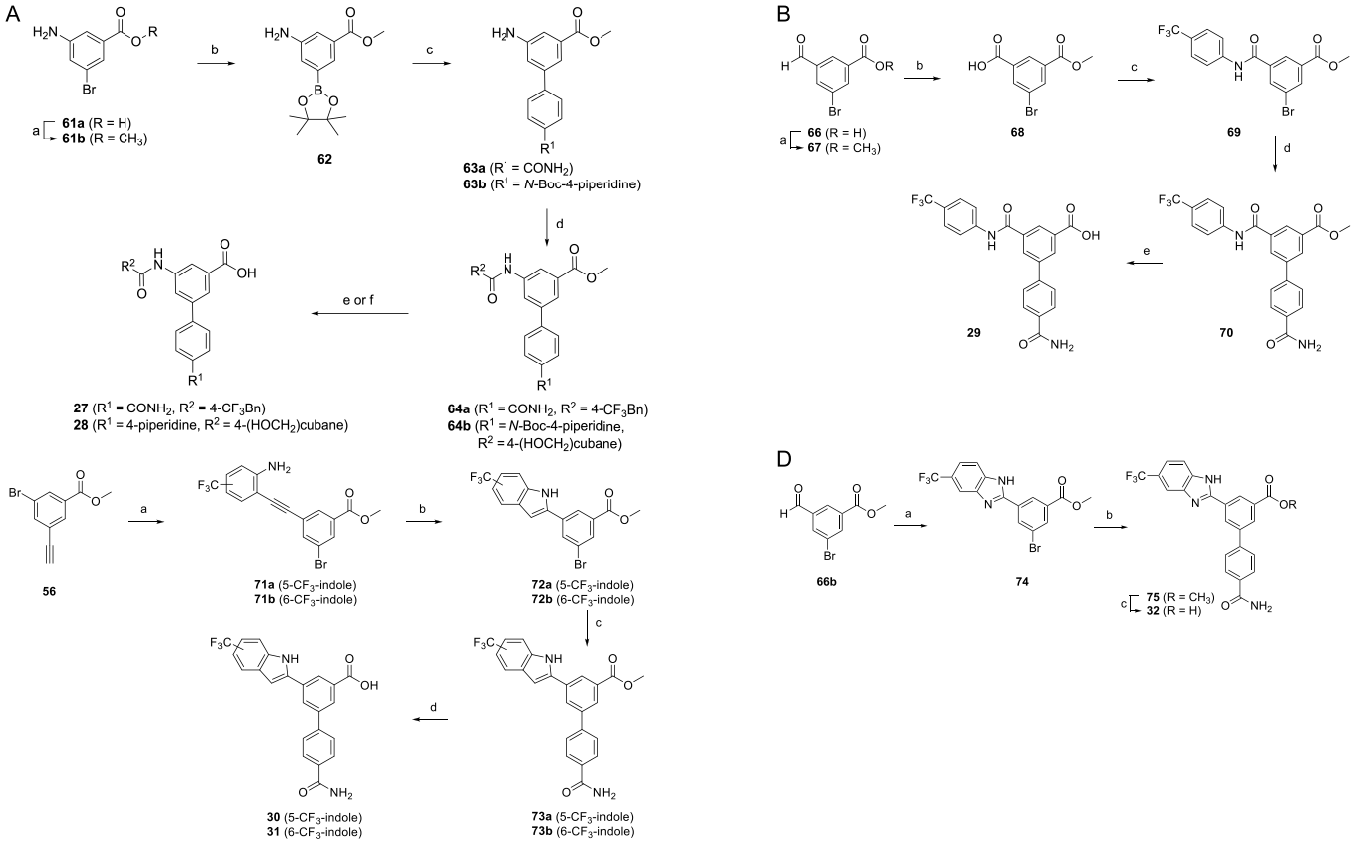

[a](A) Reagents and conditions: (a) $SOCl_2$, MeOH, rt, 15 h, 98%; (b) $B_2(pin)_2$, KOAc, $PdCl_2(dppf)$, dioxane, 95 °C, 15 h, 68%; (c) 4-BrPhCONH$_2$ or *tert*-butyl 4-(4-bromophenyl)piperidine-1-carboxylate, $Pd(PPh)_4$, K_2CO_3, DMF, 80 °C, 15 h, 63% (**63a**) or 41% (**63b**); (d) *p*-CF_3PhCOOH or 4-(HOCH$_2$)cubane-1-COOH, HATU, DIPEA, DMF, rt, 15 h, 99% (**64a**) or 69% (**64b**); (e) KOH, MeOH, H_2O, 50 °C, 15 h, 70% for **27**; (f) (i) 1 N HCl, dioxane, rt, 15 h, 67%; (ii) KOH, MeOH, H_2O, 50 °C, 15 h, 39% for **28**. (B) Reagents and conditions: (a) H_2SO_4, CH_3OH, 60 °C, 15 h, 54%; (b) oxone, DMF, rt, 15 h, 78%; (c) (i) $SOCl_2$, Et_3N, DCM, 0 °C, 1 h; (ii) *p*-trifluoromethylaniline, Et_3N, DCM, rt, 15 h, 45%; (d) 4-aminocarbonylphenylboronic acid pinacol ester, $PdCl_2(PPh_3)_2$, Na_2CO_3, dioxane, H_2O, 80 °C, 2 h, 63%; (e) KOH, MeOH, H_2O, 50 °C, 15 h, 72%. (C) Reagents and conditions: (a) iodo-(trifluoromethyl)aniline, $PdCl_2(PPh)_2$, CuI, Et_3N, rt, 1 h, 82% (**71a**) or 87% (**71b**); (b) $PdCl_2$, DMF, 110 °C, 10 min, μW, 65% (**72a**) or 62% (**72b**); (c) 4-aminocarbonylphenylboronic acid pinacol ester, $PdCl_2(PPh)_2$, Na_2CO_3, dioxane, H_2O, 80 °C, 15 h, 55% (**73a**) or 72% (**73b**); (d) KOH, MeOH, H_2O, 70 °C, 3 h, 59% (**30**) or 67% (**31**). (D) Reagents and conditions: (a) $Na_2S_2O_5$, 4-trifluoromethyloxy-phenylenediamine, DMF, 130 °C, 15 h, 97%; (b) 4-aminocarbonyl-phenylboronic acid pinacol ester, $PdCl_2(PPh_3)_2$, Na_2CO_3, dioxane, H_2O, 80 °C, 15 h, 38%; (c) KOH, MeOH, H_2O, 70 °C, 3 h, 99%.

In search of an alternative assay to the fluorescence binding assay using **36**, we prepared [^{3}H]**1** as a potential radioligand, as shown in Scheme 5. The piperidine alkene intermediate **39**, containing both Boc and ester protecting groups, was catalytically hydrogenated with tritium gas in ethyl acetate as the solvent to yield **93**. The protecting groups were used, rather than one-step catalytic reduction of **3**, because having no easily ionizable groups present improved the solubility of both the hydrogenation substrate and the product. Facile, sequential removal of the protecting groups provided the desired tritiated compound [^{3}H]**1** in high purity following preparative HPLC (Supporting Information). The catalytic reduction sequence shown in Scheme 5 was first performed using nonradioactive hydrogen gas.

In Vitro Pharmacological Assays. Feasibility testing of [^{3}H]**1** as a radioligand in cell membranes was disappointing as the compound demonstrated low solubility in the aqueous medium and adsorbed to plastic surfaces at higher μM concentrations. In hP2Y$_{14}$R-expressing cell membranes, a signal for specific receptor binding was lacking due to the high nonspecific binding. Therefore, the affinity measurement of the new antagonist analogues was performed using the previously reported fluorescence binding assay, using as tracer the AF488 conjugate **36** prepared according to Yu et al.,[23] by flow cytometry of whole Chinese hamster ovary (CHO) cells stably expressing the hP2Y$_{14}$R in a 96-well format.

Various small *N*-alkyl and *N*-acyl derivatives of the piperidine ring of **1** were previously shown to have moderate hP2Y$_{14}$R antagonist potency.[12,23] Here, as shown in Table 1A, the loss of affinity in the fluorescence assay of small *N*-alkyl derivatives of **1** was in the range of 13- to 33-fold (compounds **5**–**7**). Notably, an *N*-acetyl derivative **8**, which is no longer a zwitterion, showed only 3-fold lower affinity than **1**. Derivatives with other simple modifications of the piperidine rings of **1** and **2**, i.e., alkene **3** and piperazine **4** derivatives, respectively, bound relatively well to the hP2Y$_{14}$R with affinity reduction of only 3- to 7-fold. The IC$_{50}$ value of **3** in inhibition of binding of **36** was 18 nM, i.e., it ranked among the most potent analogues in this study. However, the Boc derivative **10** showed relatively weak affinity. Therefore, not all modifications

https://dx.doi.org/10.1021/acs.jmedchem.0c00745
J. Med. Chem. XXXX, XXX, XXX–XXX

Scheme 4. (A–C) Synthesis of Analogues of 2 in Which the Central Phenyl Ring Has Been Modified[a]

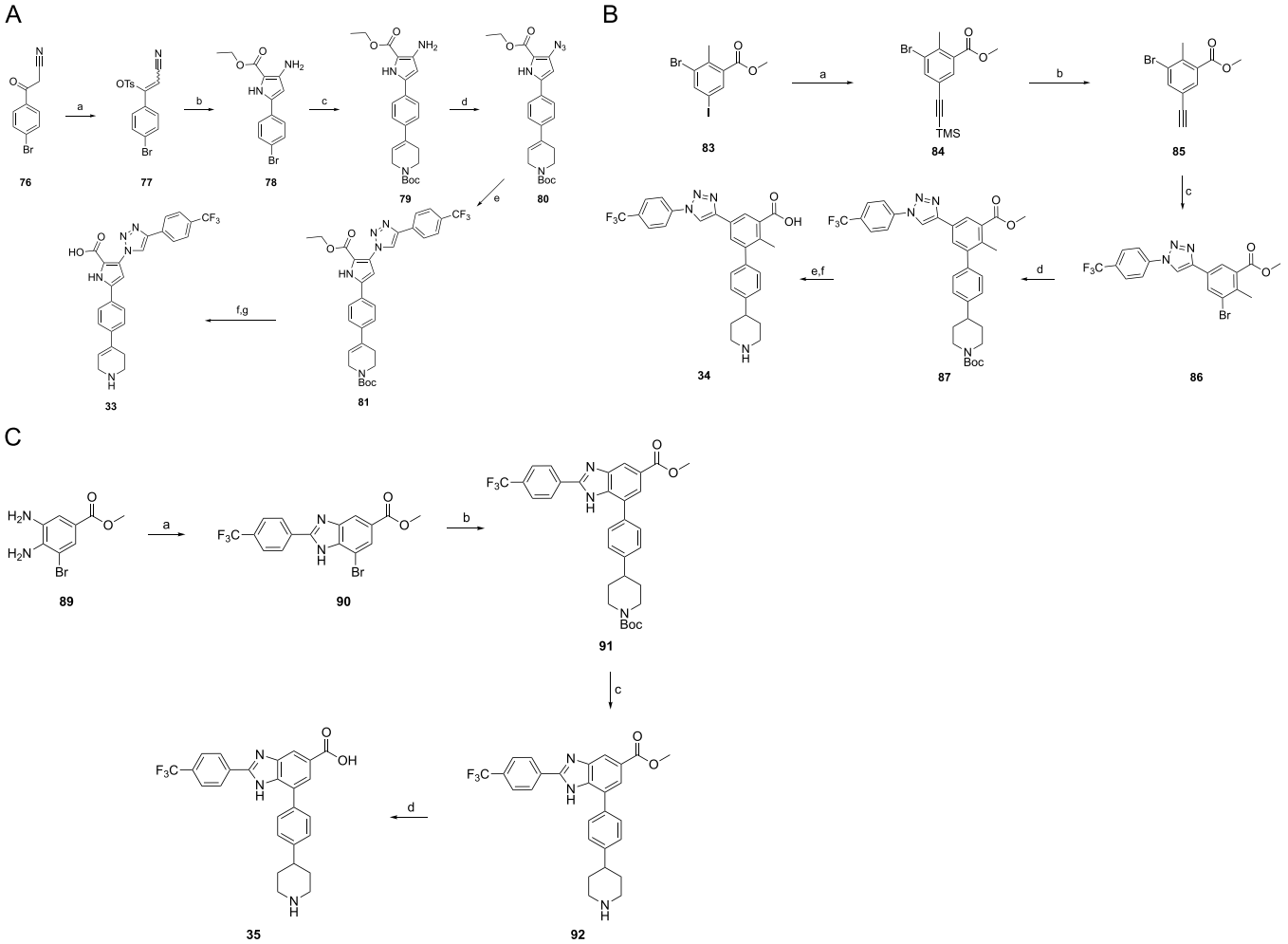

[a](A) Reagents and conditions: (a) Ts_2O, TEA, DCM, rt, 3 h; (b) NaOEt, diethyl aminomalonate hydrochloride, EtOH, THF, rt, 0.5 h, 40%; (c) *tert*-butyl 4-(4,4,5,5-tetramethyl-1,3,2-dioxaborolan-2-yl)-3,6-dihydropyridine-1(2*H*)-carboxylate, $PdCl_2$(dppf), NaOH, DMF, rt, 1 h, 78%; (d) $NaNO_2$, NaN_3, 4 M HCl(aq), 0 °C to rt, 0.5 h, 75%; (e) 4-ethynyl-*α*,*α*,*α*-trifluorotoluene, sodium ascorbate, $CuSO_4 \cdot 5H_2O$, dimethyl sulfoxide/water = 9:1, rt, 1 h, 77%; (f) TFA/THF = 2:1, rt, 0.5 h, 60%; (g) KOH, MeOH, H_2O, 50 °C, 5 h, 30%. (B) Reagents and conditions: (a) TMS-acetylene, $PdCl_2(PPh_3)_2$, CuI, Et_3N, DMF, rt, 5 h, 99%; (b) TBAF, THF, rt, 0.5 h, 93%; (c) 1-azido-4-(trifluoromethyl)benzene, $CuSO_4 \cdot 5H_2O$, Na ascorbate, THF/H_2O, rt, 1 h, 66%; (d) *tert*-butyl 4-(4-(4,4,5,5-tetramethyl-1,3,2-dioxaborolan-2-yl)phenyl)piperidine-1-carboxylate, $Pd(PPh)_4$, K_2CO_3, DMF, 85 °C, 12 h, 70%; (e) TFA/THF = 2:1, rt, 0.5 h, 79%; (f) KOH, MeOH, H_2O, 50 °C, 5 h, 72%. (C) Reagents and conditions: (a) 4-(trifluoromethyl)benzaldehyde, $Na_2S_2O_5$, DMF, 130 °C, 12 h, 65%; (b) *tert*-butyl 4-(4-(4,4,5,5-tetramethyl-1,3,2-dioxaborolan-2-yl)phenyl)-piperidine-1-carboxylate, $Pd(PPh_3)_4$, Na_2CO_3, 1,4-dioxane/water (10:1), 80 °C, 12 h, 43%; (c) TFA/THF = 2:1, rt, 0.5 h, 82%; (d) KOH, MeOH, H_2O, 50 °C, 5 h, 63%.

of the piperidine nitrogen were tolerated. The $(PEG)_6$ amide-linked conjugates **11–14** were intermediate in binding affinity ($IC_{50} \approx 1–3$ μM), although at least 160-fold weaker than the parent compound **1**.

The approach of modifying the piperidine ring as bicyclic ring systems was especially fruitful. Phenylquinuclidine derivative **17** proved to have high affinity at the $hP2Y_{14}R$ with an IC_{50} value of 20 nM, i.e., ∼3-fold lower than its reference naphthalene **1**. Similarly, the corresponding triazole derivative **18** showed a $P2Y_{14}R$ affinity ∼3-fold lower than its reference **2**. Bridged cyclopropyl derivatives **19** and **20** (both racemic) showed 11-fold and 20-fold lower affinity, respectively, than the reference triazole **2**. The quaternized *N*-methylquinuclidinium derivative **21** had an improved cLogP and showed only ∼6-fold lower $hP2Y_{14}R$ affinity than parent zwitterion **1**.

Compounds with modifications elsewhere on the scaffold (Table 1B) were generally of much lower $P2Y_{14}R$ affinity than the reference compounds. Cubane **28**, pyrrole **33**, and benzimidazole **35** derivatives had affinities that were too low to be measured (estimated >100 μM) using the current method and given the solubility limitations of the compounds. Benzimidazole **32** and aryl-methyl **34** derivatives only weakly inhibited binding, with IC_{50} values > 10 μM. More effective preservation of $P2Y_{14}R$ affinity was achieved with amides **27** and **29** and trifluoromethyl-indoles **30** and **31**, which had IC_{50} values between 1 and 10 μM. Amide **27** with NH on the central phenyl ring had 11-fold lower affinity than its reference triazole derivative **22**, and it bound to the $P2Y_{14}R$ with twice the affinity of the corresponding reversed amide **29**. Among the analogues in Table 1B, the best retention of $P2Y_{14}R$ affinity was observed with the rotated triazole derivatives **24–26**, which differed in the R^1 substituent. Nevertheless, the affinities

https://dx.doi.org/10.1021/acs.jmedchem.0c00745
J. Med. Chem. XXXX, XXX, XXX–XXX

Scheme 5. Synthesis of [^{3}H]1[a]

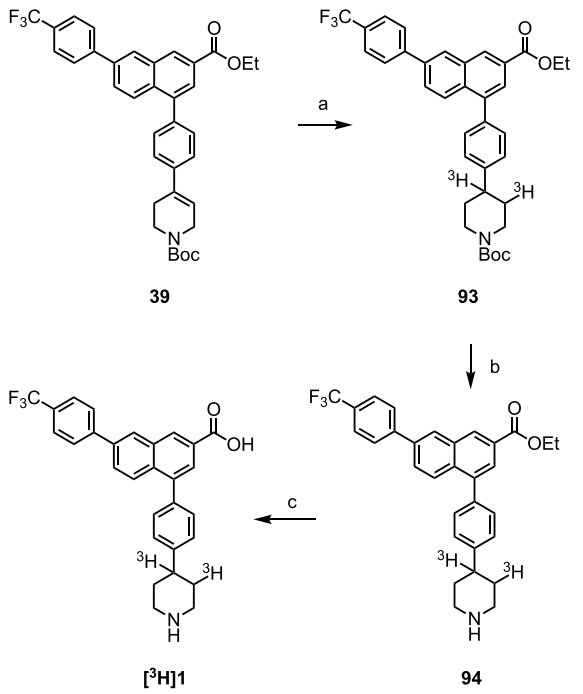

[a]Reagents and conditions: (a) Pd/C, $^3H_2$, EtOAc, rt, 100 psi; (b) TFA/THF = 2:1, rt, 0.5 h; (c) KOH, MeOH, H_2O, 50 °C, 5 h.

were moderately reduced (fold) compared to respective reference compound: **24** (6.2-fold vs **22**), **25** (20-fold vs **2**), and **26** (15-fold vs **23**). The IC_{50} value of primary carboxamide derivative **25** was 0.644 μM, i.e., 20-fold weaker than reference triazole **2**.

To examine the species dependence of affinity, the mP2Y_{14}R was stably transfected in human embryonic kidney (HEK) 293 cells.[12] The intact cell binding of **36** in mP2Y_{14}R-expressing HEK293 cells was almost completely inhibited in the presence of 1 μM **1**, as shown in fluorescence micrographs.[12] The primary screen of binding affinity was P2Y_{14}R fluorescence binding quantified using flow cytometry. The affinity of selected compounds at the mP2Y_{14}R was determined (Table 2). Representative fluorescence binding inhibition curves at the two species homologues are shown for key antagonists (Figure 1). Compound **17** showed the same affinity at the two P2Y_{14}R species homologues and also the same affinity as **1** at the mP2Y_{14}R. PEG derivative **12** and rotated triazole **25** showed 2-fold greater affinity at the mouse homologue than at the hP2Y_{14}R, while other compounds had higher IC_{50} values at mP2Y_{14}R than at hP2Y_{14}R: **1** (3.6-fold), **2** (4.5-fold), **4** (2.1-fold), **8** (1.7-fold), **18** (8.0-fold), **19** (3.3-fold), **22** (3.4-fold), and **23** (2.3-fold). Thus, in the quinuclidine series, the naphthalene moiety of **17** better preserved mP2Y_{14}R affinity than the triazole core structure of **18**.

The pH dependence of hP2Y_{14}R affinity was examined for two potent derivatives, **1** and **17**. These antagonists showed only a minor increase in IC_{50} values when the pH was lowered from 7.4 to 6.0 (Figure 1C and Table 3). Thus, the antagonists can be expected to be effective under slightly acidic conditions as might occur during inflammation, cancer, and ischemia.[31]

One objective was to overcome the low aqueous solubility of **1**. The cLogP values (Tables 1A and 1B) were calculated for the antagonists as an indication of partition between aqueous and organic phases. There was no correlation between the cLogP and IC_{50} values (Supporting Information), indicating that the binding affinity was not a function of hydrophobicity as one would expect if association with a lipid membrane was required, for example with a P2Y_1R allosteric antagonist.[32] The five antagonists of highest affinity, **1**, **2**, **3**, **17**, and **18**, were relatively nonpolar, with cLogP values of 5−6, but the cLogP was consistently lower in the triazole compared to the naphthalene series. Compound **23** showed a balance between moderately high affinity and hydrophilicity, with a cLogP of 0.84.[23]

Table 2. Inhibitory Potency of Antagonists at the mP2Y_{14}R Expressed in HEK293 Cells, Using the Fluorescence Binding Method, Compared to the hP2Y_{14}R Expressed in CHO Cells

compound	mP2Y_{14}R, IC_{50} (nM)[a]	hP2Y_{14}R, IC_{50} (nM)[a]
1	21.6 ± 7.0	6.0 ± 0.1
2	142 ± 58	31.7 ± 8.0
4	499 ± 57	233 ± 26
7a	130 ± 30	76.3 ± 24.4
8	29.7 ± 9.3	27.6 ± 4.3
12	487 ± 130	963 ± 417
17	21.4 ± 7.9	20.0 ± 4.4
18	845 ± 150	105 ± 10
19	1160 ± 330	359 ± 69
21	56.3 ± 19.0	38.3 ± 2.2
22	902 ± 344	269 ± 121
23	384 ± 88	169 ± 42
25	246 ± 63	644 ± 175

[a]IC_{50} values were determined by flow cytometry of mP2Y_{14}R-HEK293 cells using fluorescent antagonist tracer **36** and expressed as mean ± SEM (n = 3−5). hP2Y_{14}R values were from Tables 1A and 1B.

The solubility of six analogues was determined using the pION method (Table 4), and lipophilicity was determined based on the HPLC retention time relative to **1** (methods in the Supporting Information). The mean aqueous solubility at pH 7.4 varied in the order **12** > **8**, **21** > **18** > **17**, **1**. Thus, modest improvements in the solubility at physiological pH were observed, especially for the PEG conjugate **12** (7.16 μg/mL) compared to parent reference compound **1** (0.36 μg/mL). At pH 4.0, the solubility was greater than at pH 7.4, except for the nonzwitterionic carboxylic acid **8**, but the same compound showed reduced lipophilicity relative to **1**. For in vivo administration, aqueous DMSO was used as a solubilizing vehicle. Quinuclidine derivative **17** was readily soluble at 1 mM in DMSO as a zwitterion, while the parent **1** as a zwitterion failed to dissolve in DMSO at 1 mM, unless it was treated with aqueous NaOH or HCl. Compound **17** dissolved readily in DMSO without basification and was not subjected to precipitation upon dilution; it was completely soluble at 1 mg/mL in 10% DMSO in water.

OFF-TARGET AND ADME-TOXICITY TESTING

Although the novel antagonists in this study were not evaluated for P2Y_{14}R selectivity within the P2Y family, there is precedent for exclusive interaction with P2Y_{14}R as compounds **1** and **2** and other members of the triazole series were inactive at other P2YRs.[8,17] Off-target non-P2YR interactions of selected antagonists (**4**, **6b**, **7a**, **8**, **12**, **17**−**19**, and **22**−**26**) were determined at 46 receptors, transporters,

https://dx.doi.org/10.1021/acs.jmedchem.0c00745
J. Med. Chem. XXXX, XXX, XXX−XXX

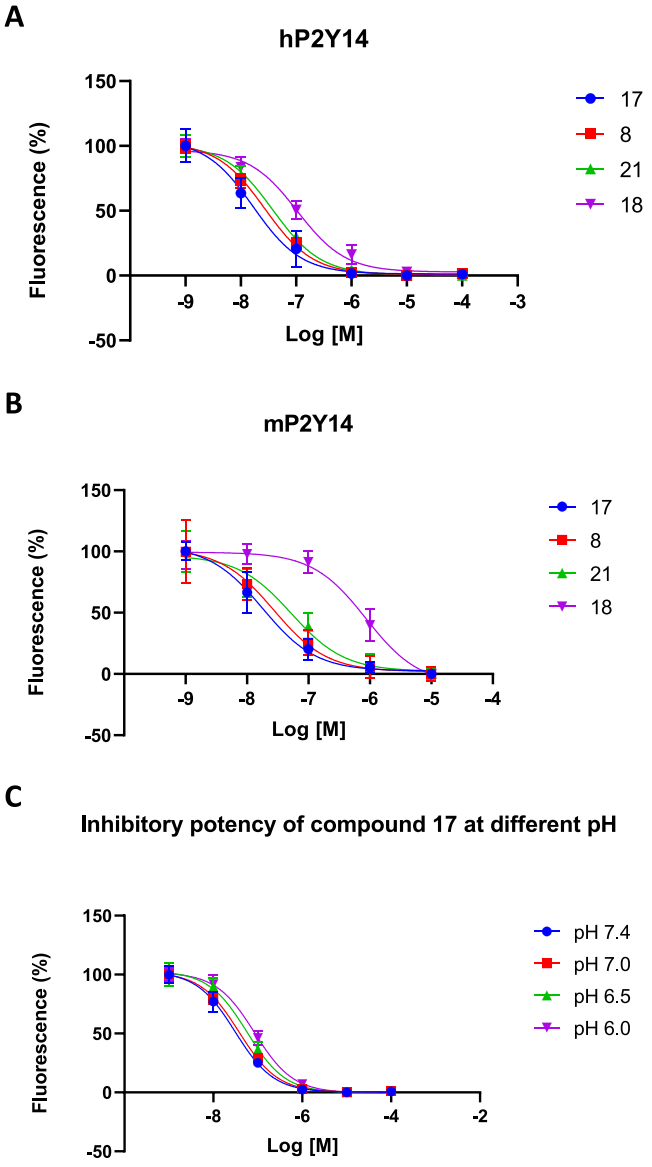

Figure 1. (A, B) Fluorescence inhibition assay by flow cytometry in (A) $hP2Y_{14}R$-expressing CHO cells and (B) $mP2Y_{14}R$-expressing HEK293 cells with the AF488-labeled tracer **36**. The IC_{50} values are given in Tables 1A and 1B. In (C), the pH was varied between 7.4 and 6.0, and binding was measured using $hP2Y_{14}R$-expressing CHO cells.

and ion channels (comprehensive screen) by the Psychoactive Drug Screening Program (PDSP, Supporting Information).[33] Compound **1** was previously reported to bind to the D_3 dopamine and δ-opioid (DOR) receptors with K_i values of 6.79 and 2.75 μM, respectively, and compounds **2**, **6b**, and **7a** had no detected off-target interactions.[8,9] Several off-target interactions were noted for the new analogues (K_i, μM, receptor): **4**, 6.7 ± 0.5 (σ_2R); **8**, 4.31 ± 0.11 (D_3R), 4.38 ± 0.62 (D_5R), 1.75 ± 0.54 ($5HT_{1D}$R), and 0.51 (TSPO); **17**, 2.29 ± 0.81 (σ_2R); **18**, 1.37 ± 0.04 (σ_2R); **19**, 2.63 ± 0.13 (DOR) and 0.30 ± 0.13 (σ_2R); **21**, 0.42 (σ_2R); **22**, 6.89 ($5HT_6$R); **23**, 3.26 ± 0.64 (DOR) and 4.34 ($5HT_{1D}$R); **24**, 2.48 (DOR), 0.50 (σ_1R), and 2.91 (σ_2R); **25**, 3.79 (DOR), 0.96 (α_{2A}R), 5.33 (α_{2B}R), 2.71 ± 0.21 (α_{2C}R), 1.48 (σ_1R), and 2.09 (σ_2R); and **26**, 2.96 (DOR) and 1.11 (σ_1R). Furthermore, compounds **1** and **25** were inactive (EC_{50}, IC_{50} > 10 μM) as

Table 3. pH Dependence of IC_{50} of Two Antagonists in Inhibition of Fluorescent Antagonist 36 Binding at $hP2Y_{14}R$-Expressing CHO Cells (n = 3, Measured in Triplicate)

compound	pH[a]	IC_{50} ± SEM (nM)
1	7.4	6.01 ± 0.87
	7.0	9.75 ± 3.29
	6.5	14.5 ± 5.8
	6.0	19.0 ± 2.8
17	7.4	30.8 ± 2.2
	7.0	38.1 ± 2.1
	6.5	57.0 ± 8.7
	6.0	84.5 ± 1.1

[a]The levels of total fluorescence binding were comparable at the different pH values (arbitrary fluorescence units): pH 7.4, 71.37 ± 3.82; pH 7.0, 76.98 ± 4.39; pH 6.5, 78.80 ± 7.83; and pH 6.0, 79.29 ± 6.49.

Table 4. Solubility and Relative Lipophilicity Determined for Selected $P2Y_{14}R$ Antagonists

	solubility (μg/mL)[a]		
compound	pH 4.0	pH 7.4	lipophilicity (Δk), relative to **1**[b]
1	1.10 ± 0.07	0.36 ± 0.03	0
8	0.09 ± 0.02	2.32 ± 0.18	−0.48 ± 0.01
12	8.02 ± 1.01	7.16 ± 1.16	0.71 ± 0.03
17	1.50 ± 0.04	0.55 ± 0.02	1.24 ± 0.78
18	2.87 ± 0.10	1.10 ± 0.09	−0.09 ± 0.13
21	2.24 ± 0.19	1.72 ± 0.07	0.24 ± 0.03

[a]Determined using the pION method at the pH indicated (Supporting Information). [b]Determined from the RP-HPLC retention time (C18 column), with a 20 min gradient of 10 to 100% acetonitrile in 10 mM triethylammonium acetate.

functional agonist or antagonist of CB1 and CB2 cannabinoid receptors, as determined by PDSP (Supporting Information). An indication that the representative tested compounds were not promiscuous, i.e., pan-assay interference compounds (PAINS),[34] was the lack of appreciable binding at other sites in the PDSP screen.

ADME-toxicity properties were predicted for compounds **7a**, **8**, and **25** using online resources.[35,36] None of the three were predicted to inhibit hERG-I. The only CYP interactions predicted were as follows: all three as CYP3A4 substrates and **8** additionally as the CYP2C9 inhibitor. Furthermore, compounds **17** and **18** were tested for bioavailability when administered ip (1, 3, and 10 mg/kg compared to 0.5 mg/kg iv) in the rat and in other in vitro tests predictive of ADME-toxicity properties (Table 5). Several unusual pharmacokinetic features were observed (Supporting Information), the first of which was >100% F for ip administration of both **17** and **18**. The bioavailability was dose-correlated such that the highest dose of 10 mg/kg showed a faster clearance than at 1 and 3 mg/kg. The 10 mg/kg dose also had a higher volume of distribution. The maximal plasma concentrations of **17** and **18** (~900 ng/mL at the highest dose of 10 mg/kg) were reached at 3−4 h (Figure S6, Supporting Information). The highest dose still maintained a concentration of ~200−400 ng/kg at the 12 h time point. At the 1 mg/kg dose, the plasma concentrations of compounds **17** and **18** were 165 and 206 nM (2 h) and 292 and 163 nM (4 h), respectively. The $t_{1/2}$ values of compounds **17** and **18** were 5.1 and 4.6 h, respectively (1

https://dx.doi.org/10.1021/acs.jmedchem.0c00745
J. Med. Chem. XXXX, XXX, XXX−XXX

Table 5. In Vitro and In Vivo ADME-Tox Data for Two Representative $P2Y_{14}R$ Antagonists[a]

test	22[b]	17	18
simulated intestinal fluid (% remaining at 120 min)	100	99.7	102
simulated gastric fluid (% remaining at 120 min)	100	74.2	106
CYP1A2 (IC_{50}, μM)	>30	8.69	14.1
CYP2C9 (IC_{50}, μM)	>30	>30	>30
CYP2C19 (IC_{50}, μM)	>30	>30	>30
CYP2D6 (IC_{50}, μM)	>30	>30	>30
CYP3A4 (IC_{50}, μM)	>30	3.29	9.94
plasma stability (three species)[d](% remaining at 120 min)	94−100	100 (h); 79.9 (r); 100 (m)	86.8 (h); 89.4 (r); 79.5 (m)
microsomal stability($t_{1/2}$, min)	145 (m), 108 (r), 145 (h)	67.2 (m), 80.0 (r), >240 (h)	311 (m), 108 (r), 192 (h)
hERG, IC_{50} (μM)	0.166	16.4	16.8
$t_{1/2}$ (h), administration mode[e]	0.20 (iv)	5.1 (1 mg/kg, ip); 3.46 (iv)	4.6 (1 mg/kg, ip); 0.72 (iv)
aqueous solubility[c] (pH 7.4, μg/mL)	138 ± 4	0.44 ± 0.06	<0.1
aqueous solubility[c] (pH 4.0, μg/mL)	ND[f]	14.3 ± 0.5	14.4 ± 0.3

[a]Procedure is in the Supporting Information. [b]Data determined by Yu et al.[23] [c]Mean ± SD, pION method. [d]Species tested for plasma stability were human, rat, and mouse; species as indicated for microsomal stability. [e]By iv administration: 0.5 mg/kg dose. [f]ND, not determined.

mg/kg, ip). Thus, the in vivo clearance of both compounds was low, but there was a lag observed in the entry into circulation with ip but not iv administration. Caco-2 cell permeability values of **17** and **18** (P_{app}, apical to basal) were 0.00 and 0.09, respectively, and they were not cytotoxic to Hep-G2 cells (IC_{50} > 20 μM, Table S2). Compounds **17** and **18** were stable in plasma and simulated body fluids and showed an acceptable hERG inhibition, which was greatly improved over the earlier compound **22**. In addition, the plasma protein binding of compounds **12**, **17**, **18**, **21**, **23**, and **25** tested in three species was high, with **21** and **25** having a more favorable free fraction in human and mouse but not rat (Table 6).

Table 6. Plasma Protein Binding at 10 μM in Three Species, Expressed as Unbound Percent[a]

compound	human, % free[b]	mouse, % free[b]	rat, % free
12	0.48	0.29	0.00
21	1.13	0.94	0.00
23	0.00	0.83	0.00
25	1.25	1.33	0.00

[a]Procedure is in the Supporting Information. Verapamil and warfarin served as positive controls. [b]Mean ± SD.

Evaluation of Selected Analogues in an In Vivo Assay of Antiasthmatic Activity. The ability of selected analogues to reduce allergic lung inflammation was studied in an *Aspergillus* protease-mediated mouse model of allergic asthma.[37] The test compounds were injected intraperitoneally at 10 mg/kg 30 min prior to allergen challenge, and airway inflammation was assessed 2 days post-challenge (Figure 2)[11] by cell differential counts in the bronchoalveolar lavage fluid (BALF) of mice. As shown previously, $mP2Y_{14}R$ blockade by reference antagonist **1** strongly attenuated eosinophilic airway inflammation.[11] A comparison of activity for other derivatives revealed that the highest potency of reducing eosinophil infiltration was associated with the previously reported *N*-hexynyl **7a** (10 mg/kg, ip) and that in vivo effects of quinuclidine **17** and primary amino **23** derivatives were similar to **1**. *N*-Acetyl **8** and rotated triazole **25** derivatives had a less pronounced but still significant anti-inflammatory activity. By contrast, a PEG derivative **12** and reference triazole **2** at the same dose were inactive when applied in this rodent model of asthma. Although many of the tested compounds had similar $mP2Y_{14}R$ affinity in vitro, the differences in in vivo activity probably arose from varying pharmacokinetic properties.

Evaluation of 12 in Chronic Constriction Injury Mouse Model of Neuropathic Pain. Since the PEG conjugate **12** showed ∼20-fold greater aqueous solubility at pH 7.4 than the reference compound **1**, we measured its in vivo efficacy in a mouse model of chronic neuropathic pain (7 days post-chronic constriction injury, CCI, of the sciatic nerve in adult male mice), as we recently reported for various $P2Y_{14}R$ antagonists in the work of Mufti et al.[12] Compound **12** was fully efficacious in reversing established, CCI-induced mechano-allodynia (Figure 3) at a dose that was already shown to be effective for other more potent $P2Y_{14}R$ antagonists such as **1** and **8** (10 μmol/kg, ip). Peak protection was achieved at 1−2 h post-injection. No effect of the drug was seen on the hind paw response contralateral to the injury.

Molecular Modeling. We used our previously published homology model of $hP2Y_{14}R$ based on a high-resolution X-ray structure of the closely related $hP2Y_{12}R$ as a template.[22] The agonist-bound $P2Y_{12}R$ structure served as the template (PDB ID: 4PXZ[20]), instead of a non-nucleotide antagonist-bound structure, because the extracellular loops (ELs) are defined. This model was used effectively in our previous docking and MD simulation of $hP2Y_{14}R$ antagonist binding,[22,23] so it was applicable to the current study.

This study has two principal aims: investigating piperidine substitution of lead compound **1** with bicyclic analogues and the replacement of the naphthalene or phenyl-triazole moieties of lead compounds **1** and **2** with alternative scaffolds. Focusing on the first aim, piperidine substitution with a conformationally constrained quinuclidine was proposed, and molecular modeling tested the $hP2Y_{14}R$ binding site fit of the potent protonated quinuclidinium form of analogue **17**. The initial docking pose of **17** (Figure 4) indicates a binding mode resembling that of **1** and **2** (Figure S7A). The carboxylate group of the central naphthalene/phenyl ring of **1** and **2** interacted with three residues in the transmembrane domains (TMs) 2, 3, and 7, which was used as an essential predictor of $P2Y_{14}R$ affinity among newly synthesized antagonist analogues.[22,23] The carboxylate engaged in electrostatic and H-bond interactions with the side chains of $Lys77^{2.60}$ (using Ballesteros−Weinstein convention for residue numbering[38]) and $Lys277^{7.35}$ and H-bonding with the $Tyr102^{3.33}$ phenolic group. Compound **17** made interactions with $Lys77^{2.60}$ and

https://dx.doi.org/10.1021/acs.jmedchem.0c00745
J. Med. Chem. XXXX, XXX, XXX−XXX

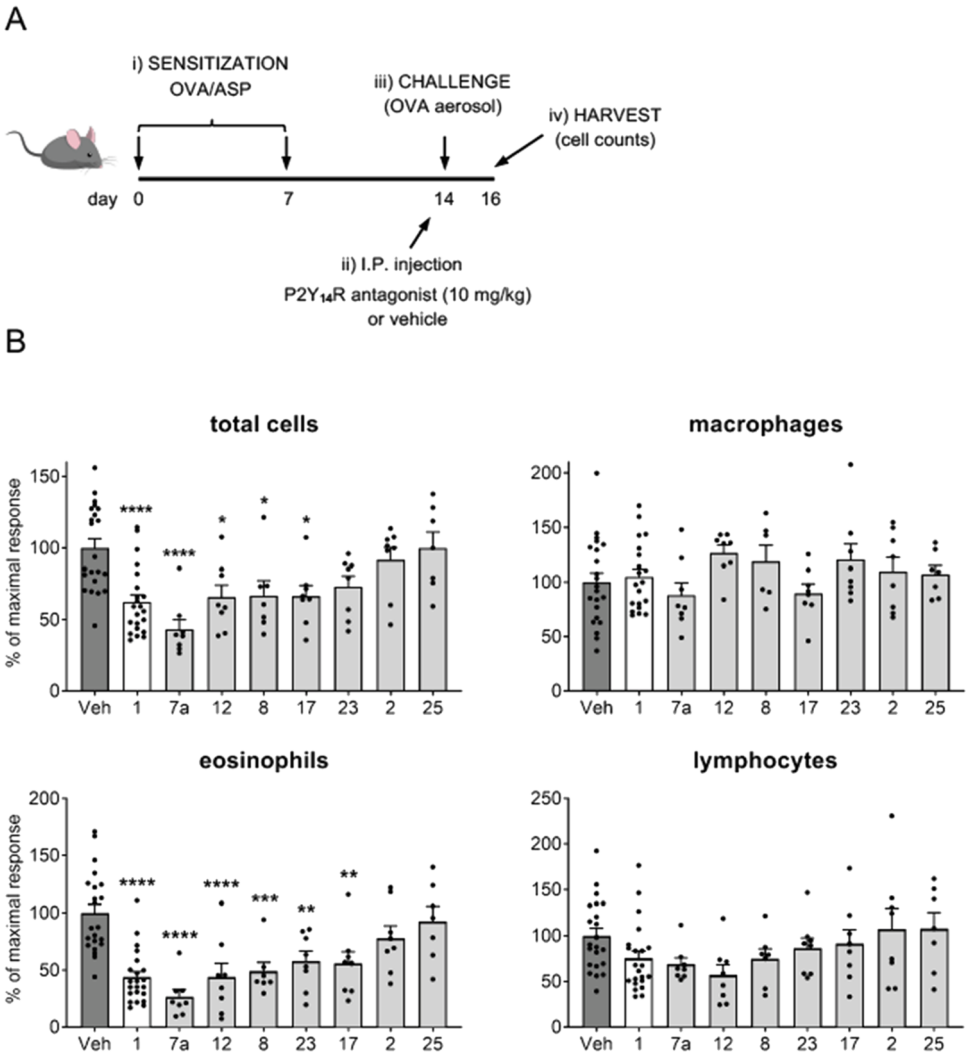

Figure 2. $P2Y_{14}R$ blockade during allergen challenge reduces eosinophilic airway inflammation in the protease model of asthma. (A) Timeline for ASP/OVA sensitization, $P2Y_{14}R$ antagonist treatment, and OVA challenge. (B) Effect on BALF leukocytes of ip injection of the $P2Y_{14}R$ antagonists 2 days post-challenge of ASP/OVA-sensitized mice. *$P < 0.05$, **$P < 0.01$, ***$P < 0.001$, and ****$P < 0.0001$ vs vehicle by one-way ANOVA followed by Dunnett's test.

Lys277$^{7.35}$, but an ideal H-bond with Tyr102$^{3.33}$ was not observed, even if the conformation of the compound was in proximity to allow this kind of interaction. To further test the requirement of the carboxylate, the carboxamide-substituted **15**, analogue of **2**, was docked to $hP2Y_{14}R$, and the pose lacked the predicted important carboxylate interactions with the three amino acid residues (Figure S7B), consistent with the loss of affinity.

Compound **17** occupied the binding pocket spanning from the transmembrane helical domain 2 (TM2), TM3, and TM7 regions, i.e., the carboxylate interface, to trifluoromethyl moiety insertion at TM4 and TM5. The 7-phenyl moiety of the naphthalene ring was stabilized by a charge−π and a $\pi-\pi$ interaction with Arg253$^{6.55}$ and His184$^{5.36}$, respectively, while the 4-phenyl ring made a charge−π interaction with Arg274$^{7.32}$. The protonated phenyl-quinuclidinium form of **17** pointed toward the $P2Y_{14}R$ extracellular region, surrounded by TM4, TM5, extracellular loop 1 (EL1), and EL2. In the previous study,[22] the piperidine of compound **1**, simulated in the more stable chair conformation, made a H-bond with Gly80$^{2.63}$ and deviated to interact with Ile170^{EL2} during MD simulation, while the reverse behavior was observed for compound **2**. The direct or water-mediated interaction mainly involved an axial piperidine N proton. The quinuclidine may be considered as a constrained boat form of the piperidine, and the single hydrogen atom bound to the protonated nitrogen has a geometry different than the piperidine axial hydrogen. In fact, in the predicted docking pose of **17**, the quinuclidine protonated nitrogen did not interact with any residue. Given similar binding affinity of compounds **17** and **1**, we explored if some quinuclidine interactions could be observed by increasing the flexibility level of the model. For this reason, we subjected the complex obtained through docking to MD simulations, and five 50 ns replicates were simulated. In all the replicates, the ligand deviated only slightly from its initial geometry, with an average RMSD over the five replicates of 3.05 Å (Table S4). Except for replicate 2, H-bonds with Lys77$^{2.60}$ and/or Lys277$^{7.35}$ were maintained during much of the simulation time, with the addition of the previously observed H-bond with Tyr102$^{3.33}$ for >50% of the simulation in replicate 4. Eleven residues were in contact (≤4 Å) with the ligand for >50% of the time in all the replicates (Figure S8), suggesting their involvement in binding: Asn90$^{3.21}$, Cys94$^{3.25}$, Ala98$^{3.29}$,

https://dx.doi.org/10.1021/acs.jmedchem.0c00745
J. Med. Chem. XXXX, XXX, XXX−XXX

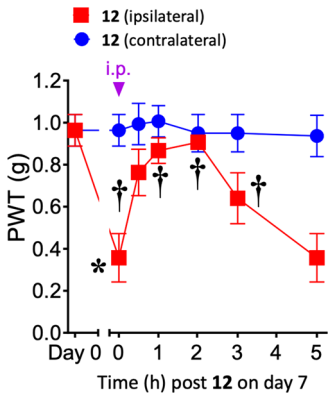

Figure 3. In vivo efficacy of compound **12** in a mouse model of unilateral chronic neuropathic pain (7 days post-chronic constriction injury, CCI, of the sciatic nerve in adult male ICR mice), as described by Mufti et al.[12] The dose was 10 μmol/kg, ip, injected in a volume of 0.2 mL in a vehicle of 30% DMSO in phosphate-buffered saline. Mechano-allodynia in the ipsilateral and contralateral hind paws was measured manually using von Frey filaments. Data (mean ± SD) were analyzed by two-way ANOVA, $^{*}P < 0.05$ versus day 0 and $^{\dagger}P < 0.05$ versus day 7, $n = 3$.

Val99$^{3.30}$, Tyr102$^{3.33}$, Cys172^{EL2}, His184$^{5.36}$, Asn188$^{5.40}$, Phe191$^{5.43}$, Arg253$^{6.55}$, and Lys277$^{7.35}$.

The geometrical rearrangement of the complex enabled ligand interactions with residues of EL1 and EL2 (Figure S8). We focused on the two replicates with an intrareplicate ligand RMSD below the interreplicate average, i.e., replicates 3 and 4 (with an intrareplicate average RMSD values of 2.22 and 2.97 Å, respectively, as reported in Table S4). In both replicates, the H-bond with Lys277$^{7.35}$ was largely maintained, while the Lys77$^{2.60}$ H-bond was more persistent in replicate 3 and the Tyr102$^{3.33}$ H-bond was more persistent during replicate 4 (Table S4 and Figures S9 and S10C). The ligand electrostatic interactions of those residues, in addition to Arg253$^{6.55}$, were intensely negative during the simulations (Figures S9 and S10D). Moreover, additional electrostatic interactions and transient hydrogen bonds were observed between the ligand and residues in EL1 and EL2, according to the replicate. In the case of replicate 3, negative electrostatic interactions were observed between the protonated quinuclidinium form of **17** and residues Gly80$^{2.63}$, Leu84^{EL1}, and Gly85$^{2.63}$ (Figure S9D), with water-mediated H-bonds with Leu84^{EL1} and Gly85$^{2.63}$ appearing (Video S1). In replicate 4, the quinuclidinium moiety showed negative electrostatic interactions with Gly80$^{2.63}$, Gly83$^{2.66}$, Thr168^{EL2}, Gln169^{EL2}, and Ile170^{EL2} (Figure S10D), with the last three residues observed to be in proximity of the ligand during most of replicates 1, 2, and 5 as well as reported in Figure S8. Transient direct H-bonds were observed with Thr168^{EL2}, but for most of the simulation, a water molecule mediated H-bonds between the ligand and Thr168^{EL2}, Gln169^{EL2}, and Leu84^{EL1} (Video S2).

The simulations showed a possible involvement of EL1 and EL2 in stabilizing the ligand-bound state. Electrostatic interactions are a molecular mechanics approximation of either ionic or dipolar interactions; in our simulations, no ionic interaction was observed between the cationic quinuclidinium ion and anionic residues, instead suggesting charge−dipole interactions. However, limitations to our observations of other possible relevant interactions arise from the use of a homology model and from the conformational uncertainty of the sequence variable and highly flexible EL regions. However, potentially interacting proximal residues include the negatively charged E166^{EL2} in EL2. Moreover, the high affinity of *N*-methyl-quaternized **21**, similar to **17**, suggests that the electrostatic interaction within the hP2Y$_{14}$R binding site is more important than H-bonding of the quinuclidine nitrogen atom.

The second aim of this work was the investigation of possible substitution of the naphthalene or phenyl-triazole scaffolds of lead compounds **1** and **2**. We investigated the amide analogues **27** and **29**, indoles (**30** and **31**), and benzimidazole (**32**) obtained by the fusion of the 4-

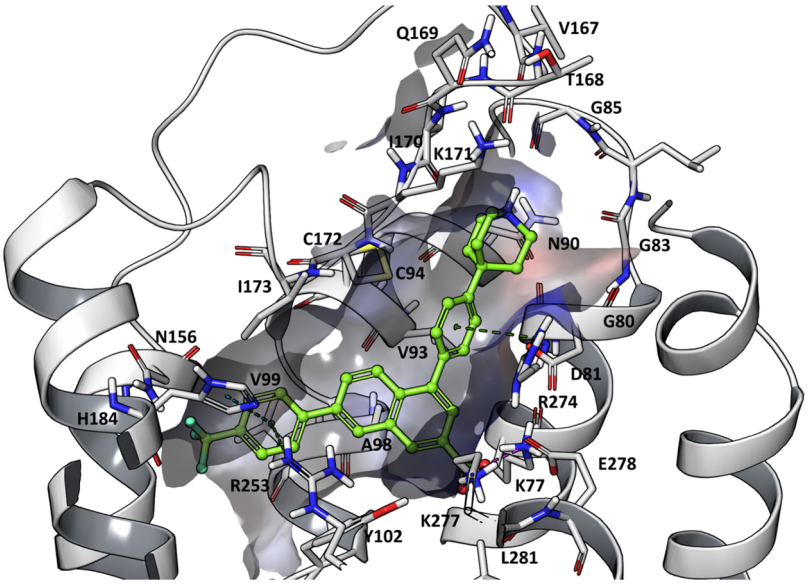

Figure 4. Docking pose of compound **17** at the hP2Y$_{14}$R putative binding site. The P2Y$_{12}$R crystal structure (PDB ID: 4PXZ)[20] was used as a starting point for molecular modeling. The ligand is represented by lime sticks, and the receptor by light gray ribbon. Residues within 3 Å from the ligand, in addition to EL1 and EL2 residues interacting with the ligand during MD simulations, are depicted by gray sticks, and their surface is colored according to the Coulombic potential.

https://dx.doi.org/10.1021/acs.jmedchem.0c00745
J. Med. Chem. XXXX, XXX, XXX−XXX

trifluoromethyl-phenyl and triazole rings of **2**, and the pyrrole analogue of the central trisubstituted phenyl ring of **2** (**33**). Unlike compound **1**, where the trifluoromethyl-carboxylate distance (around 11.5 Å) was conformation independent, in all these compounds, the distance between those two (trifluoromethyl and carboxylate) moieties varied with the ligand conformation. However, the docking poses of these ligands resembled the bound conformations of **1** and **2** (Figure S7C,D). In fact, even with greatly reduced affinities, these ligands were able to occupy the putative binding site (with the exception of **33**, which lacked affinity and showed a slightly modified docking pose and slightly less deep in the binding pocket, as reported in Figure S7E). To test the relevance of compound geometry for the SAR, we designed a benzimidazole analogue **35**, by fusing the central trisubstituted phenyl and triazole moieties of compound **2**. Compound **35** had a conformation-independent fixed trifluoromethyl-carboxylate distance similar to compound **1** (Figure S7F), but an alignment of those moieties to receptor-bound **1** reflected a different geometry of the compound, forcing the phenyl-piperidine to point in a region virtually occupied by EL2. In fact, no docking pose was obtained for this compound, and the experimental lack of affinity of **35** for hP2Y$_{14}$R was consistent with our model's topology.

DISCUSSION

In previous SAR studies of P2Y$_{14}$R antagonists, the affinity of **1** was seldom surpassed.[19,22,23] Attempts to enhance the drug-likeness in this chemical series often resulted in much lower affinity and in at least one case, i.e., **22**, rapid metabolism in vivo.[23] In the SAR progression in our previous three studies,[19,22,23] there was a tendency toward lower affinity at the hP2Y$_{14}$R (IC$_{50}$ value), i.e., in the progression of **1** (6.0 nM) to **2** (31.7 nM) to **23** (169 nM).Therefore, we re-examined the entire scaffold of both **1** and **2** to identify alternative scaffold variations with greater flexibility of substitution and retention of receptor affinity.

In an effort to improve the assay method, we synthesized tritiated **1** and found that it was not only of limited solubility but also tended to adsorb to plastic surfaces and was therefore not suitable as a radiolabeled tracer for drug screening. Thus, we applied the fluorescent tracer **36** using our previous method to determine the binding affinity of the newly synthesized analogues at both the hP2Y$_{14}$R (expressed in CHO cells) and mP2Y$_{14}$R (expressed in HEK293 cells). Fluorescence micrographs show the presence of specific mP2Y$_{14}$R binding in the HEK293 cells,[12] which were used to demonstrate that the species differences in antagonist affinity were relatively minor, compared to species differences in other GPCRs, such as the A$_3$ adenosine receptor.[13] Furthermore, we compared data obtained for three compounds in the fluorescence (whole cell binding) assay with our previously published forskolin-stimulated cAMP inhibition (Table S1, Supporting Information). The cAMP assay values were lower by 18 ± 6-fold, indicating that the fluorescence binding consistently underestimates the intrinsic affinity of these antagonists.

We have previously implicated the naphthalene moiety as a source of the unfavorable physicochemical properties of the potent, amphiphilic antagonist **1**.[8] Nevertheless, naphthalene is a component of many useful drug substances.[21] Therefore, we now focus on modification of other scaffold regions, particularly the piperidine ring as a means of enhancing the drug-like properties of this antagonist series. We found that steric constraint of this piperidine ring is especially suitable for retaining high P2Y$_{14}$R affinity. Specifically, bicyclic substitution of the piperidine ring to decrease the conformational flexibility led to the most successful analogues, i.e., quinuclidine analogue **17**, which was only 3-fold less potent than **1** with an IC$_{50}$ value of 20 nM. Similarly, **18** was 3-fold less potent than its piperidine equivalent **2**. Also, a single alkene group in **3** preserved affinity, and substitution with a piperazine in **4** only moderately reduced affinity. The previously reported amino derivative **23**, which had a more favorable cLogP (0.84 compared to 4.64 for **2**), was active in vivo in reducing the eosinophil content in the BALF.

Previously, rotating a bridging 1,2,3-triazole ring by one position (equivalent to its inversion) in other GPCR pharmacophores was shown to preserve biological activity, e.g., in adenosine receptor agonists.[39] Furthermore, amides and 1,2,3-triazole groups have been identified as bioisosteres, and amides may have better water-solubilizing properties than the triazoles.[58] The "reversed" triazole derivative **25** maintained moderate affinity and in vivo activity. However, extension of the piperidine nitrogen in the form of a water-solubilizing PEG group in **12** resulted in inactivity. The most effective antagonist in lowering the eosinophil content in the BALF was the hexynyl derivative **7a**.

Modification of the central phenyl ring and its carboxylate group, e.g., nitrile **16**, pyrrole **33**, and C-methyl derivative **34**, or fusion of two aryl groups, e.g., benzimidazoles **32** and **35**, in general, dramatically reduced the affinity. This indicated that the "upper" part of the scaffold is conformationally constrained in its deeper P2Y$_{14}$R binding pocket. Also, planarity of this part of the scaffold seems to be required as an attempt to introduce three-dimensionality in cubane derivative **28** failed. Thus, the overall placement and orientation of this ligand series in the orthosteric P2Y$_{14}$R binding site are consistent with the piperidine moiety of **1** and **2** facing the extracellular medium. This region is less sterically constrained than the deeper binding pocket that is mainly hydrophobic, except for its small hydrophilic region for electrostatic interaction of the essential carboxylate. Replacement of this carboxylate group of **2** with a polar and H bonding but uncharged carboxamide group of **15** eliminated its binding ability.

Bicyclic substitution of the piperidine ring, e.g., quinuclidine **17** (IC$_{50}$ = 20 nM) in the naphthalene series and **18** (IC$_{50}$ ≈ 100 nM) in the triazole series, preserved P2Y$_{14}$R affinity. Molecular modeling of the interaction of quinuclidine derivative **17** with the hP2Y$_{14}$R showed a binding mode similar to the parent compound **1**. MD simulations showed the conservation of electrostatic interactions with Lys77$^{2.60}$, Lys277$^{7.35}$, and Tyr102$^{3.33}$ and additional interactions with residues of EL1 and EL2. *N*-Methyl quinuclidinium analogue **21** showed nearly as high affinity as the parent quinuclidine **17**, suggesting that a positively charged, non-H-bonding N atom is as suitable for high hP2Y$_{14}$R affinity as a neutral, H-bonding N atom in **8**. Thus, multiple modes of interaction between the piperidine/quinuclidine ring at the receptor are possible.

CONCLUSIONS

P2Y$_{14}$R antagonism is one of the potential therapeutic strategies for pain and renal and pulmonary conditions. Exploration of alternative scaffolds for P2Y$_{14}$R antagonists containing a biaryl core has yielded high affinity derivatives in which the piperidine moiety is constrained. Other modifications, such as reversal of a triazole moiety maintained only

https://dx.doi.org/10.1021/acs.jmedchem.0c00745
J. Med. Chem. XXXX, XXX, XXX−XXX

moderate affinity. Thus, other regions of the antagonist scaffold are highly sensitive to structural changes. Quinuclidine **17** showed high affinity receptor binding by flow cytometric analysis at hP2Y$_{14}$R (IC_{50} = 20 nM) and mP2Y$_{14}$R (IC_{50} = 21 nM) and in vivo efficacy. Modest improvement in aqueous solubility was achieved for several analogues, including a PEG conjugate **12** with 20-fold higher solubility than potent antagonist **1**. Moreover, in vivo efficacy in models of asthma and chronic neuropathic pain was demonstrated. Future studies potentially will be able to identify leads for clinically useful drug candidates for kidney inflammation, chronic neuropathic pain, pulmonary diseases, and other conditions.

EXPERIMENTAL SECTION

Reagents and Instrumentation. All reagents and solvents were purchased from Sigma-Aldrich (St. Louis, MO) or Ark Pharm, Inc. (Libertyville, IL; compound **83**).[1] ^{1}H NMR spectra were obtained using a Bruker 400 spectrometer with $CDCl_3$, CD_3OD, and DMSO-d_6 as solvents. Chemical shifts are expressed in δ values (ppm) with tetramethylsilane (δ 0.00) for $CDCl_3$ and water (δ 3.30) for CD_3OD. NMR spectra were collected using a Bruker AV spectrometer equipped with a z-gradient [^{1}H, ^{13}C, ^{15}N]-cryoprobe. TLC analysis was carried out on glass sheets precoated with silica gel F_{254} (0.2 mm) from Sigma-Aldrich. The purity of final compounds was checked using a Hewlett−Packard 1100 HPLC equipped with a Zorbax SB-Aq 5 μm analytical column (50 × 4.6 mm, Agilent Technologies Inc., Palo Alto, CA). Mobile phase: linear gradient solvent system, 5 mM tetrabutylammonium dihydrogen phosphate−CH_3CN from 100:0 to 0:100 in 15 min; the flow rate was 0.5 mL/min. Peaks were detected by UV absorption with a diode array detector at 210, 254, and 280 nm. All derivatives tested for biological activity showed >95% purity by HPLC analysis (detection at 254 nm). Low-resolution mass spectrometry was performed using a JEOL SX102 spectrometer with 6 kV Xe atoms following desorption from a glycerol matrix or on an Agilent LC/MS 1100 MSD, with a Waters (Milford, MA) Atlantis C18 column. High-resolution mass spectroscopy (HRMS) measurements were performed on a proteomics optimized Q-TOF-2 (MicromassWaters) using external calibration with polyalanine, unless noted. Observed mass accuracies are those expected based on known instrument performance as well as trends in masses of standard compounds observed at intervals during the series of measurements. Reported masses are observed masses uncorrected for this time-dependent drift in mass accuracy. The total polar surface area (tPSA) was calculated using ChemDraw Professional (PerkinElmer, Boston, MA, v. 16.0). cLogP was calculated as reported.[36] Simulated pharmacokinetic parameters were calculated as reported.[3]

General Procedure: Deprotection Reaction. *Method A.* A mixture of compound containing an ester (1 equiv) and potassium hydroxide (5 equiv) in methanol/water (2:1) was stirred at 50 °C. This mixture was neutralized with 1 N HCl until pH was 5−6. The slightly acidic mixture was evaporated under reduced pressure and purified by silica gel column chromatography (dichloromethane/methanol/acetic acid = 95:5:0.1) or semipreparative HPLC (10 mM triethylammonium acetate buffer/acetonitrile = 80:20 to 20:80 in 40 min) to afford the compound as a white solid.

Method B. A solution of compound in trifluoroacetic acid/tetrahydrofuran (1:1 or 2:1) was stirred at room temperature. The solvent was evaporated with toluene under reduced pressure. The residue was purified by silica gel column chromatography (dichloromethane/methanol = 95:5) or semipreparative HPLC (10 mM triethylammonium acetate buffer/acetonitrile = 80:20 to 20:80 in 40 min) to afford the compound as a white solid.

*4-(4-(1,2,3,6-Tetrahydropyridin-4-yl)phenyl)-7-(4-(trifluoromethyl)phenyl)-2-naphthoic Acid (**3**).* Method A: yield, 88%; HPLC purity, 95% (R_t = 14.76 min); ^{1}H NMR (400 MHz, CD_3OD): δ 8.58 (s, 1H), 8.36 (s, 1H), 8.06−7.98 (m, 4H), 7.86−7.78 (m, 3H), 7.63 (d, J = 8.00 Hz, 2H), 7.55 (d, J = 8.00 Hz, 2H), 6.31 (broad s, 1H), 3.66 (broad s, 2H), 3.25 (broad s, 2H), 2.71 (broad s, 2H); MS (ESI, m/z): 474.2 [M + 1]$^+$; ESI-HRMS calcd m/z for $C_{29}H_{23}NO_2F_3$, 474.1681; found, 474.1683 [M + 1]$^+$.

*4′-(Piperazin-1-yl)-5-(4-(4-(trifluoromethyl)phenyl)-1H-1,2,3-triazol-1-yl)-[1,1′-biphenyl]-3-carboxylic Acid (**4**).* Method A: yield, 59%; HPLC purity, 95% (R_t = 6.41 min); ^{1}H NMR (400 MHz, CD_3OD): δ 9.17 (s, 1H), 8.45 (s, 1H), 8.37 (s, 1H), 8.23 (s, 1H), 8.16 (m, 2H), 7.81−7.75 (m, 4H), 7.20−7.14 (m, 2H), 3.51 (broad s, 4H), 3.40 (broad s, 4H); MS (ESI, m/z): 494.1 [M + 1]$^+$; ESI-HRMS calcd m/z for $C_{26}H_{23}N_5O_2F_3$, 494.1804; found, 494.1807 [M + 1]$^+$.

*4-(4-(1-Methylpiperidin-4-yl)phenyl)-7-(4-(trifluoromethyl)-phenyl)-2-naphthoic Acid (**5**).* Method A: yield, 65%; HPLC purity, 95% (R_t = 12.49 min); ^{1}H NMR (400 MHz, DMSO-d_6): δ 8.59 (s, 1H), 8.52 (s, 1H), 8.06 (d, J = 8.28 Hz, 2H), 7.96−7.86 (m, 5H), 7.46 (d, J = 8.48 Hz, 2H), 7.43 (d, J = 8.52 Hz, 2H), 2.93 (d, J = 11.56 Hz, 2H), 2.23 (s, 3H), 2.06−2.00 (m, 2H), 1.91−1.77 (m, 4H); MS (ESI, m/z): 490.2 [M + 1]$^+$; ESI-HRMS calcd m/z for $C_{30}H_{27}NO_2F_3$, 490.1994; found, 490.1988 [M + 1]$^+$.

*4-(4-(1-(Prop-2-yn-1-yl)piperidin-4-yl)phenyl)-7-(4-(trifluoromethyl)phenyl)-2-naphthoic Acid (**6a**).* Method A: yield, 52%; HPLC purity, 99% (R_t = 13.64 min); ^{1}H NMR (400 MHz, CD_3OD): δ 8.72 (s, 1H), 8.41 (s, 1H), 8.06−7.98 (m, 4H), 7.91−7.89 (m, 1H), 7.80 (d, J = 8.08 Hz, 2H), 7.50−7.45 (m, 4H), 3.74 (broad s, 2H), 3.45−3.42 (m, 2H), 3.05 (m, 1H), 2.88−2.80 (m, 3H), 2.15−1.94 (m, 4H); MS (ESI, m/z): 514.2 [M + 1]$^+$; ESI-HRMS calcd m/z for $C_{32}H_{27}NO_2F_3$, 514.1994; found, 514.2001 [M + 1]$^+$.

*4-(4-(1-Propylpiperidin-4-yl)phenyl)-7-(4-(trifluoromethyl)-phenyl)-2-naphthoic Acid (**6b**).* Method A: yield, 56%; ^{1}H NMR (400 MHz, CD_3OD): δ 8.63 (s, 1H), 8.35 (s, 1H), 8.05 (s, 1H), 7.98−7.94 (m, 3H), 7.81−7.78 (m, 3H), 7.46 (d, J = 7.64 Hz, 2H), 7.41 (d, J = 7.84 Hz 2H), 3.65 (d, J = 11.80 Hz, 2H), 3.19−3.09 (m, 4H), 2.19−2.03 (m, 3H), 1.97 (s, 2H), 1.88−1.82 (m, 2H), 1.08 (t, J = 7.32 Hz, 3H); MS (ESI, m/z): 518.2 [M + 1]$^+$; ESI-HRMS calcd m/z for $C_{32}H_{31}NO_2F_3$, 518.2307; found, 518.2301 [M + 1]$^+$.

*4-(4-(1-(Hex-5-yn-1-yl)piperidin-4-yl)phenyl)-7-(4-(trifluoromethyl)phenyl)-2-naphthoic Acid (**7a**).* Method A: yield, 48%; HPLC purity, 100% (R_t = 13.71 min); ^{1}H NMR (400 MHz, CD_3OD): δ 8.74 (s, 1H), 8.41 (d, J = 1.76 Hz, 1H), 8.04−7.95 (m, 4H), 7.91 (dd, J = 1.88, 8.91 Hz, 1H), 7.80 (d, J = 8.28 Hz, 2H), 7.50 (q, J = 8.28 Hz, 4H), 3.76 (d, J = 12.05 Hz, 2H), 3.26−3.14 (m, 4H), 3.10−3.00 (m, 1H), 2.38−2.30 (m, 3H), 2.26 (d, J = 14.05 Hz, 2H), 2.17−2.06 (m, 2H), 2.01−1.90 (m, 2H), 1.65 (quin, J = 7.15 Hz, 2H); negative ion ESI-MS m/z (rel intensity): 554 [M − H$^+$, 100]; ESI-HRMS [M − H$^+$] calcd m/z for $C_{35}H_{31}F_3NO_2$, 554.2307; found, 554.2288.

*4-(4-(1-Hexylpiperidin-4-yl)phenyl)-7-(4-(trifluoromethyl)-phenyl)-2-naphthoic Acid (**7b**).* To a solution of compound **7a** (4 mg, 0.007 mmol) in methanol (0.5 mL) and ethyl acetate (0.5 mL) was added the Rh/C catalyst. The resulting reaction mixture was stirred at room temperature in a hydrogen atmosphere (100 psi) for 14 h. The mixture was filtered through a cake of Celite, and the filtrate was evaporated under reduced pressure. The residue was purified by semipreparative HPLC (10 mM triethylammonium acetate buffer/acetonitrile = 80:20 to 20:80 in 40 min) to afford the compound **9** (3.7 mg, 92%) as a white solid; HPLC purity, 95% (R_t = 13.98 min); ^{1}H NMR (400 MHz, CD_3OD): δ 8.58 (s, 1H), 8.36 (s, 1H), 8.02 (s, 1H), 7.98−7.92 (m, 3H), 7.81−7.77 (m, 3H), 7.46 (d, J = 8.20 Hz, 2H), 7.40 (d, J = 8.16 Hz, 2H), 3.60 (d, J = 11.56 Hz, 2H), 3.04−2.89 (m, 4H), 2.15−2.01 (m, 3H), 1.77−1.74 (m, 1H), 1.45−1.34 (m, 8H), 0.95 (t, J = 6.80 Hz, 3H), 0.91−0.87 (m, 1H); MS (ESI, m/z): 560.3 [M + 1]$^+$; ESI-HRMS calcd m/z for $C_{35}H_{37}NO_2F_3$, 560.2776; found, 560.2782 [M + 1]$^+$.

*4-(4-(1-(Acetyl)piperidin-4-yl)phenyl)-7-(4-(trifluoromethyl)-phenyl)-2-naphthoic Acid (**8**) and 4-(4-(1-(Propionyl)piperidin-4-yl)phenyl)-7-(4-(trifluoromethyl)phenyl)-2-naphthoic Acid (**9**).* Synthetic procedures followed, and confirmation of structural identity and purity were recently reported.[12]

*4-(4-(1-(tert-Butoxycarbonyl)piperidin-4-yl)phenyl)-7-(4-(trifluoromethyl)phenyl)-2-naphthoic Acid (**10**).* Method A: yield, 71%; HPLC purity, 95% (R_t = 16.26 min); ^{1}H NMR (400 MHz, CD_3OD): δ 8.74 (s, 1H), 8.43 (s, 1H), 8.05−7.99 (m, 4H), 7.93 (d, J

https://dx.doi.org/10.1021/acs.jmedchem.0c00745
J. Med. Chem. XXXX, XXX, XXX−XXX

= 8.72 Hz, 1H), 7.82 (d, *J* = 8.20 Hz, 2H), 7.48 (d, *J* = 8.08 Hz, 2H), 7.44 (d, *J* = 8.12 Hz, 2H), 4.28 (d, *J* = 12.6 Hz, 2H), 2.95−2.85 (m, 3H), 1.96 (d, *J* = 12.40 Hz, 2H), 1.77−1.685 (m, 2H), 1.52 (s, 9H); MS (ESI, *m/z*): 520.1 [M + 1-*tert*-butyl]$^+$, 476.2 [M + 1-Boc]$^+$.

*4-(4-(1-(2,5,8,11,14,17-Hexaoxaicosan-20-oyl)piperidin-4-yl)-phenyl)-7-(4-(trifluoromethyl)phenyl)-2-naphthoic Acid (**11**).* Method A: yield, 65%; HPLC purity, 97% (R_t = 14.01 min); ^{1}H NMR (400 MHz, CD_3OD): δ 8.71 (s, 1H), 8.41 (s, 1H), 8.04−7.99 (m, 4H), 7.90 (d, *J* = 8.92 Hz, 1H), 7.81 (d, *J* = 8.20 Hz, 2H), 7.48 (d, *J* = 8.16 Hz, 2H), 7.44 (d, *J* = 8.20 Hz, 2H), 4.77 (d, *J* = 13.22 Hz, 1H), 4.23 (d, *J* = 13.6 Hz, 1H), 3.87−3.77 (m, 2H), 3.66−3.59 (m, 21H), 3.53−3.50 (m, 2H), 3.29−3.26 (m, 1H), 3.01−2.95 (m, 1H), 2.88−2.77 (m, 2H), 2.72−2.65 (m, 1H), 2.02 (t, *J* = 11.88 Hz, 2H), 1.87−1.67 (m, 2H); MS (ESI, *m/z*): 782.4 [M + 1]$^+$, 799.4 [M + NH_4^+]$^+$; ESI-HRMS calcd *m/z* for $C_{43}H_{51}NO_9F_3$, 782.3516; found, 782.33530 [M + 1]$^+$.

*4-(4-(1-(1-Amino-3,6,9,12,15,18-hexaoxahenicosan-21-oyl)-piperidin-4-yl)phenyl)-7-(4-(trifluoromethyl)phenyl)-2-naphthoic Acid (**12**).* Method B: yield, 91%; ^{1}H NMR (400 MHz, CD_3OD): δ 8.74 (s, 1H), 8.42 (s, 1H), 8.04−7.98 (m, 4H), 7.91 (d, *J* = 8.84 Hz, 1H), 7.81 (d, *J* = 8.20 Hz, 2H), 7.48 (d, *J* = 8.24 Hz, 2H), 7.45 (d, *J* = 8.32 Hz, 2H), 4.79 (d, *J* = 12.6 Hz, 1H), 4.19 (d, *J* = 13.4 Hz, 1H), 3.83 (t, *J* = 6.06 Hz, 2H), 3.79 (t, *J* = 8.08 Hz, 2H), 3.73−3.67 (m, 21H), 3.16 (t, *J* = 4.86 Hz, 2H), 3.02−2.96 (m, 1H), 2.88−2.71 (m, 3H), 2.07−2.01 (m, 2H), 1.86−1.67 (m, 2H); MS (ESI, *m/z*): 811.4 [M + 1]$^+$; ESI-HRMS calcd *m/z* for $C_{44}H_{54}N_2O_9F_3$, 811.3781; found, 811.3793 [M + 1]$^+$.

*4-(4-(1-(2-Oxo-6,9,12,15,18,21-hexaoxa-3-azatetracosan-24-oyl)piperidin-4-yl)phenyl)-7-(4-(trifluoromethyl)phenyl)-2-naphthoic Acid (**13**).* To a solution of compound **12** (6.3 mg, 7.77 μmol) in pyridine (0.5 mL) was added acetic anhydride (8 μL, 84 μmol), and then this reaction mixture was stirred at room temperature for 1 h. After all volatiles were evaporated under reduced pressure, the residue was purified by silica gel column chromatography (dichloromethane/methanol = 20:1) to afford compound **13** (3.7 mg, 59%) as a white solid; HPLC purity, 99% (R_t = 13.38 min); ^{1}H NMR (400 MHz, CD_3OD): δ 8.73 (s, 1H), 8.37 (s, 1H), 7.98−7.80 (m, 7H), 7.43 (s, 4H), 4.77 (d, *J* = 9.04 Hz, 1H), 4.22 (d, *J* = 11.04 Hz, 1H), 3.82 (d, *J* = 5.24 Hz, 2H), 3.66−3.60 (m, 20H), 3.52−3.50 (m, 2H), 3.29−3.25 (m, 1H), 2.96−2.70 (m, 4H), 2.00 (m, 2H), 1.94 (s, 3H), 1.83−1.68 (m, 2H); MS (ESI, *m/z*): 853.4 [M + 1]$^+$, 870.5 [M + NH_4^+]$^+$; ESI-HRMS calcd *m/z* for $C_{46}H_{56}N_2O_{10}F_3$, 853.3887; found, 853.3893 [M + 1]$^+$.

*4-(4-(1-(2,2-Dimethyl-4-oxo-3,8,11,14,17,20,23-heptaoxa-5-azahexacosan-26-oyl)piperidin-4-yl)phenyl)-7-(4-(trifluoromethyl)-phenyl)-2-naphthoic Acid (**14**).* Method A: yield, 79%; HPLC purity, 97% (R_t = 14.17 min); ^{1}H NMR (400 MHz, CD_3OD): δ 8.71 (s, 1H), 8.40 (s, 1H), 8.02−7.98 (m, 4H), 7.88 (d, *J* = 8.92 Hz, 1H), 7.80 (d, *J* = 8.20 Hz, 2H), 7.46 (d, *J* = 8.20 Hz, 2H), 7.43 (d, *J* = 8.16 Hz, 2H), 4.76 (d, *J* = 12.6 Hz, 1H), 4.22 (d, *J* = 12.7 Hz, 1H), 3.86−3.77 (m, 2H), 3.66−3.57 (m, 20H), 3.49 (t, *J* = 9.52 Hz, 2H), 3.27−3.25 (m, 1H), 3.21 (t, *J* = 5.52 Hz, 2H), 2.99−2.93 (m, 1H), 2.87−2.76 (m, 2H), 2.71−2.65 (m, 1H), 2.01 (t, *J* = 11.82 Hz, 2H), 1.86−1.80 (m, 1H), 1.75−1.68 (m, 1H), 1.43 (s, 9H); MS (ESI, *m/z*): 811.4 [M + 1-Boc]$^+$, 911.4 [M + 1]$^+$, 928.4 [M + NH_4^+]$^+$; ESI-HRMS calcd *m/z* for $C_{49}H_{62}N_2O_{11}F_3$, 911.4306; found, 911.4300 [M + 1]$^+$.

*4-(4-(Quinuclidin-4-yl)phenyl)-7-(4-(trifluoromethyl)phenyl)-2-naphthoic Acid (**17**).* Method A: yield, 53%; HPLC purity, 98% (R_t = 10.13 min); melting point, 203−205 °C; ^{1}H NMR (400 MHz, CD_3OD): δ 8.76 (s, 1H), 8.43 (s, 1H), 8.01−7.92 (m, 5H), 7.82−7.80 (m, 2H), 7.65−7.54 (m, 4H), 3.58−3.54 (m, 6H), 2.37−2.33 (m, 6H); MS (ESI, *m/z*): 502.2 [M + 1]$^+$; ^{13}C NMR (100 MHz, DMSO-d_6): δ 167.2, 145.2, 143.2, 139.2, 137.3, 136.5, 133.1, 132.2, 130.5, 129.7, 128.7, 128.0, 127.7, 127.4, 126.7, 126.4, 126.1, 125.8, 125.6, 124.7, 45.9, 31.3, 28.4; ESI-HRMS calcd *m/z* for $C_{31}H_{27}NO_2F_3$, 502.1994; found, 502.1993 [M + 1]$^+$.

*4′-(Quinuclidin-4-yl)-5-(4-(4-(trifluoromethyl)phenyl)-1H-1,2,3-triazol-1-yl)-[1,1′-biphenyl]-3-carboxylic Acid (**18**).* Method A: yield, 66%; HPLC purity, 99% (R_t = 8.70 min); melting point, 308−310 °C; ^{1}H NMR (400 MHz, CD_3OD): δ 9.24 (s, 1H), 8.51 (broad s, 1H), 8.39 (broad s, 1H), 8.37 (broad s, 1H), 8.17 (d, *J* = 8.00 Hz, 2H), 7.83−7.75 (m, 4H), 7.58 (d, *J* = 8.00 Hz, 2H), 3.58−3.49 (m, 6H), 2.31−2.24 (m, 6H); MS (ESI, *m/z*): 519.2 [M + 1]$^+$; ^{13}C NMR (100 MHz, DMSO-d_6): δ 166.2, 146.7, 146.1, 146.0, 141.7, 137.2, 136.2, 134.0, 129.3, 128.2, 127.1, 126.1, 125.9, 125.8, 125.5, 124.2, 121.5, 121.2, 45.7, 31.3, 28.3; ESI-HRMS calcd *m/z* for $C_{29}H_{26}N_4O_2F_3$, 519.2008; found, 519.2013 [M + 1]$^+$.

*4′-(3-Azabicyclo[4.1.0]heptan-6-yl)-5-(4-(4-(trifluoromethyl)-phenyl)-1H-1,2,3-triazol-1-yl)-[1,1′-biphenyl]-3-carboxylic Acid (**19**).* Method B: yield, 79%; HPLC purity, 99% (R_t = 24.09 min); ^{1}H NMR (400 MHz, CD_3OD): δ 9.09 (s, 1H), 8.45 (s, 1H), 8.34 (s, 1H), 8.17 (s, 1H), 8.13−8.04 (m, 2H), 7.75−7.63 (m, 4H), 7.50−7.40 (m, 2H), 3.83−3.77 (m, 1H), 3.30−3.22 (m, 2H), 2.94−2.87 (m, 1H), 2.35 (broad s, 2H), 1.60−1.56 (m, 1H), 1.31−1.23 (m, 1H), 1.12−1.10 (m, 1H); MS (ESI, *m/z*): 505.2 [M + 1]$^+$; ESI-HRMS calcd *m/z* for $C_{28}H_{24}N_4O_2F_3$, 505.1851; found, 505.1848 [M + 1]$^+$.

*4′-(7,7-Difluoro-3-azabicyclo[4.1.0]heptan-6-yl)-5-(4-(4-(trifluoromethyl)phenyl)-1H-1,2,3-triazol-1-yl)-[1,1′-biphenyl]-3-carboxylic Acid (**20**).* Method B: yield, 35%; HPLC purity, 99% (R_t = 11.78 min); ^{1}H NMR (400 MHz, CD_3OD): δ 9.19 (s, 1H), 8.50 (s, 1H), 8.38−8.30 (m, 2H), 8.17−8.11 (m, 2H), 7.83−7.72 (m, 4H), 7.59−7.54 (m, 2H), 3.98−3.86 (m, 1H), 3.73 (broad s, 1H), 3.43−3.37 (m, 1H), 3.04−2.96 (m, 1H), 2.66−2.46 (m, 2H), 2.33−2.22 (m, 1H); MS (ESI, *m/z*): 541.2 [M + 1]$^+$; ESI-HRMS calcd *m/z* for $C_{28}H_{22}N_4O_2F_5$, 541.1663; found, 541.1668 [M + 1]$^+$.

*4-(4-(1-Methylquinuclidin-1-ium-4-yl)phenyl)-7-(4-(trifluoromethyl)phenyl)-2-naphthoate (**21**).* Method A: yield, 71%; HPLC purity, 97% (R_t = 9.57 min); ^{1}H NMR (400 MHz, CD_3OD): δ 8.58 (s, 1H), 8.36 (s, 1H), 8.02−7.93 (m, 4H), 7.79−7.77 (m, 3H), 7.54−7.52 (m, 3H), 3.69−3.65 (m, 6H), 3.09 (s, 3H), 2.40−2.37 (m, 6H); MS (ESI, *m/z*): 516.2 [M + 1]$^+$; ESI-HRMS calcd *m/z* for $C_{32}H_{29}NO_2F_3$, 516.2150; found, 516.2159 [M + 1]$^+$.

*4′-Carbamoyl-5-(1-(4-(trifluoromethyl)phenyl)-1H-1,2,3-triazol-4-yl)-[1,1′-biphenyl]-3-carboxylic Acid (**24**).* Method A: yield, 88%; HPLC purity, 99% (R_t = 11.77 min); ^{1}H NMR (400 MHz, CD_3OD): δ 9.28 (s, 1H), 8.64 (s, 1H), 8.51 (s, 1H), 8.35 (s, 1H), 8.21 (d, *J* = 8.40 Hz, 2H), 8.04 (d, *J* = 8.28 Hz, 2H), 7.96 (d, *J* = 8.52 Hz, 2H), 7.88 (d, *J* = 8.24 Hz, 2H); MS (ESI, *m/z*): 453.1 [M + 1]$^+$; ESI-HRMS calcd *m/z* for $C_{23}H_{16}N_4O_3F_3$, 453.1175; found, 453.1169 [M + 1]$^+$.

*4′-(Piperidin-4-yl)-5-(1-(4-(trifluoromethyl)phenyl)-1H-1,2,3-triazol-4-yl)-[1,1′-biphenyl]-3-carboxylic Acid (**25**).* Synthetic procedures followed, and confirmation of structural identity and purity were recently reported.[12]

*3-(5-((3-Aminopropyl)carbamoyl)thiophen-2-yl)-5-(1-(4-(trifluoromethyl)phenyl)-1H-1,2,3-triazol-4-yl)benzoic Acid (**26**).* Method B: yield, 45%; HPLC purity, 98% (R_t = 10.23 min); ^{1}H NMR (400 MHz, DMSO-d_6): δ 9.75 (s, 1H), 8.82 (broad s, 1H; NH), 8.53 (s, 1H), 8.46 (s, 1H), 8.25 (d, *J* = 8.44 Hz, 2H), 8.23 (s, 1H), 8.06 (d, *J* = 8.52 Hz, 2H), 7.89 (s, 1H), 7.75 (d, *J* = 3.36 Hz, 1H), 3.35 (merged with water peak), 2.90 (t, *J* = 7.24 Hz, 2H), 1.84 (t, *J* = 7.02 Hz, 2H); MS (ESI, *m/z*): 516.1 [M + 1]$^+$; ESI-HRMS calcd *m/z* for $C_{24}H_{21}N_5O_3F_3{}^{32}S$, 516.1317; found, 516.1316 [M + 1]$^+$.

*4′-Carbamoyl-5-(4-(trifluoromethyl)benzamido)-[1,1′-biphenyl]-3-carboxylic Acid (**27**).* Method A: yield, 70%; HPLC purity, 96% (R_t = 11.11 min); ^{1}H NMR (400 MHz, CD_3OD): δ 8.42 (s, 1H), 8.37 (s, 1H), 8.17 (d, *J* = 7.96 Hz, 2H), 8.14 (s, 1H), 8.02 (d, *J* = 7.76 Hz, 2H), 7.86 (d, *J* = 7.96 Hz, 2H), 7.81 (d, *J* = 7.80 Hz, 2H); MS (ESI, *m/z*): 429.1 [M + 1]$^+$; ESI-HRMS calcd *m/z* for $C_{22}H_{16}N_2O_4F_3$, 429.1062; found, 429.1069 [M + 1]$^+$.

*5-(4-(Hydroxymethyl)cubane-1-carboxamido)-4′-(piperidin-4-yl)-[1,1′-biphenyl]-3-carboxylic Acid (**28**).* Method A: yield, 39%; HPLC purity, 96% (R_t = 7.39 min); ^{1}H NMR (400 MHz, DMSO-d_6): δ 9.69 (s, 1H), 8.13 (s, 2H), 7.90 (s, 1H), 7.57 (d, *J* = 7.88 Hz, 2H), 7.35 (d, *J* = 7.96 Hz, 2H), 4.15 (t, *J* = 4.68 Hz, 3H), 3.80 (t, *J* = 4.50 Hz, 3H), 3.55 (s, 2H), 3.20 (d, *J* = 11.76 Hz, 2H), 2.79−2.75 (m, 2H), 1.80−1.76 (m, 3H); MS (ESI, *m/z*): 457.2 [M + 1]$^+$; ESI-HRMS calcd *m/z* for $C_{28}H_{29}N_2O_4$, 457.2127; found, 457.2129 [M + 1]$^+$.

https://dx.doi.org/10.1021/acs.jmedchem.0c00745
J. Med. Chem. XXXX, XXX, XXX−XXX

*4′-Carbamoyl-5-((4-(trifluoromethyl)phenyl)carbamoyl)-[1,1′-biphenyl]-3-carboxylic Acid (**29**).* Method A: yield, 72%; HPLC purity, 99% (R_t = 11.30 min); ^{1}H NMR (400 MHz, CD_3OD): δ 8.61 (s, 1H), 8.53 (s, 1H), 8.44 (s, 1H), 8.03 (d, J = 8.12 Hz, 2H), 7.99 (d, J = 8.48 Hz, 2H), 7.87 (d, J = 8.12 Hz, 2H), 7.68 (d, J = 8.48 Hz, 2H); MS (ESI, m/z): 429.1 $[M + 1]^+$; ESI-HRMS calcd m/z for $C_{22}H_{16}N_2O_4F_3$, 429.1062; found, 429.1065 $[M + 1]^+$.

*4′-Carbamoyl-5-(5-(trifluoromethyl)-1H-indol-2-yl)-[1,1′-biphenyl]-3-carboxylic Acid (**30**).* The suspension of compound **73a** (8 mg, 18.2 μmol) and potassium hydroxide (5.2 mg, 91.2 μmol) in methanol (1 mL) and water (0.5 mL) was stirred at 70 °C for 3 h. The reaction mixture was acidified with acetic acid, and the solvent was evaporated under reduced pressure. The residue was purified by silica gel column chromatography (dichloromethane/methanol/acetic acid = 10:1:0.01) to afford compound **30** (4.6 mg, 59%) as a white solid; HPLC purity, 96% (R_t = 11.75 min); (96%); ^{1}H NMR (400 MHz, CD_3OD): δ 8.62 (s, 1H), 8.34 (s, 1H), 8.29 (s, 1H), 8.05 (d, J = 7.84 Hz, 2H), 7.93 (s, 1H), 7.89 (d, J = 7.92 Hz, 2H), 7.58 (d, J = 8.48 Hz, 1H), 7.40 (d, J = 8.44 Hz, 1H), 7.14 (s, 1H); MS (ESI, m/z): 425.1 $[M + 1]^+$; ESI-HRMS calcd m/z for $C_{23}H_{16}N_2O_3F_3$, 425.1113; found, 425.1112 $[M + 1]^+$.

*4′-Carbamoyl-5-(6-(trifluoromethyl)-1H-indol-2-yl)-[1,1′-biphenyl]-3-carboxylic Acid (**31**).* Compound **73b** (20 mg, 50.2 μmol) was converted to compound **31** (13 mg, 67%) as a white solid, using a similar procedure used in the preparation of compound **30**; HPLC purity, 97% (R_t = 11.94 min); ^{1}H NMR (400 MHz, CD_3OD): δ 8.54 (s, 1H), 8.38 (s, 1H), 8.31 (s, 1H), 8.06 (d, J = 8.24 Hz, 2H), 7.90 (d, J = 8.28 Hz, 2H), 7.75−7.74 (m, 2H), 7.30 (d, J = 8.64 Hz, 1H), 7.12 (s, 1H); MS (ESI, m/z): 425.1 $[M + 1]^+$; ESI-HRMS calcd m/z for $C_{23}H_{16}N_2O_3F_3$, 425.1113; found, 425.1108 $[M + 1]^+$.

*4′-Carbamoyl-5-(5-(trifluoromethyl)-1H-benzo[d]imidazol-2-yl)-[1,1′-biphenyl]-3-carboxylic Acid (**32**).* Compound **75** (5 mg, 11.4 μmol) was converted to compound **32** (5 mg, 99%) as a white solid, using a similar procedure used in the preparation of compound **30**; HPLC purity, 99% (R_t = 10.64 min); ^{1}H NMR (400 MHz, CD_3OD): δ 8.77 (s, 1H), 8.62 (s, 1H), 8.49 (s, 1H), 8.04 (d, J = 7.48 Hz, 2H), 7.96 (s, 1H), 7.91 (d, J = 7.52 Hz, 2H), 7.79 (d, J = 7.92 Hz, 1H), 7.58 (d, J = 8.48 Hz, 1H); MS (ESI, m/z): 426.1 $[M + 1]^+$; ESI-HRMS calcd m/z for $C_{22}H_{15}N_3O_3F_3$, 426.1066; found, 426.1063 $[M + 1]^+$.

*5-(4-(1,2,3,6-Tetrahydropyridin-4-yl)phenyl)-3-(4-(4-(trifluoromethyl)phenyl)-1H-1,2,3-triazol-1-yl)-1H-pyrrole-2-carboxylic Acid (**33**).* Method A: yield, 30%; HPLC purity, 99% (R_t = 10.35 min); ^{1}H NMR (400 MHz, CD_3OD): δ 9.23 (s, 1H), 8.13−8.05 (m, 2H), 7.80−7.68 (m, 3H), 7.58−49 (m, 2H), 7.37−7.31 (m, 1H), 7.01−6.92 (m, 1H), 6.22 (broad s, 1H), 3.83−3.76 (m, 2H), 3.48−3.37 (m, 2H), 2.84−2.74 (m, 2H); MS (ESI, m/z): 480.1 $[M + 1]^+$; ESI-HRMS calcd m/z for $C_{25}H_{21}N_5O_2F_3$, 480.1647; found, 480.1649 $[M + 1]^+$.

*2-Methyl-4′-(piperidin-4-yl)-5-(1-(4-(trifluoromethyl)phenyl)-1H-1,2,3-triazol-4-yl)-[1,1′-biphenyl]-3-carboxylic Acid (**34**).* Method A: yield, 72%; HPLC purity, 99% (R_t = 10.37 min); ^{1}H NMR (400 MHz, DMSO-d_6): δ 8.31 (s, 1H), 8.22 (d, J = 8.40 Hz, 2H), 8.04 (d, J = 8.40 Hz, 2H), 7.88 (s, 1H), 7.39−7.34 (m, 3H), 7.01 (d, J = 8.40 Hz, 1H), 6.72 (d, J = 8.000 Hz, 1H), 3.42−3.35 (m, 2H), 3.05−2.91 (m, 3H), 2.38 (s, 3H), 2.01−1.83 (m, 4H); MS (ESI, m/z): 507.2 $[M + 1]^+$; ESI-HRMS calcd m/z for $C_{28}H_{26}N_4O_2F_3$, 507.2008; found, 507.2009 $[M + 1]^+$.

*4-(4-(Piperidin-4-yl)phenyl)-2-(4-(trifluoromethyl)phenyl)-1H-benzo[d]imidazole-6-carboxylic Acid (**35**).* Method B: yield, 63%; HPLC purity, 99% (R_t = 5.59 min); ^{1}H NMR (400 MHz, CD_3OD): δ 8.37 (d, J = 8.00 Hz, 2H), 8.28 (broad s, 1H), 8.12−8.02 (m, 3H), 7.89 (d, J = 8.40 Hz, 2H), 7.53−7.45 (m, 2H), 3.58 (d, J = 12.80 Hz, 2H), 3.25 (t, J = 13.20 Hz, 2H), 3.08−3.00 (m, 1H), 2.23−2.15 (m, 2H), 2.06−1.95 (m, 2H); MS (ESI, m/z): 466.2 $[M + 1]^+$; ESI-HRMS calcd m/z for $C_{26}H_{23}N_3O_2F_3$, 466.1742; found, 466.1747 $[M + 1]^+$.

*tert-Butyl 4-(4-(3-(Ethoxycarbonyl)-6-(4-(trifluoromethyl)-phenyl)naphthalen-1-yl)phenyl)-3,6-dihydropyridine-1(2H)-carboxylate (**38**).* A mixture of compound **37** (60 mg, 0.121 mmol, synthesized according to literature procedures reported), *tert*-butyl 4-(4-(4,4,5,5-tetramethyl-1,3,2-dioxaborolan-2-yl)phenyl)-3,6-dihydropyridine-1(2*H*)-carboxylate (47 mg, 0.121 mmol), $PdCl_2(PPh_3)_2$ (8 mg, 0.012 mmol), and Na_2CO_3 (47 mg, 0.240 mmol) in 1,4-dioxane/water (10:1, 5 mL) was purged with nitrogen gas for 15 min and then stirred at 80 °C for 12 h under a nitrogen atmosphere. After cooling at room temperature, the mixture was partitioned with ethyl acetate (20 mL) and water (10 mL). The aqueous layer was extracted with ethyl acetate (10 mL × 2), and then the combined organic layer was washed with brine (3 mL), dried over $MgSO_4$, filtered, and evaporated under reduced pressure. The residue was purified by silica gel column chromatography (hexane/ethyl acetate = 3:1) to afford compound **38** (35 mg, 48%) as a white solid; ^{1}H NMR (400 MHz, $CDCl_3$): δ 8.68 (s, 1H), 8.23 (s, 1H), 8.06−8.03 (m, 2H), 7.83−7.74 (m, 5H), 7.55−7.49 (m, 4H), 6.17 (broad s, 1H), 4.46 (q, J = 7.12 Hz, 2H), 4.14 (broad s, 2H), 3.71−3.68 (m, 2H), 2.63 (broad s, 2H), 1.51 (s, 9H), 1.45 (t, J = 7.12 Hz, 3H); MS (ESI, m/z): 546.2 $[M + 1\text{-}tert\text{-butyl}]^+$; ESI-HRMS calcd m/z for $C_{32}H_{27}NO_4F_3$, 546.1892; found, 546.1902 $[M + 1\text{-}tert\text{-butyl}]^+$.

*Ethyl 4-(4-(1,2,3,6-Tetrahydropyridin-4-yl)phenyl)-7-(4-(trifluoromethyl)phenyl)-2-naphthoate (**39**).* Method B: yield, 90%; ^{1}H NMR (400 MHz, $CDCl_3$): δ 8.69 (s, 1H), 8.24 (s, 1H), 8.05−8.00 (m, 2H), 7.83−7.74 (m, 5H), 7.58−7.52 (m, 4H), 6.16 (broad s, 1H), 4.46 (q, J = 7.12 Hz, 2H), 3.95 (broad s, 2H), 3.56−3.48 (m, 2H), 2.93 (broad s, 2H), 1.45 (t, J = 7.12 Hz, 3H); MS (ESI, m/z): 502.3 $[M + 1]^+$; ESI-HRMS calcd m/z for $C_{31}H_{27}NO_2F_3$, 502.1994; found, 502.1996 $[M + 1]^+$.

*Ethyl 4-(4-(1-Methylpiperidin-4-yl)phenyl)-7-(4-(trifluoromethyl)-phenyl)-2-naphthoate (**43a**).* To a solution of compound **42** (10 mg, 16.2 μmol; synthesized according to literature procedures reported) in acetonitrile (1 mL) were added potassium carbonate (6.7 mg, 48.6 μmol) and iodomethane (36 μL, 17.8 μmol, 0.5 M solution in acetonitrile), and then this reaction mixture was stirred at room temperature for 15 h. The reaction mixture was evaporated under reduced pressure. The residue was purified by silica gel column chromatography (dichloromethane/methanol = 10:1) to afford compound **43a** (5 mg, 55%) as a white solid; ^{1}H NMR (400 MHz, CD_3OD): δ 8.74 (s, 1H), 8.44 (s, 1H), 8.04−7.93 (m, 5H), 7.82 (d, J = 7.96 Hz, 2H), 7.52−7.47 (m, 4H), 4.50−4.45 (dd, J = 7.03 Hz, 2H), 3.28 (m, 2H), 2.86−2.80 (m, 1H), 2.64−2.60 (m, 5H), 2.08 (d, J = 12.00 Hz, 2H), 2.03−1.94 (m, 2H), 1.47 (t, J = 7.00 Hz, 3H); MS (ESI, m/z): 518.2 $[M + 1]^+$; ESI-HRMS calcd m/z for $C_{32}H_{31}NO_2F_3$, 518.2307; found, 518.2297 $[M + 1]^+$.

*Ethyl 4-(4-(1-(Prop-2-yn-1-yl)piperidin-4-yl)phenyl)-7-(4-(trifluoromethyl)phenyl)-2-naphthoate (**43b**).* To a solution of compound **42** (24 mg, 0.04 mmol), which was synthesized according to literature procedures reported, in acetonitrile (2 mL) was added potassium carbonate (17.0 mg, 0.12 mmol), and then propargyl bromide (4 μL, 0.047 mmol, 1 M solution in acetonitrile) was added to the reaction mixture by dropwise addition under a N_2 atmosphere. This reaction mixture was stirred at 50 °C temperature for 15 h. This mixture was partitioned with ethyl acetate (5 mL) and water (10 mL). The aqueous layer was extracted with ethyl acetate (5 mL × 2), and then the combined organic layer was washed with brine (3 mL), dried over $MgSO_4$, filtered, and evaporated under reduced pressure. The residue was purified by silica gel column chromatography (hexane/ethyl acetate = 3:1) to afford compound **43b** (14 mg, 65%) as a white solid; ^{1}H NMR (400 MHz, $CDCl_3$): δ 8.67 (s, 1H), 8.22 (s, 1H), 8.08−8.04 (m, 2H), 7.82 (d, J = 8.24 Hz, 2H), 7.79−7.73 (m, 3H), 7.48 (d, J = 8.04 Hz, 2H), 7.40 (d, J = 8.04 Hz, 2H), 4.45 (q, J = 7.12 Hz, 2H), 3.42 (broad s, 2H), 3.11−3.07 (m, 2H), 2.64−2.60 (m, 1H), 2.48−2.38 (m, 1H), 2.05−1.92 (m, 4H), 1.64−1.54 (m, 2H), 1.44 (t, J = 7.12 Hz, 3H); MS (ESI, m/z): 542.2 $[M + 1]^+$; ESI-HRMS calcd m/z for $C_{34}H_{31}NO_2F_3$, 542.2307; found, 542.2305 $[M + 1]^+$.

*Ethyl 4-(4-(1-Propylpiperidin-4-yl)phenyl)-7-(4-(trifluoromethyl)-phenyl)-2-naphthoate (**43c**).* To a solution of compound **42** (5 mg, 8.10 μmol), which was synthesized according to literature procedures reported, in acetonitrile (1 mL) were added potassium carbonate (6.7 mg, 48.6 μmol) and 1-iodopropane (9 μL, 8.91 μmol, 1 M solution in acetonitrile), and then this reaction mixture was stirred at room temperature for 15 h. The reaction mixture was evaporated under

https://dx.doi.org/10.1021/acs.jmedchem.0c00745
J. Med. Chem. XXXX, XXX, XXX−XXX

reduced pressure. The residue was purified by silica gel column chromatography (dichloromethane/methanol = 20:1) to afford compound **43c** (3 mg, 68%) as a white solid; ^{1}H NMR (400 MHz, $CDCl_3$): δ 8.70 (s, 1H), 8.25 (s, 1H), 8.06−8.04 (m, 2H), 7.86−7.77 (m, 5H), 7.51 (d, J = 8.08 Hz, 2H), 7.45 (d, J = 8.08 Hz, 2H), 4.48 (q, J = 7.12 Hz, 2H), 3.59 (d, J = 6.52 Hz, 2H), 2.91−2.85 (m, 2H), 2.71−2.60 (m, 3H), 2.13 (d, J = 12.88 Hz, 2H), 1.97−1.92 (m, 2H), 1.47 (t, J = 7.12 Hz, 3H), 1.05 (t, J = 7.32 Hz, 3H); MS (ESI, m/z): 546.2 $[M + 1]^+$; ESI-HRMS calcd m/z for $C_{34}H_{35}NO_2F_3$, 546.2620; found, 546.2627 $[M + 1]^+$.

*Ethyl 4-(4-(1-(Hex-5-yn-1-yl)piperidin-4-yl)phenyl)-7-(4-(trifluoromethyl)phenyl)-2-naphthoate (**43d**).* To a solution of compound **42** (50 mg, 0.081 mmol), which was synthesized according to literature procedures reported, in DMF (*N*,*N*-dimethylformamide, 3 mL) were added potassium carbonate (34 mg, 0.024 mmol) and 6-bromohex-1-yne (65 mg, 0.405 mmol, 1 M solution in DMF), and then this reaction mixture was stirred at room temperature for 15 h. This mixture was partitioned with ethyl acetate (5 mL) and water (10 mL). The aqueous layer was extracted with ethyl acetate (5 mL × 2), and then the combined organic layer was washed with brine (3 mL), dried over $MgSO_4$, filtered, and evaporated under reduced pressure. The residue was purified by silica gel column chromatography (hexane/ethyl acetate = 3:1) to afford compound **43d** (50 mg, 95%) as a white solid; ^{1}H NMR (400 MHz, $CDCl_3$): δ 8.70 (s, 1H), 8.24 (d, J = 1.80 Hz, 1H), 8.05 (d, J = 1.60 Hz, 1H), 8.02 (d, J = 8.84 Hz, 1H), 7.84 (d, J = 8.16 Hz, 2H), 7.81−7.76 (m, 3H), 7.52 (d, J = 8.20 Hz, 2H), 7.47 (d, J = 8.20 Hz, 2H), 4.48 (q, J = 7.08 Hz, 2H), 3.77 (d, J = 10.36 Hz, 2H), 3.10−3.04 (m, 2H), 2.92−2.79 (m, 4H), 2.36−2.32 (m, 2H), 2.20−2.14 (m, 4H), 2.03 (t, J = 2.62 Hz, 1H), 1.72−1.65 (m, 2H), 1.47 (t, J = 7.12 Hz, 3H); MS (ESI, m/z): 584.3 $[M + 1]^+$; ESI-HRMS calcd m/z for $C_{37}H_{37}NO_2F_3$, 584.2776; found, 584.2783 $[M + 1]^+$.

*Ethyl 4-(4-(1-Acetylpiperidin-4-yl)phenyl)-7-(4-(trifluoromethyl)-phenyl)-2-naphthoate (**43e**).* To a solution of compound **42** (30.0 mg, 0.060 mmol) in acetonitrile (2.0 mL) was added triethylamine (12 μL, 0.120 mmol) by dropwise addition at room temperature. After this reaction mixture was stirred for 5 min, acetic anhydride (18 μL, 0.180 mmol) was added to the reaction mixture. Then, this reaction mixture was stirred at room temperature for 30 min. This mixture was partitioned with ethyl acetate (5 mL) and brine (10 mL). The aqueous layer was extracted with ethyl acetate (5 mL × 2), and then the combined organic layer was dried with $MgSO_4$, filtered, and evaporated under reduced pressure. The residue was purified by silica gel column chromatography (hexane/ethyl acetate = 1:1) to afford **43e** (26 mg, 49%) as a white solid; ^{1}H NMR (400 MHz, $CDCl_3$): δ 8.68 (s, 1H), 8.23 (s, 1H), 8.05−8.03 (m, 2H), 7.83−7.74 (m, 5H), 7.49 (d, J = 7.96 Hz, 2H), 7.37 (d, J = 7.88 Hz, 2H), 4.86−4.83 (m, 1H), 4.47 (q, J = 7.08 Hz, 2H), 4.01−3.98 (m, 1H), 3.27−3.20 (m, 1H), 2.89−2.83 (m, 1H), 2.72−2.66 (m, 1H), 2.17 (s, 3H), 2.04−1.98 (m, 2H), 1.75−1.70 (m, 2H), 1.45 (t, J = 7.08 Hz, 3H); MS (ESI, m/z): 546.2 $[M + 1]^+$; ESI-HRMS calcd m/z for $C_{33}H_{31}NO_3F_3$, 546.2256; found, 546.2250 $[M + 1]^+$.

*Ethyl 4-(4-(1-Propionylpiperidin-4-yl)phenyl)-7-(4-(trifluoromethyl)phenyl)-2-naphthoate (**43f**).* To a solution of compound **42** (33 mg, 0.065 mmol) in DMF (2.0 mL) were added propionic acid (5 μL, 0.072 mmol), HATU (27.0 mg, 0.072 mmol), and *N*,*N*-diisopropylethylamine (15 μL, 0.085 mmol), and then this reaction mixture was stirred at room temperature for 2 h. The reaction mixture was partitioned with ethyl acetate (5 mL) and water (5 mL), and the aqueous layer was extracted with ethyl acetate (5 mL × 2). The combined organic layer was washed with brine (3 mL), dried with $MgSO_4$, filtered, and evaporated under reduced pressure. The residue was purified by silica gel column chromatography (hexane/ethyl acetate = 3:1) to afford compound **43f** (20 mg, 54%) as a white solid; ^{1}H NMR (400 MHz, CD_3OD): δ 8.60 (s, 1H), 8.28 (s, 1H), 7.92−7.87 (m, 4H), 7.79−7.73 (m, 3H), 7.35 (s, 4H), 4.74−4.70 (m, 1H), 4.42 (q, J = 7.12 Hz, 2H), 4.12−4.07 (m, 1H), 3.26−3.19 (m, 1H), 2.94−2.86 (m, 1H), 2.77−2.70 (m, 1H), 2.48 (q, J = 7.48 Hz, 2H), 2.02−1.91 (m, 2H), 1.76−1.58 (m, 2H), 1.42 (t, J = 7.12 Hz, 3H), 1.16 (t, J = 7.48 Hz, 3H); MS (ESI, m/z): 560.2 $[M + 1]^+$; ESI-HRMS calcd m/z for $C_{34}H_{33}NO_3F_3$, 560.2413; found, 560.2419 $[M + 1]^+$.

*Ethyl 4-(4-(1-(2,2-Dimethyl-4-oxo-3,8,11,14,17,20,23-heptaoxa-5-azahexacosan-26-oyl)piperidin-4-yl)phenyl)-7-(4-(trifluoromethyl)phenyl)-2-naphthoate (**44a**).* To a solution of compound **42** (5 mg, 8.10 μmol) in DMF (0.5 mL) were added Boc-NH-PEG_6-CH_2-CH_2-COOH (7 mg, 15.4 μmol), HATU (3.4 mg, 8.94 μmol), and *N*,*N*-diisopropylethylamine (4 μL, 24.3 μmol), and then this reaction mixture was stirred at room temperature for 1 h. The reaction mixture was partitioned with ethyl acetate (5 mL) and water (5 mL), and the aqueous layer was extracted with ethyl acetate (5 mL × 2). The combined organic layer was washed with brine (3 mL), dried over $MgSO_4$, filtered, and evaporated under reduced pressure. The residue was purified by silica gel column chromatography (dichloromethane/methanol = 50:1) to afford compound **44a** (7 mg, 94%) as a white solid; ^{1}H NMR (400 MHz, $CDCl_3$): δ 8.70 (s, 1H), 8.25 (s, 1H), 8.08−8.06 (m, 2H), 7.84 (d, J = 8.16 Hz, 2H), 7.82−7.77 (m, 3H), 7.50 (d, J = 7.92 Hz, 2H), 7.38 (d, J = 8.00 Hz, 2H), 5.09 (s, 1H), 4.86 (d, J = 13.24 Hz, 1H), 4.48 (q, J = 7.12 Hz, 2H), 4.09 (d, J = 13.32 Hz, 1H), 3.86 (t, J = 6.58 Hz, 2H), 3.71−3.65 (m, 20H), 3.56 (t, J = 5.08 Hz, 2H), 3.33 (d, J = 4.88 Hz, 2H), 3.25−3.19 (m, 1H), 2.92−2.86 (m, 1H), 2.76 (t, J = 6.68 Hz, 2H), 2.07−2.00 (m, 2H), 1.80−1.70 (m, 2H), 1.49−1.46 (m, 12H); MS (ESI, m/z): 939.5 $[M + 1]^+$, 956.4 $[M + NH_4]^+$; ESI-HRMS calcd m/z for $C_{51}H_{66}N_2O_{11}F_3$, 939.4619; found, 939.4625 $[M + 1]^+$.

*Ethyl 4-(4-(1-(2,5,8,11,14,17-Hexaoxaicosan-20-oyl)piperidin-4-yl)phenyl)-7-(4-(trifluoromethyl)phenyl)-2-naphthoate (**44b**).* Compound **42** (11 mg, 14.9 μmol) with mPEG$_5$-CH_2-CH_2-COOH (7.4 mg, 22.8 μmol) was converted to compound **44b** (11 mg, 93%) as a white foam, using a similar procedure used in the preparation of compound **44a**; ^{1}H NMR (400 MHz, $CDCl_3$): δ 8.70 (s, 1H), 8.25 (s, 1H), 8.07 (d, J = 7.88 Hz, 2H), 7.86−7.77 (m, 5H), 7.50 (d, J = 7.88 Hz, 2H), 7.38 (d, J = 7.88 Hz, 2H), 4.84 (d, J = 13.8 Hz, 1H), 4.48 (q, J = 7.10 Hz, 2H), 4.10 (d, J = 13.6 Hz, 1H), 3.89−3.82 (m, 2H), 3.70−3.65 (m, 18H), 3.59−3.57 (m, 2H), 3.51 (s, 1H), 3.40 (s, 3H), 3.24 (t, J = 12.8 Hz, 1H), 2.90 (t, J = 12.1 Hz, 1H), 2.76 (t, J = 12.7 Hz, 2H), 2.04 (t, J = 13.5 Hz, 2H), 1.81−1.71 (m, 2H), 1.47 (t, J = 7.15 Hz, 3H); MS (ESI, m/z): 810.4 $[M + 1]^+$; ESI-HRMS calcd m/z for $C_{45}H_{55}NO_9F_3$, 810.3829; found, 810.3831 $[M + 1]^+$.

*Ethyl 4-(4-(Quinuclidin-4-yl)phenyl)-7-(4-(trifluoromethyl)-phenyl)-2-naphthoate (**45a**).* The mixture of compound **40** (10 mg, 0.021 mmol), $Pd(PPh_3)_4$ (2 mg, 1.73 μmol), and potassium carbonate (8 mg, 0.057 mmol) in DMF (2 mL) was purged with nitrogen gas for 15 min, and then 4-(4-bromophenyl)quinuclidine (**96**, 7 mg, 0.025 mmol) was added to the mixture. The mixture was stirred at 80 °C for 3 h and then allowed to be cooled to room temperature. This mixture was partitioned with ethyl acetate (5 mL) and water (10 mL). The aqueous layer was extracted with ethyl acetate (5 mL × 2), and then the combined organic layer was washed with brine (3 mL), dried over $MgSO_4$, filtered, and evaporated under reduced pressure. The residue was purified by silica gel column chromatography (hexane/ethyl acetate = 4:1) to afford compound **45a** (10 mg, 88%) as a white solid; ^{1}H NMR (400 MHz, CD_3OD): δ 8.75 (s, 1H), 8.44 (s, 1H), 8.01−7.92 (m, 5H), 7.82 (d, J = 8.12 Hz, 2H), 7.62 (d, J = 8.16 Hz, 2H), 7.57 (d, J = 8.24 Hz, 2H), 4.49 (q, J = 7.12 Hz, 2H), 3.58−3.54 (m, 6H), 2.37−2.33 (m, 6H), 1.47 (t, J = 7.12 Hz, 3H); MS (ESI, m/z): 530.2 $[M + 1]^+$; ESI-HRMS calcd m/z for $C_{33}H_{31}NO_2F_3$, 530.2307; found, 530.2302 $[M + 1]^+$.

*4-(4-(3-(Ethoxycarbonyl)-6-(4-(trifluoromethyl)phenyl)-naphthalen-1-yl)phenyl)-1-methylquinuclidin-1-ium (**45b**).* To a solution of compound **45a** (10.0 mg, 0.018 mmol) in acetonitrile/methanol (1:1, 1 mL) were added potassium carbonate (10.0 mg, 0.075 mmol) and iodomethane (6.0 μL, 0.094 mmol), and then this reaction mixture was stirred at room temperature for 1 h. The reaction mixture was evaporated under reduced pressure. The residue was purified by silica gel column chromatography (chloroform/methanol = 10:1) to afford compound **45b** (5.6 mg, 55%) as a white solid; ^{1}H NMR (400 MHz, CD_3OD): δ 8.77 (s, 1H), 8.45 (s, 1H), 8.03−7.96 (m, 5H), 7.84 (d, J = 8.00 Hz, 2H), 7.66−7.55 (m, 4H), 4.48 (q, J = 7.12 Hz, 2H), 3.79−3.71 (m, 6H), 3.17 (s, 3H), 2.47−

https://dx.doi.org/10.1021/acs.jmedchem.0c00745
J. Med. Chem. XXXX, XXX, XXX−XXX

2.43 (m, 6H), 1.47 (t, J = 7.12 Hz, 3H); MS (ESI, m/z): 544.3 $[M + 1]^+$.

*tert-Butyl 4-(3′-(Methoxycarbonyl)-5′-(4-(4-(trifluoromethyl)-phenyl)-1H-1,2,3-triazol-1-yl)-[1,1′-biphenyl]-4-yl)piperazine-1-carboxylate (**48a**).* The mixture of compound **47** (30 mg, 0.063 mmol), $Pd(PPh_3)_4$ (5.0 mg, 4.32 μmol), and potassium carbonate (25 mg, 0.180 mmol) in DMF (1.5 mL) was purged with nitrogen gas for 15 min, and then *tert*-butyl 4-(4-bromophenyl)piperazine-1-carboxylate (26 mg, 0.076 mmol) was added to the mixture. The mixture was stirred at 80 °C for 3 h and then allowed to be cooled to room temperature. This mixture was partitioned with ethyl acetate (5 mL) and water (10 mL). The aqueous layer was extracted with ethyl acetate (5 mL × 2), and then the combined organic layer was washed with brine (3 mL), dried over $MgSO_4$, filtered, and evaporated under reduced pressure. The residue was purified by silica gel column chromatography (hexane/ethyl acetate = 4:1) to afford compound **48a** (14 mg, 36%) as a colorless oil; ^{1}H NMR (400 MHz, $CDCl_3$): δ 8.39 (s, 1H), 8.34 (s, 1H), 8.29 (s, 1H), 8.25 (s, 1H), 8.07 (d, J = 7.96 Hz, 2H), 7.77 (d, J = 7.96 Hz, 2H), 7.65 (d, J = 8.60 Hz, 2H), 7.04 (d, J = 8.60 Hz, 2H), 4.01 (s, 3H), 3.62 (broad s, 4H), 3.24 (broad s, 4H), 1.49 (s, 9H); MS (ESI, m/z): 608.3 $[M + 1]^+$; ESI-HRMS calcd m/z for $C_{32}H_{33}N_5O_4F_3$, 608.2485; found, 608.2483 $[M + 1]^+$.

*Methyl 4′-(Quinuclidin-4-yl)-5-(4-(4-(trifluoromethyl)phenyl)-1H-1,2,3-triazol-1-yl)-[1,1′-biphenyl]-3-carboxylate (**48b**).* Compound **47** (43 mg, 0.091 mmol) and compound **96** (29 mg, 0.109 mmol) were coupled to compound **48b** (20 mg, 41%) as a white solid, using a similar procedure used in the preparation of compound **48a**; ^{1}H NMR (400 MHz, CD_3OD): δ 9.26 (s, 1H), 8.50 (s, 1H), 8.42 (s, 1H), 8.35 (s, 1H), 8.15 (d, J = 8.00 Hz, 2H), 7.83−7.75 (m, 4H), 7.59−7.55 (m, 2H), 4.00 (s, 3H), 3.55−3.46 (m, 6H), 2.30−2.23 (m, 6H); MS (ESI, m/z): 533.2 $[M + 1]^+$; ESI-HRMS calcd m/z for $C_{30}H_{28}N_4O_2F_3$, 533.2164; found, 533.2170 $[M + 1]^+$.

*tert-Butyl 6-(3′-(Methoxycarbonyl)-5′-(4-(4-(trifluoromethyl)-phenyl)-1H-1,2,3-triazol-1-yl)-[1,1′-biphenyl]-4-yl)-3-azabicyclo-[4.1.0]heptane-3-carboxylate (**48c**).* Compound **47** (36 mg, 0.076 mmol) and compound **99** (32 mg, 0.091 mmol) were coupled to compound **48c** (15 mg, 32%) as a white solid, using a similar procedure used in the preparation of compound **48a**; ^{1}H NMR (400 MHz, CD_3OD): δ 9.18 (s, 1H), 8.40 (s, 1H), 8.31 (s, 1H), 8.26 (s, 1H), 8.11 (d, J = 8.04 Hz, 2H), 7.77 (d, J = 8.08 Hz, 2H), 7.65 (d, J = 8.04 Hz, 2H), 7.39 (d, J = 8.08 Hz, 2H), 3.97 (s, 3H), 3.78 (broad s, 2H), 3.41−3.36 (m, 2H), 2.20−2.11 (m, 2H), 1.48 (s, 9H), 1.29−1.24 (m, 1H), 1.08−1.04 (m, 1H), 0.89−0.86 (m, 1H); MS (ESI, m/z): 619.2 $[M + 1]^+$; ESI-HRMS calcd m/z for $C_{34}H_{34}N_4O_4F_3$, 619.2532; found, 619.2524 $[M + 1]^+$.

*tert-Butyl 7,7-Difluoro-6-(3′-(methoxycarbonyl)-5′-(4-(4-(trifluoromethyl)phenyl)-1H-1,2,3-triazol-1-yl)-[1,1′-biphenyl]-4-yl)-3-azabicyclo[4.1.0]heptane-3-carboxylate (**48d**).* Compound **47** (53 mg, 0.112 mmol) and compound **101** (36 mg, 0.093 mmol) were coupled to compound **48d** (25 mg, 41%) as a white solid, using a similar procedure used in the preparation of compound **48a**; ^{1}H NMR (400 MHz, CD_3OD): δ 9.27 (s, 1H), 8.53 (s, 1H), 8.43 (s, 1H), 8.37 (s, 1H), 8.17 (d, J = 8.00 Hz, 2H), 7.82−7.76 (m, 4H), 7.50 (d, J = 8.40 Hz, 2H), 4.00 (s, 3H), 3.93 (broad s, 1H), 3.79 (broad s, 1H), 3.53 (broad s, 1H), 3.20−3.09 (m, 1H), 2.38−2.15 (m, 2H), 1.99−1.93 (m, 1H), 1.50 (s, 9H); MS (ESI, m/z): 655.2 $[M + 1]^+$.

*Methyl 4′-(Piperazin-1-yl)-5-(4-(4-(trifluoromethyl)phenyl)-1H-1,2,3-triazol-1-yl)-[1,1′-biphenyl]-3-carboxylate (**49a**).* Method B: yield, 76%; ^{1}H NMR (400 MHz, CD_3OD): δ 9.26 (s, 1H), 8.46 (s, 1H), 8.40 (s, 1H), 8.35 (s, 1H), 8.16 (d, J = 8.12 Hz, 2H), 7.81−7.75 (m, 4H), 7.20 (d, J = 8.60 Hz, 2H), 4.01 (s, 3H), 3.54 (broad s, 4H), 3.42 (broad s, 4H); MS (ESI, m/z): 508.2 $[M + 1]^+$; ESI-HRMS calcd m/z for $C_{27}H_{25}N_5O_2F_3$, 508.1960; found, 508.1964 $[M + 1]^+$.

*4′-(3-(tert-Butoxycarbonyl)-3-azabicyclo[4.1.0]heptan-6-yl)-5-(4-(4-(trifluoromethyl)phenyl)-1H-1,2,3-triazol-1-yl)-[1,1′-biphenyl]-3-carboxylic Acid (**49c**).* Method A: yield, 76%; ^{1}H NMR (400 MHz, CD_3OD): δ 9.24 (s, 1H), 8.49 (s, 1H), 8.38 (d, J = 6.6 Hz, 2H), 8.16 (d, J = 8.04 Hz, 2H), 7.79 (d, J = 8.12 Hz, 2H), 7.72 (d, J = 8.04 Hz, 2H), 7.45 (d, J = 7.96 Hz, 2H), 3.79 (broad s, 2H), 3.41−3.36 (m, 2H), 2.21−2.11 (m, 2H), 1.48 (s, 9H), 1.25 (d, J = 6.40 Hz, 1H), 1.11−1.06 (m, 1H), 0.91−0.86 (m, 1H); MS (ESI, m/z): 549.2 $[M + 1\text{-}tert\text{-butyl}]^+$.

*4′-(3-(tert-Butoxycarbonyl)-7,7-difluoro-3-azabicyclo[4.1.0]-heptan-6-yl)-5-(4-(4-(trifluoromethyl)phenyl)-1H-1,2,3-triazol-1-yl)-[1,1′-biphenyl]-3-carboxylic Acid (**49d**).* Method A: yield, 94%; ^{1}H NMR (400 MHz, CD_3OD): δ 9.26 (s, 1H), 8.54 (s, 1H), 8.41 (d, J = 7.20 Hz, 2H), 8.17 (d, J = 8.00 Hz, 2H), 7.83−7.76 (m, 4H), 7.51 (d, J = 8.00 Hz, 2H), 3.98−3.73 (m, 2H), 3.53 (broad s, 1H), 3.19−3.12 (m, 1H), 2.38−2.15 (m, 2H), 2.00−1.93 (m, 1H), 1.50 (s, 9H); MS (ESI, m/z): 641.2 $[M + 1]^+$; ESI-HRMS calcd m/z for $C_{33}H_{30}N_4O_4F_5$, 641.2187; found, 641.2179 $[M + 1]^+$.

*Synthesis of Methyl 3-Bromo-5-iodobenzoate (**54**), Methyl 3-Bromo-5-((trimethylsilyl)ethynyl)benzoate (**55**), Methyl 3-Bromo-5-ethynylbenzoate (**56**), Methyl 3-Bromo-5-(1-(4-(trifluoromethyl)-phenyl)-1H-1,2,3-triazol-4-yl)benzoate (**57**), Methyl 3-(4,4,5,5-Tetramethyl-1,3,2-dioxaborolan-2-yl)-5-(1-(4-(trifluoromethyl)-phenyl)-1H-1,2,3-triazol-4-yl)benzoate (**58**), and tert-Butyl 4-(3′-(Methoxycarbonyl)-5′-(1-(4-(trifluoromethyl)phenyl)-1H-1,2,3-triazol-4-yl)-[1,1′-biphenyl]-4-yl)piperidine-1-carboxylate (**59b**).* Synthesis of compounds **54**−**59** is reported by Mufti et al.[12]

*Methyl 4′-Carbamoyl-5-(1-(4-(trifluoromethyl)phenyl)-1H-1,2,3-triazol-4-yl)-[1,1′-biphenyl]-3-carboxylate (**59a**).* A mixture of compound **58** (51 mg, 0.106 mmol), 4-bromobenzamide (26 mg, 0.127 mmol), and $PdCl_2$(dppf) (9 mg, 10.6 μmol) in dimethoxyethane (2 mL) and 2 M Na_2CO_3 aqueous solution (0.2 mL) was stirred at 50 °C for 3 h. After cooling at room temperature, the mixture was partitioned with diethyl ether (5 mL) and water (10 mL). The aqueous layer was extracted with diethyl ether (5 mL × 2), and then the combined organic layer was washed with brine (3 mL), dried over $MgSO_4$, filtered, and evaporated under reduced pressure. The residue was purified by silica gel column chromatography (hexane/ethyl acetate = 1:1) to afford compound **59a** (24 mg, 46%) as a white solid; ^{1}H NMR (400 MHz, $CDCl_3$): δ 8.53−8.52 (m, 2H), 8.45 (s, 1H), 8.34 (s, 1H), 8.02 (d, J = 8.40 Hz, 2H), 7.97 (d, J = 8.16 Hz, 2H), 7.88 (d, J = 8.48 Hz, 2H), 7.83 (d, J = 8.16 Hz, 2H), 4.03 (s, 3H); MS (ESI, m/z): 467.1 $[M + 1]^+$; ESI-HRMS calcd m/z for $C_{24}H_{18}N_4O_3F_3$, 467.1331; found, 467.1325 $[M + 1]^+$.

*Methyl 3-(5-((3-((tert-Butoxycarbonyl)amino)propyl)-carbamoyl)thiophen-2-yl)-5-(1-(4-(trifluoromethyl)phenyl)-1H-1,2,3-triazol-4-yl)benzoate (**59c**).* Compound **58** (45 mg, 0.095 mmol) and *tert*-butyl (3-(5-bromothiophene-2-carboxamido)propyl) carbamate (38 mg, 0.105 mmol) were converted to compound **59c** (31 mg, 52%) as a white solid, using a similar procedure used in the preparation of compound **59a**; ^{1}H NMR (400 MHz, $CDCl_3$): δ 8.47 (s, 1H), 8.45−8.44 (m, 2H), 8.31 (s, 1H), 8.02 (d, J = 8.44 Hz, 2H), 7.87 (d, J = 8.56 Hz, 2H), 7.61 (d, J = 3.64 Hz, 1H), 7.47 (d, J = 3.88 Hz, 1H), 7.36 (broad s, 1H), 4.92 (broad s, 1H), 4.01 (s, 3H), 3.53 (q, J = 6.03 Hz, 2H), 3.30 (q, J = 5.97 Hz, 2H), 1.79−1.73 (m, 2H), 1.50 (s, 9H); MS (ESI, m/z): 530.1 $[M + 1\text{-Boc}]^+$; ESI-HRMS calcd m/z for $C_{25}H_{23}N_5O_3F_3{}^{32}S$, 530.1474; found, 530.1476 $[M + 1\text{-Boc}]^+$.

*4′-(1-(tert-Butoxycarbonyl)piperidin-4-yl)-5-(1-(4-(trifluoromethyl)phenyl)-1H-1,2,3-triazol-4-yl)-[1,1′-biphenyl]-3-carboxylic Acid (**60b**).* Method A: yield, 60%; ^{1}H NMR (400 MHz, CD_3OD): δ 9.20 (s, 1H), 8.53 (s, 1H), 8.39 (s, 1H), 8.25 (s, 1H), 8.18 (d, J = 7.92 Hz, 2H), 7.93 (d, J = 8.20 Hz, 2H), 7.68 (d, J = 7.76 Hz, 2H), 7.37 (d, J = 7.84 Hz, 2H), 4.25 (d, J = 13.12 Hz, 2H), 2.91 (broad s, 2H), 2.80 (t, J = 12.02 Hz, 1H), 1.88 (d, J = 12.68 Hz, 2H), 1.70−1.60 (m, 2H), 1.51 (s, 9H).

*3-(5-((3-((tert-Butoxycarbonyl)amino)propyl)carbamoyl)-thiophen-2-yl)-5-(1-(4-(trifluoromethyl)phenyl)-1H-1,2,3-triazol-4-yl)benzoic Acid (**60c**).* Method A: yield, 99%; ^{1}H NMR (400 MHz, CD_3OD): δ 9.13 (s, 1H), 8.48 (s, 1H), 8.34 (s, 1H), 8.23 (s, 1H), 8.13 (s, 2H), 7.90 (s, 2H), 7.65 (s, 1H), 7.50 (s, 1H), 3.41 (s, 2H), 3.16 (s, 2H), 1.78 (s, 2H), 1.46 (s, 9H); MS (ESI, m/z): 516.1 $[M + 1\text{-Boc}]^+$; ESI-HRMS calcd m/z for $C_{24}H_{21}N_5O_3F_3{}^{32}S$, 516.1317; found, 516.1316 $[M + 1\text{-Boc}]^+$.

*Methyl 3-Amino-5-bromobenzoate (**61b**).* 3-Bromo-5-aminobenzoic acid (**61a**, 1.01 g, 4.62 mmol) was stirred in methanol (15 mL) with ice cooling, and the yellow solution was treated with thionyl chloride (4.00 mL, 55.0 mmol) dropwise over 20 min. The resulting mixture was warmed up to room temperature and left stirring for 15 h.

https://dx.doi.org/10.1021/acs.jmedchem.0c00745
J. Med. Chem. XXXX, XXX, XXX−XXX

The reaction mixture was quenched with aqueous saturated $NaHCO_3$ solution at 0 °C. The solvent was then removed under vacuum, and the residue was suspended in ethyl acetate (200 mL). The organic phase was washed with brine (100 mL), dried over Na_2SO_4, and concentrated in vacuo to afford the title compound **61b** (1.08 g, 98%) as a yellow solid; ^{1}H NMR (400 MHz, DMSO-d_6): δ 7.16 (dd, J = 1.48, 2.12 Hz, 1H), 7.13 (t, J = 1.64 Hz, 1H), 6.96 (t, J = 2.00 Hz, 1H), 5.74 (s, 2H), 3.81 (s, 3H); MS (ESI, m/z): 231 $[M + 1]^+$; ESI-HRMS calcd m/z for $C_8H_8BrNO_2$, 229.9817; found, 229.9818 $[M + 1]^+$.

*Methyl 3-Amino-5-(4,4,5,5-tetramethyl-1,3,2-dioxaborolan-2-yl)benzoate (**62**).* To a solution of methyl 3-amino-5-bromobenzoate (**61b**, 219 mg, 0.950 mmol) in 1,4-dioxane (20 mL) were added bis(pinacolato)diboron (290 mg, 1.14 mmol), $PdCl_2$(dppf) (23 mg, 28.5 μmol), and potassium acetate (279 mg, 2.85 mmol), and then this reaction mixture was stirred at 95 °C for 15 h. The reaction mixture was partitioned with ethyl acetate (20 mL) and water (10 mL), and the aqueous layer was extracted with ethyl acetate (10 mL × 2). The combined organic layer was washed with brine (5 mL), dried over $MgSO_4$, filtered, and evaporated under reduced pressure. The residue was purified by silica gel column chromatography (hexane/ethyl acetate = 4:1) to afford compound **62** (180 mg, 68%) as a white solid; ^{1}H NMR (400 MHz, $CDCl_3$): δ 7.88 (s, 1H), 7.46 (s, 1H), 7.31 (d, J = 2.4 Hz, 1H), 3.91 (s, 3H), 1.36 (s, 12H); MS (ESI, m/z): 278.2 $[M + 1]^+$; ESI-HRMS calcd m/z for $C_{14}H_{21}NO_4{}^{11}B$, 278.1564; found, 278.1565 $[M + 1]^+$.

*Methyl 5-Amino-4′-carbamoyl-[1,1′-biphenyl]-3-carboxylate (**63a**).* To a solution of compound **62** (90 mg, 0.325 mmol) in 1,2-dimethoxyethane (4 mL) were added compound 4-bromobenzamide (71 mg, 0.357 mmol), $Pd(PPh_3)_4$ (7.5 mg, 6.5 μmol), and potassium carbonate (90 mg, 0.650 mmol), and then this reaction mixture was purged with nitrogen for 30 min and stirred at 80 °C for 15 h. The reaction mixture was partitioned with ethyl acetate (20 mL) and water (10 mL), and the aqueous layer was extracted with ethyl acetate (20 mL × 2). The combined organic layer was washed with brine (3 mL), dried over $MgSO_4$, filtered, and evaporated under reduced pressure. The residue was purified by silica gel column chromatography (hexane/ethyl acetate = 1:1) to afford compound **63a** (55 mg, 63%) as a white solid; ^{1}H NMR (400 MHz, $CDCl_3$): δ 7.90 (d, J = 8.20 Hz, 2H), 7.70−7.68 (m, 3H), 7.40 (s, 1H), 7.11 (s, 1H), 3.95 (s, 3H), 3.92 (broad s, 1.5H; NH_2); MS (ESI, m/z): 271.1 $[M + 1]^+$; ESI-HRMS calcd m/z for $C_{15}H_{15}N_2O_3$, 271.1083; found, 271.1080 $[M + 1]^+$.

*tert-Butyl 4-(3′-Amino-5′-(methoxycarbonyl)-[1,1′-biphenyl]-4-yl)piperidine-1-carboxylate (**63b**).* Compound **62** (90 mg, 0.325 mmol) was converted to compound **63b** (54 mg, 41%) as a white solid, using a similar procedure used in the preparation of compound **63a**; ^{1}H NMR (400 MHz, $CDCl_3$): δ 7.68 (s, 1H), 7.56 (d, J = 8.16 Hz, 2H), 7.34 (s, 1H), 7.30 (merged with C*H*Cl_3 peak, 2H), 7.09−7.08 (m, 1H), 4.03 (broad s, 2H), 3.93 (s, 3H), 2.84 (t, J = 12.06 Hz, 2H), 2.75−2.67 (m, 1H), 1.88 (d, J = 13.6 Hz, 2H), 1.73−1.62 (m, 2H), 1.51 (s, 9H); MS (ESI, m/z): 355.1 $[M + 1\text{-}tert\text{-butyl}]^+$, 323.1 $[M + 1\text{-Boc}]^+$.

*Methyl 4′-Carbamoyl-5-(4-(trifluoromethyl)benzamido)-[1,1′-biphenyl]-3-carboxylate (**64a**).* To a solution of compound **63a** (20 mg, 0.074 mmol) in DMF (2 mL) were added 4-(trifluoromethyl)-benzoic acid (21 mg, 0.111 mmol), HATU (31 mg, 0.081 mmol), and *N*,*N*-diisopropylethylamine (39 μL, 0.222 mmol), and then this reaction mixture was stirred at room temperature for 15 h. The reaction mixture was partitioned with ethyl acetate (10 mL) and water (10 mL), and the aqueous layer was extracted with ethyl acetate (10 mL × 2). The combined organic layer was washed with brine (3 mL), dried over $MgSO_4$, filtered, and evaporated under reduced pressure. The residue was purified by silica gel column chromatography (hexane/ethyl acetate = 1:1) to afford compound **64a** (33 mg, 99%) as a white solid; ^{1}H NMR (400 MHz, $CDCl_3$): δ 8.42 (s, 1H), 8.15 (d, J = 9.60 Hz, 2H), 8.07 (s, 1H), 8.05 (s, 1H), 7.94 (d, J = 7.80 Hz, 2H), 7.83 (d, J = 8.12 Hz, 2H), 7.78 (d, J = 8.16 Hz, 2H), 4.00 (s, 3H); MS (ESI, m/z): 443.1 $[M + 1]^+$; ESI-HRMS calcd m/z for $C_{23}H_{18}N_2O_4F_3$, 443.1219; found, 443.1227 $[M + 1]^+$.

*tert-Butyl 4-(3′-(4-(Hydroxymethyl)cubane-1-carboxamido)-5′-(methoxycarbonyl)-[1,1′-biphenyl]-4-yl)piperidine-1-carboxylate (**64b**).* Compound **63b** (28 mg, 68.2 μmol) and 4-(hydroxymethyl)-cubane-1-carboxylic acid (13 mg, 75.0 μmol) were converted to compound **64b** (27 mg, 69%) as a white solid, using a similar procedure used in the preparation of compound **64a**; ^{1}H NMR (400 MHz, $CDCl_3$): δ 8.30 (s, 1H), 8.04 (s, 1H), 7.61 (d, J = 7.96 Hz, 2H), 7.34 (s, 1H), 7.30 (d, J = 8.28 Hz, 2H), 4.27 (s, 5H), 3.98 (s, 3H), 3.96 (s, 3H), 3.85 (s, 2H), 2.91−2.82 (m, 2H), 2.75−2.69 (m, 1H), 1.87 (d, J = 12.24 Hz, 2H), 1.73−1.65 (m, 2H), 1.51 (s, 9H).

*Methyl 5-(4-(Hydroxymethyl)cubane-1-carboxamido)-4′-(piperidin-4-yl)-[1,1′-biphenyl]-3-carboxylate (**65**).* The reaction mixture of compound **64b** (20 mg, 35.0 μmol) in 1 N HCl/dioxane solution (1 mL) was stirred at room temperature for 15 h. After all volatiles was evaporated under reduced pressure, the residue was purified by silica gel column chromatography (dichloromethane/methanol = 3:1) to afford a methyl ester compound (**65**, 11 mg, 67%) as a white solid; ^{1}H NMR (400 MHz, CD_3OD): δ 8.27 (s, 1H), 8.25 (s, 1H), 8.00 (t, J = 1.50 Hz, 1H), 7.65 (d, J = 8.28 Hz, 2H), 7.41 (d, J = 8.24 Hz, 2H), 4.25 (t, J = 4.90 Hz, 3H), 3.96 (s, 3H), 3.93 (t, J = 4.94 Hz, 3H), 3.73 (s, 2H), 3.49 (d, J = 12.52 Hz, 2H), 3.18−3.11 (m, 2H), 3.00−2.94 (m, 1H), 2.11 (d, J = 12.84 Hz, 2H), 2.03−1.93 (m, 2H); MS (ESI, m/z): 471.2 $[M + 1]^+$; ESI-HRMS calcd m/z for $C_{29}H_{31}N_2O_4$, 471.2284; found, 471.2282 $[M + 1]^+$.

*Methyl 3-Bromo-5-formylbenzoate (**67**).* To a solution of 3-bromo-5-formylbenzoic acid (**66**, 500 mg, 2.18 mmol) in methanol (25 mL) was added concentrated H_2SO_4 (1.16 mL, 21.8 mmol) at room temperature, and this reaction mixture was stirred at 60 °C for 15 h. After the solvent was evaporated under reduced pressure, the residue was partitioned with ethyl acetate (20 mL) and saturated sodium bicarbonate solution (20 mL), and the aqueous phase was extracted with ethyl acetate (20 mL × 2). The combined organic layer was washed with brine (5 mL), dried over $MgSO_4$, filtered, and evaporated under reduced pressure. The residue was purified by silica gel column chromatography (hexane/ethyl acetate = 50:1) to afford compound **67** (287 mg, 54%) as a white solid; ^{1}H NMR (400 MHz, $CDCl_3$): δ 10.04 (s, 1H), 8.47 (s, 1H), 8.43 (s, 1H), 8.22 (s, 1H), 4.00 (s, 3H); MS (ESI, m/z): 243.0, 245.0 $[M + 1]^+$; ESI-HRMS calcd m/z for $C_9H_8O_3{}^{79}Br$, 242.9657; found, 242.9656 $[M + 1]^+$.

*3-Bromo-5-(methoxycarbonyl)benzoic Acid (**68**).* To a solution of compound **67** (30 mg, 0.123 mmol) in DMF (1 mL) was added oxone (38 mg, 0.123 mmol), and this reaction mixture was stirred at room temperature for 15 h. The reaction mixture was partitioned with ethyl acetate (5 mL) and saturated $NaHCO_3$ aqueous solution (5 mL), and the organic layer was extracted with saturated $NaHCO_3$ aqueous solution (5 mL × 2). The basic aqueous layer was acidified with 4 N aqueous HCl and extracted with ethyl acetate (10 mL × 2). The combined organic layer was washed with brine (5 mL), dried over $MgSO_4$, filtered, and evaporated under reduced pressure to afford compound **68** (25 mg, 78%) as a white solid; ^{1}H NMR (400 MHz, $CDCl_3$): δ 8.69 (s, 1H), 8.43 (s, 2H), 3.99 (s, 3H); MS (ESI, m/z): 259.0, 261.0 $[M + 1]^+$; ESI-HRMS calcd m/z for $C_9H_8O_4{}^{79}Br$, 258.9606; found, 258.9609 $[M + 1]^+$.

*Methyl 3-Bromo-5-((4-(trifluoromethyl)phenyl)carbamoyl)-benzoate (**69**).* To a solution of compound **68** (20 mg, 0.0778 mmol) in dichloromethane (3 mL) were added thionyl chloride (86 μL, 0.0856 mmol; 1 M solution in dichloromethane) and triethylamine (16 μL, 0.117 mmol) at 0 °C, and this reaction mixture was stirred at the same temperature for 1 h. After removal of the solvent under reduced pressure, the residue was dissolved in dichloromethane. *p*-(Trifluoromethyl)aniline (30 μL, 0.234 mmol) and triethylamine (16 μL, 0.117 mmol) were added, and the reaction mixture was stirred at room temperature for 15 h. The reaction mixture was partitioned with dichloromethane (10 mL) and water (5 mL), and the aqueous phase was extracted with dichloromethane (10 mL × 2). The combined organic layer was dried over $MgSO_4$, filtered, and evaporated under reduced pressure. The residue was purified by silica gel column chromatography (hexane/ethyl acetate = 6:1) to afford compound **69** (14 mg, 45%) as a white solid; ^{1}H NMR (400 MHz, $CDCl_3$): δ 8.42 (s, 1H), 8.38 (s, 1H), 8.29 (s, 1H), 8.03 (s,

https://dx.doi.org/10.1021/acs.jmedchem.0c00745
J. Med. Chem. XXXX, XXX, XXX−XXX

1H), 7.81 (d, J = 8.44 Hz, 2H), 7.67 (d, J = 8.52 Hz, 2H), 4.00 (s, 3H); MS (ESI, m/z): 402.0, 404.0 $[M + 1]^+$; ESI-HRMS calcd m/z for $C_{16}H_{12}NO_3F_3{}^{79}Br$, 401.9953; found, 401.9950 $[M + 1]^+$.

*Methyl 4′-Carbamoyl-5-((4-(trifluoromethyl)phenyl)carbamoyl)-[1,1′-biphenyl]-3-carboxylate (**70**).* To a solution of compound **69** (13 mg, 32.3 μmol) in 1,4-dioxane (2 mL) and water (0.2 mL) were added 4-aminocarbonylphenylboronic acid pinacol ester[9] (16 mg, 64.6 μmol), $PdCl_2(PPh_3)_2$ (2.3 mg, 3.23 μmol), and sodium carbonate (6.5 mg, 64.6 μmol), and then this reaction mixture was stirred at 80 °C for 2 h. The reaction mixture was partitioned with ethyl acetate (10 mL) and water (5 mL), and the aqueous layer was extracted with ethyl acetate (5 mL × 2). The combined organic layer was washed with brine (3 mL), dried over $MgSO_4$, filtered, and evaporated under reduced pressure. The residue was purified by silica gel column chromatography (dichloromethane/ethyl acetate = 1:1) to afford compound **70** (9 mg, 63%) as a white solid; ^{1}H NMR (400 MHz, CD_3OD): δ 8.64 (s, 1H), 8.54 (s, 1H), 8.53 (s, 1H), 8.05 (d, J = 8.20 Hz, 2H), 8.00 (d, J = 8.36 Hz, 2H), 7.89 (d, J = 8.28 Hz, 2H), 7.70 (d, J = 8.72 Hz, 2H), 4.02 (s, 3H); MS (ESI, m/z): 443.1 $[M + 1]^+$; ESI-HRMS calcd m/z for $C_{23}H_{18}N_2O_4F_3$, 443.1219; found, 443.1217 $[M + 1]^+$.

*Methyl 3-((2-Amino-5-(trifluoromethyl)phenyl)ethynyl)-5-bromobenzoate (**71a**).* To a solution of 2-iodo-4-(trifluoromethyl)-aniline (119 mg, 0.417 mmol), $PdCl_2(PPh_3)_2$ (2.4 mg, 3.47 μmol), and copper iodide (0.7 mg, 3.47 μmol) in triethylamine (6 mL) was added dropwise a solution of **56** (83 mg, 0.347 mmol) in triethylamine (4 mL), and then the reaction mixture was stirred at room temperature for 1 h. The reaction mixture was partitioned with ethyl acetate (20 mL) and water (10 mL), and the aqueous layer was extracted with ethyl acetate (10 mL × 2). The combined organic layer was washed with brine (3 mL), dried over $MgSO_4$, filtered, and evaporated under reduced pressure. The residue was purified by silica gel column chromatography (hexane/ethyl acetate = 4:1) to afford compound **71a** (113 mg, 82%) as a white solid; ^{1}H NMR (400 MHz, $CDCl_3$): δ 8.17 (s, 1H), 8.13 (s, 1H), 7.86 (s, 1H), 7.64 (s, 1H), 7.40 (d, J = 8.52 Hz, 1H), 6.78 (d, J = 8.56 Hz, 1H), 4.61(broad s, 2H), 3.97 (s, 3H); MS (ESI, m/z): 398.0, 400.0 $[M + 1]^+$; ESI-HRMS calcd m/z for $C_{17}H_{12}NO_2F_3{}^{79}Br$, 398.0003; found, 398.0007 $[M + 1]^+$.

*Methyl 3-((2-Amino-4-(trifluoromethyl)phenyl)ethynyl)-5-bromobenzoate (**71b**).* Compound **70** (60 mg, 0.251 mmol) and 2-iodo-5-(trifluoromethyl)aniline (97 mg, 0.301 mmol) were converted to compound **71b** (87 mg, 87%) as a white solid, using a similar procedure used in the preparation of compound **71a**; ^{1}H NMR (400 MHz, $CDCl_3$): δ 8.18 (s, 1H), 8.14 (s, 1H), 7.87 (s, 1H), 7.46 (d, J = 8.52 Hz, 1H), 6.99−6.97 (m, 2H), 4.49 (broad s, 2H), 3.98 (s, 3H); MS (ESI, m/z): 398.0, 400.0 $[M + 1]^+$; ESI-HRMS calcd m/z for $C_{17}H_{12}NO_2F_3{}^{79}Br$, 398.0003; found, 398.0009 $[M + 1]^+$.

*Methyl 3-Bromo-5-(5-(trifluoromethyl)-1H-indol-2-yl)benzoate (**72a**).* The mixture of compound **71a** (20 mg, 50.2 μmol) and $PdCl_2$ (1 mg, 5.02 μmol) in DMF (2 mL) was stirred at 110 °C for 10 min in microwave. After microwave irradiation, the solvent was removed under reduced pressure. The residue was purified by silica gel column chromatography (hexane/ethyl acetate = 6:1) to afford compound **72a** (13 mg, 65%) as a white solid; ^{1}H NMR (400 MHz, $CDCl_3$): δ 8.68 (s, 1H), 8.27 (s, 1H), 8.16 (s, 1H), 8.03 (s, 1H), 7.96 (s, 1H), 7.51 (d, J = 8.48 Hz, 1H), 7.48 (d, J = 8.56 Hz, 1H), 7.01 (s, 1H), 4.00 (s, 3H); MS (ESI, m/z): 398.0, 400.0 $[M + 1]^+$; ESI-HRMS calcd m/z for $C_{17}H_{12}NO_2F_3{}^{79}Br$, 398.0003; found, 398.0000 $[M + 1]^+$.

*Methyl 3-Bromo-5-(6-(trifluoromethyl)-1H-indol-2-yl)benzoate (**72b**).* Compound **71b** (76 mg, 0.191 mmol) was converted to compound **72b** (47 mg, 62%) as a white solid, using a similar procedure used in the preparation of compound **72a**; ^{1}H NMR (400 MHz, $CDCl_3$): δ 8.65 (broad s, 1H), 8.28 (s, 1H), 8.17 (s, 1H), 8.04 (s, 1H), 7.76−7.72 (m, 2H), 7.40 (d, J = 8.44 Hz, 1H), 7.00 (s, 1H), 4.01 (s, 3H); MS (ESI, m/z): 398.0, 400.0 $[M + 1]^+$; ESI-HRMS calcd m/z for $C_{17}H_{12}NO_2F_3{}^{79}Br$, 398.0003; found, 398.0002 $[M + 1]^+$.

*Methyl 4′-Carbamoyl-5-(5-(trifluoromethyl)-1H-indol-2-yl)-[1,1′-biphenyl]-3-carboxylate (**73a**).* Compound **72a** (13 mg, 32.6 μmol) was converted to compound **73a** (8 mg, 55%) as a white solid, using a similar procedure used in the preparation of compound **69** at 80 °C for 15 h; ^{1}H NMR (400 MHz, $CDCl_3$): δ 8.54 (s, 1H), 8.40 (s, 1H), 8.29 (s, 1H), 8.06 (d, J = 7.24 Hz, 2H), 7.95 (s, 1H), 7.90 (d, J = 7.25 Hz, 2H), 7.59 (d, J = 8.48 Hz, 1H), 7.41 (d, J = 8.20 Hz, 1H), 7.18 (s, 1H), 4.03 (s, 3H); MS (ESI, m/z): 439.1 $[M + 1]^+$; ESI-HRMS calcd m/z for $C_{24}H_{18}N_2O_3F_3$, 439.1270; found, 439.1272 $[M + 1]^+$.

*Methyl 4′-Carbamoyl-5-(6-(trifluoromethyl)-1H-indol-2-yl)-[1,1′-biphenyl]-3-carboxylate (**73b**).* Compound **72b** (25 mg, 62.8 μmol) was converted to compound **73b** (20 mg, 72%) as a white solid, using a similar procedure used in the preparation of compound **69** at 80 °C for 15 h; ^{1}H NMR (400 MHz, CD_3OD): δ 8.52 (s, 1H), 8.38 (s, 1H), 8.28 (s, 1H), 8.05 (d, J = 8.16 Hz, 2H), 7.88 (d, J = 8.24 Hz, 2H), 7.76−7.74 (m, 2H), 7.30 (d, J = 8.60 Hz, 1H), 7.13 (s, 1H), 4.01 (s, 3H); MS (ESI, m/z): 439.1 $[M + 1]^+$; ESI-HRMS calcd m/z for $C_{24}H_{18}N_2O_3F_3$, 439.1270; found, 439.1272 $[M + 1]^+$.

*Methyl 3-Bromo-5-(5-(trifluoromethyl)-1H-benzo[d]imidazol-2-yl)benzoate (**74**).* To a solution of compound **66b** (20 mg, 0.083 mmol) in DMF (3 mL) was added 4-trifluoromethyl-*O*-phenylenediamine (29 mg, 0.166 mmol) and sodium metabisulfite (32 mg, 0.166 mmol) at room temperature, and this reaction mixture was stirred at 130 °C for 15 h. After cooling, the reaction mixture was partitioned with ethyl acetate (20 mL) and water (20 mL), and the aqueous phase was extracted with ethyl acetate (20 mL × 2). The combined organic layer was washed with brine (5 mL), dried over $MgSO_4$, filtered, and evaporated under reduced pressure. The residue was purified by silica gel column chromatography (hexane/ethyl acetate = 6:1) to afford compound **74** (32 mg, 97%) as a white solid; ^{1}H NMR (400 MHz, $CDCl_3$): δ 8.57−8.56 (m, 2H), 8.32 (s, 1H), 8.01 (broad s, 1H), 7.76 (broad s, 1H), 7.60 (d, J = 8.24 Hz, 1H), 4.01 (s, 3H); MS (ESI, m/z): 399.0, 401.0 $[M + 1]^+$; ESI-HRMS calcd m/z for $C_{16}H_{11}N_2O_2F_3{}^{79}Br$, 398.9956; found, 398.9953 $[M + 1]^+$.

*Methyl 4′-Carbamoyl-5-(5-(trifluoromethyl)-1H-benzo[d]-imidazol-2-yl)-[1,1′-biphenyl]-3-carboxylate (**75**).* Compound **74** (12 mg, 30.1 μmol) was converted to compound **75** (5 mg, 38%) as a white solid, using a similar procedure used in the preparation of compound **69** at 80 °C for 15 h; ^{1}H NMR (400 MHz, CD_3OD): δ 8.83 (s, 1H), 8.73 (s, 1H), 8.48 (s, 1H), 8.07 (d, J = 8.04 Hz, 2H), 7.98 (broad s, 1H), 7.92 (d, J = 8.16 Hz, 2H), 7.80 (broad s, 1H), 7.60 (d, J = 8.08 Hz, 1H), 4.04 (s, 3H); MS (ESI, m/z): 440.1 $[M + 1]^+$; ESI-HRMS calcd m/z for $C_{23}H_{17}N_3O_3F_3$, 440.1222; found, 440.1223 $[M + 1]^+$.

*Ethyl 3-Amino-5-(4-bromophenyl)-1H-pyrrole-2-carboxylate (**78**).* To a mixture of (4-bromobenzoyl)acetonitrile (**76**, 287 mg, 1.28 mmol) in dichloromethane (1 mL) were added *p*-toluenesulfonic anhydride (502 mg, 1.54 mmol) and triethylamine (194 mg, 0.27 mL, 1.92 mmol), and the reaction mixture was stirred at room temperature for 3 h. The reaction mixture was partitioned with dichloromethane (10 mL) and water (10 mL), and the aqueous phase was extracted with dichloromethane (10 mL × 2). The combined organic layer was dried over $MgSO_4$, filtered, and evaporated under reduced pressure to give a beige solid (526 mg, >100%). To a solution of sodium ethoxide (262 mg, 1.25 mL, 3.85 mmol, 21 wt % ethanol solution) in ethanol (4 mL) was added a solution of the obtained beige solid (426 mg, 1.28 mmol) and diethyl aminomalonate hydrochloride (281 mg, 1.33 mmol) in ethanol (6 mL) and tetrahydrofuran (3 mL) dropwise over 10 min. This reaction mixture was stirred at room temperature for 30 min, and all solvent was removed under reduced pressure. The residue was partitioned with ethyl acetate (10 mL) and water (10 mL), and the aqueous phase was extracted with ethyl acetate (10 mL × 2). The combined organic layer was washed with brine (5 mL), dried over $MgSO_4$, filtered, and evaporated under reduced pressure. The residue was purified by silica gel column chromatography (hexane/ethyl acetate = 5:1) to afford compound **78** (127 mg, 40% from **76**) as a beige solid; ^{1}H NMR (400 MHz, $CDCl_3$): δ 7.53 (d, J = 8.40 Hz, 2H), 7.38 (d, J = 8.40 Hz, 2H), 6.03 (d, J = 2.84 Hz, 1H), 4.37 (q, J = 7.06 Hz, 2H), 1.40 (t, J = 7.10 Hz, 3H); MS (ESI, m/z): 309.0, 311.0

https://dx.doi.org/10.1021/acs.jmedchem.0c00745
J. Med. Chem. XXXX, XXX, XXX−XXX

$[M + 1]^+$; ESI-HRMS calcd m/z for $C_{13}H_{14}N_2O_2{}^{79}Br$, 309.0239; found, 309.0240 $[M + 1]^+$.

*tert-Butyl 4-(4-(4-Amino-5-(ethoxycarbonyl)-1H-pyrrol-2-yl)-phenyl)-3,6-dihydropyridine-1(2H)-carboxylate (**79**).* To a mixture of compound **78** (23 mg, 74.4 μmol), *tert*-butyl 4-(4,4,5,5-tetramethyl-1,3,2-dioxaborolan-2-yl)-3,6-dihydropyridine-1(2*H*)-carboxylate (28 mg, 89.2 μmol), and $PdCl_2$(dppf) (6 mg, 7.44 μmol) in DMF (1 mL) was added 2 M NaOH (75 μL, 0.148 mmol), and this reaction mixture was stirred at room temperature for 1 h. The mixture was partitioned with ethyl acetate (10 mL) and water (10 mL), and the aqueous layer was extracted with ethyl acetate (10 mL × 2). The combined organic layer was washed with brine (5 mL), dried over $MgSO_4$, filtered, and evaporated under reduced pressure. The residue was purified by silica gel column chromatography (hexane/ethyl acetate = 2:1) to afford compound **79** (24 mg, 78%) as a beige solid; ^{1}H NMR (400 MHz, $CDCl_3$): δ 7.49 (d, J = 8.20 Hz, 2H), 7.42 (d, J = 8.28 Hz, 2H), 6.11 (broad s, 1H), 6.05 (d, J = 2.84 Hz, 1H), 4.37 (q, J = 7.01 Hz, 2H), 4.12 (s, 2H), 3.67 (t, J = 5.66 Hz, 2H), 2.56 (s, 2H), 1.52 (s, 9H), 1.41 (t, J = 7.10 Hz, 3H); MS (ESI, m/z): 412.2 $[M + 1]^+$.

*tert-Butyl 4-(4-(4-Azido-5-(ethoxycarbonyl)-1H-pyrrol-2-yl)-phenyl)-3,6-dihydropyridine-1(2H)-carboxylate (**80**).* To a mixture of **79** (20 mg, 48.6 μmol) in DMF (1.4 mL) and water (0.6 mL) was added 4 N aqueous HCl (24 μL, 97.2 μmol). After 5 min, sodium nitrite (7 mg, 0.101 mmol) was added to the above reaction mixture at 0 °C, and then sodium azide was added after 30 min. The mixture was stirred at room temperature for 30 min and partitioned with ethyl acetate (10 mL) and water (15 mL). The aqueous layer was extracted with ethyl acetate (10 mL × 2). The combined organic layer was washed with brine (5 mL), dried over $MgSO_4$, filtered, and evaporated under reduced pressure. The residue was purified by silica gel column chromatography (hexane/ethyl acetate = 4:1) to afford compound **80** (16 mg, 75%) as a beige solid; ^{1}H NMR (400 MHz, $CDCl_3$): δ 8.94 (s, 1H), 7.51 (d, J = 8.40 Hz, 2H), 7.45 (d, J = 8.44 Hz, 2H), 6.40 (d, J = 3.08 Hz, 1H), 6.13 (s, 1H), 4.41 (q, J = 7.10 Hz, 2H), 4.12 (s, 2H), 3.68 (t, J = 5.32 Hz, 2H), 2.56 (s, 2H), 1.52 (s, 9H), 1.43 (t, J = 7.06 Hz, 3H); MS (ESI, m/z): 410.2 $[M + 1\text{-}N_2]^+$; ESI-HRMS calcd m/z for $C_{23}H_{28}N_3O_4$, 410.2080; found, 410.2086 $[M + 1\text{-}N_2]^+$.

*tert-Butyl 4-(4-(5-(Ethoxycarbonyl)-4-(4-(4-(trifluoromethyl)-phenyl)-1H-1,2,3-triazol-1-yl)-1H-pyrrol-2-yl)phenyl)-3,6-dihydropyridine-1(2H)-carboxylate (**81**).* To a mixture of compound **80** (15 mg, 34.3 μmol) and 4-ethynyl-α,α,α-trifluorotoluene (9 μL, 9.39 mg, 55.2 μmol) in dimethyl sulfoxide/water (9:1, 1 mL) were added sodium ascorbate (10 mg, 51.4 μmol) and $CuSO_4{\cdot}5H_2O$ (4 mg, 17.1 μmol) sequentially. The reaction mixture was stirred at room temperature for 1 h and partitioned between ethyl acetate (10 mL) and water (10 mL). The aqueous layer was extracted with ethyl acetate (10 mL × 2). The combined organic layer was washed with brine (5 mL), dried over $MgSO_4$, filtered, and evaporated under reduced pressure. The residue was purified by silica gel column chromatography (hexane/ethyl acetate = 2:1) to afford compound **81** (16 mg, 77%) as a beige solid; ^{1}H NMR (400 MHz, $CDCl_3$): δ 9.32 (s, 1H), 8.79 (s, 1H), 8.07 (d, J = 8.16 Hz, 2H), 7.73 (d, J = 8.00 Hz, 2H), 7.61 (d, J = 8.08 Hz, 2H), 7.51 (d, J = 7.92 Hz, 2H), 7.11 (s, 1H), 6.17 (s, 1H), 4.39 (q, J = 7.00 Hz, 2H), 4.14 (s, 2H), 3.69 (t, J = 5.40 Hz, 2H), 2.58 (s, 2H), 1.53 (s, 9H), 1.36 (t, J = 6.98 Hz, 3H); MS (ESI, m/z): 608.2 $[M + 1]^+$; ESI-HRMS calcd m/z for $C_{32}H_{33}N_5O_4F_3$, 608.2485; found, 608.2491 $[M + 1]^+$.

*Ethyl 5-(4-(1,2,3,6-Tetrahydropyridin-4-yl)phenyl)-3-(4-(4-(trifluoromethyl)phenyl)-1H-1,2,3-triazol-1-yl)-1H-pyrrole-2-carboxylate (**82**).* Method B: yield, 60%; ^{1}H NMR (400 MHz, CD_3OD): δ 8.90 (s, 1H), 8.13 (d, J = 8.04 Hz, 2H), 7.86 (d, J = 8.36 Hz, 2H), 7.80 (d, J = 8.16 Hz, 2H), 7.62 (d, J = 8.44 Hz, 2H), 7.01 (s, 1H), 6.28 (broad s, 1H), 4.29 (q, J = 7.12 Hz, 2H), 3.91−3.88 (m, 2H), 3.50 (t, J = 6.12 Hz, 2H), 2.87−2.84 (m, 2H), 0.91 (t, J = 6.12 Hz, 3H); MS (ESI, m/z): 508.2 $[M + 1]^+$; ESI-HRMS calcd m/z for $C_{27}H_{25}N_5O_2F_3$, 508.1960; found, 508.1960 $[M + 1]^+$.

*Methyl 3-Bromo-2-methyl-5-((trimethylsilyl)ethynyl)benzoate (**84**).* To a solution of compound **83** (100 mg, 0.281 mmol) in DMF (2 mL) were added $PdCl_2(PPh_3)_2$ (40 mg, 0.056 mmol), copper iodide (6 mg, 0.030 mmol), triethylamine (0.120 mL, 0.843 mmol), and TMS-acetylene (0.043 mL, 0.309 mmol), and then this reaction mixture was stirred at room temperature for 5 h. After the solvent was evaporated under reduced pressure, the residue was purified by silica gel column chromatography (hexane/ethyl acetate = 50:1) to afford compound **84** (91 mg, 99%) as a colorless syrup; ^{1}H NMR (400 MHz, $CDCl_3$): δ 7.82 (s, 1H), 7.79 (s, 1H), 3.89 (s, 3H), 2.61 (s, 3H), 0.24 (s, 9H).

*Methyl 3-Bromo-5-ethynyl-2-methylbenzoate (**85**).* To a solution of compound **84** (91 mg, 0.279 mmol) in tetrahydrofuran (10 mL) was added tetrabutylammonium fluoride (0.028 mL, 1 M solution in tetrahydrofuran), and then this reaction mixture was stirred at room temperature for 0.5 h. After being neutralized with acetic acid, the mixture was evaporated under reduced pressure. The residue was purified by silica gel column chromatography (hexane/ethyl acetate = 30:1) to afford compound **85** (66 mg, 93%) as a white solid; ^{1}H NMR (400 MHz, $CDCl_3$): δ 7.85 (s, 1H), 7.81 (s, 1H), 3.90 (s, 3H), 3.10 (s, 1H), 2.62 (s, 3H).

*Methyl 3-Bromo-2-methyl-5-(1-(4-(trifluoromethyl)phenyl)-1H-1,2,3-triazol-4-yl)benzoate (**86**).* To a solution of compound **85** (66 mg, 0.149 mmol) and 1-azido-4-(trifluoromethyl)benzene (42 mg, 0.224 mmol, synthesized according to literature procedures reported) in tetrahydrofuran/water (2 mL, 1:1) were added $CuSO_4{\cdot}5H_2O$ (19 mg, 0.076 mmol) and sodium ascorbate (43 mg, 0.217 mmol, freshly prepared 1 M aqueous solution), and then this reaction mixture was stirred at room temperature for 1 h. The reaction mixture was partitioned with diethyl ether (10 mL) and water (5 mL), and the aqueous layer was extracted with diethyl ether (10 mL × 2). The combined organic layer was washed with brine (5 mL), dried over $MgSO_4$, filtered, and evaporated under reduced pressure. The residue was purified by silica gel column chromatography (hexane/ethyl acetate = 9:1) to afford compound **86** (76 mg, 66%) as a white solid; ^{1}H NMR (400 MHz, $CDCl_3$): δ 8.30 (s, 2H), 8.27 (s, 1H), 7.97 (d, J = 8.36 Hz, 2H), 7.85 (d, J = 8.40 Hz, 2H), 3.95 (s, 3H), 2.68 (s, 3H); MS (ESI, m/z): 440.0, 442.0 $[M + 1]^+$; ESI-HRMS calcd m/z for $C_{18}H_{14}N_3O_2F_3{}^{79}Br$, 440.0221; found, 440.0227 $[M + 1]^+$.

*tert-Butyl 4-(3′-(Methoxycarbonyl)-2′-methyl-5′-(1-(4-(trifluoromethyl)phenyl)-1H-1,2,3-triazol-4-yl)-[1,1′-biphenyl]-4-yl)-piperidine-1-carboxylate (**87**).* The mixture of compound **86** (40 mg, 0.090 mmol), $Pd(PPh_3)_4$ (6 mg, 5.19 μmol), and potassium carbonate (37 mg, 0.267 mmol) in DMF (3 mL) was purged with nitrogen gas for 15 min, and then *tert*-butyl 4-(4-(4,4,5,5-tetramethyl-1,3,2-dioxaborolan-2-yl)phenyl)piperidine-1-carboxylate (53 mg, 0.136 mmol) was added to the mixture. The mixture was stirred at 85 °C for 12 h and then allowed to be cooled to room temperature. This mixture was partitioned with diethyl ether (5 mL) and water (10 mL). The aqueous layer was extracted with diethyl ether (5 mL × 2), and then the combined organic layer was washed with brine (3 mL), dried over $MgSO_4$, filtered, and evaporated under reduced pressure. The residue was purified by silica gel column chromatography (hexane/ethyl acetate = 4:1) to afford compound **87** (40 mg, 70%) as a white solid; ^{1}H NMR (400 MHz, $CDCl_3$): δ 8.35 (s, 1H), 8.28 (s, 1H), 7.96−7.92 (m, 3H), 7.84 (d, J = 8.44 Hz, 2H), 7.07 (d, J = 8.52 Hz, 2H), 6.78 (d, J = 8.56 Hz, 2H), 4.30−4.19 (m, 2H), 3.96 (s, 3H), 2.95−2.72 (m, 3H), 2.47 (s, 3H), 1.90 (d, J = 13.12 Hz, 2H), 1.80 (d, J = 13.12 Hz, 2H), 1.49 (s, 9H); MS (ESI, m/z): 621.3 $[M + 1]^+$; ESI-HRMS calcd m/z for $C_{34}H_{36}N_4O_4F_3$, 621.2689; found 621.2690 $[M + 1]^+$.

*Methyl 2-Methyl-4′-(piperidin-4-yl)-5-(1-(4-(trifluoromethyl)-phenyl)-1H-1,2,3-triazol-4-yl)-[1,1′-biphenyl]-3-carboxylate (**88**).* Method B: yield, 79%; ^{1}H NMR (400 MHz, $CDCl_3$): δ 8.35 (s, 1H), 8.29 (s, 1H), 7.96−7.92 (m, 3H), 7.84 (d, J = 8.52 Hz, 2H), 7.34−7.29 (m, 2H), 7.09 (d, J = 8.40 Hz, 1H), 6.81 (d, J = 8.40 Hz, 1H), 3.96 (s, 3H), 3.62−3.52 (m, 2H), 2.90−2.83 (m, 2H), 2.74−2.67 (m, 1H), 2.46 (s, 3H), 2.17−2.11 (m, 2H), 2.06−1.97 (m, 2H); MS (ESI, m/z): 521.2 $[M + 1]^+$; ESI-HRMS calcd m/z for $C_{29}H_{28}N_4O_2F_3$, 521.2164; found, 521.2173 $[M + 1]^+$.

*Methyl 4-Bromo-2-(4-(trifluoromethyl)phenyl)-1H-benzo[d]-imidazole-6-carboxylate (**90**).* To a solution of compound **89** (200

https://dx.doi.org/10.1021/acs.jmedchem.0c00745
J. Med. Chem. XXXX, XXX, XXX−XXX

mg, 0.816 mmol) in DMF (10 mL) was added 4-(trifluoromethyl)-benzaldehyde (0.222 mL, 1.632 mmol) and sodium metabisulfite (310 mg, 1.632 mmol) at room temperature, and this reaction mixture was stirred at 130 °C for 12 h. After cooling, the reaction mixture was partitioned with ethyl acetate (20 mL) and water (20 mL), and the aqueous phase was extracted with ethyl acetate (20 mL × 2). The combined organic layer was washed with brine (5 mL), dried over $MgSO_4$, filtered, and evaporated under reduced pressure. The residue was purified by silica gel column chromatography (hexane/ethyl acetate = 6:1) to afford compound **90** (212 mg, 65%) as a white solid; ^{1}H NMR (400 MHz, $CDCl_3$): δ 8.38 (broad s, 1H), 8.25−8.18 (m, 3H), 7.82 (d, J = 8.16 Hz, 2H), 3.97 (s, 3H); MS (ESI, m/z): 399.0, 401.0 $[M + 1]^+$; ESI-HRMS calcd m/z for $C_{16}H_{11}N_2O_2F_3{}^{79}Br$, 398.9956; found, 398.9950 $[M + 1]^+$.

*Methyl 4-(4-(1-(tert-Butoxycarbonyl)piperidin-4-yl)phenyl)-2-(4-(trifluoromethyl)phenyl)-1H-benzo[d]imidazole-6-carboxylate (**91**).* Compound **90** (30 mg, 0.075 mmol) and *tert*-butyl 4-(4-(4,4,5,5-tetramethyl-1,3,2-dioxaborolan-2-yl)phenyl)piperidine-1-carboxylate (34 mg, 0.090 mmol) were dissolved in degassed 2 M Na_2CO_3 aqueous solution (15 mg, 0.141 mmol) and 1,4-dioxane (3 mL), and then $Pd(PPh_3)_4$ (5 mg, 4.32 μmol) was added to the reaction mixture. The mixture was stirred at 80 °C for 12 h under a nitrogen atmosphere. After cooling at room temperature, the mixture was partitioned with ethyl acetate (20 mL) and water (10 mL). The aqueous layer was extracted with ethyl acetate (10 mL × 2), and then the combined organic layer was washed with brine (3 mL), dried over $MgSO_4$, filtered, and evaporated under reduced pressure. The residue was purified by silica gel column chromatography (hexane/ethyl acetate = 5:1) to afford compound **91** (19 mg, 43%) as a white solid; ^{1}H NMR (400 MHz, $CDCl_3$): δ 8.42 (broad s, 1H), 8.23−8.17 (m, 3H), 7.79 (d, J = 8.04 Hz, 2H), 7.40 (d, J = 7.84 Hz, 2H), 7.27−7.23 (m, 2H), 3.97 (s, 3H), 2.90−2.70 (m, 3H), 1.93−1.86 (m, 2H), 1.74−1.65 (m, 2H), 1.50 (s, 9H), 1.28−1.24 (m, 2H); MS (ESI, m/z): 580.2 $[M + 1]^+$; ESI-HRMS calcd m/z for $C_{32}H_{33}N_3O_4F_3$, 580.2423; found, 580.2434 $[M + 1]^+$.

*Methyl 4-(4-(Piperidin-4-yl)phenyl)-2-(4-(trifluoromethyl)-phenyl)-1H-benzo[d]imidazole-6-carboxylate (**92**).* Method B: yield, 82%; ^{1}H NMR (400 MHz, CD_3OD): δ 8.36 (d, J = 8.00 Hz, 2H), 8.28 (s, 1H), 8.06 (s, 1H), 7.97 (d, J = 8.00 Hz, 2H), 7.88 (d, J = 8.40 Hz, 2H), 7.48 (d, J = 8.00 Hz, 2H), 3.98 (s, 3H), 3.57 (d, J = 13.12 Hz, 2H), 3.25−3.17 (m, 2H), 3.08−2.98 (m, 1H), 2.23−2.15 (m, 2H), 2.06−1.95 (m, 2H); MS (ESI, m/z): 480.2 $[M + 1]^+$; ESI-HRMS calcd m/z for $C_{27}H_{25}N_3O_2F_3$, 480.1899; found, 480.1902 $[M + 1]^+$.

*tert-Butyl 4-(4-(3-(Ethoxycarbonyl)-6-(4-(trifluoromethyl)-phenyl)naphthalen-1-yl)phenyl)piperidine-1-carboxylate-3,4-t_2 (**93**).* To a solution of compound **39** (6 mg, 0.010 mmol) in ethyl acetate (0.2 mL) was added 10% Pd/C (5 mg). The reaction mixture was stirred under a tritium atmosphere for 24 h at room temperature. The reaction mixture was filtered and evaporated with methanol three times.

*Ethyl 4-(4-(Piperidin-4-yl-3,4-t_2)phenyl)-7-(4-(trifluoromethyl)-phenyl)-2-naphthoate (**94**).* To a solution of compound **93** in THF (1 mL) was added dropwise TFA (1 mL) and stirred for 4 h at room temperature. The reaction mixture was evaporated to dryness.

*4-(4-(Piperidin-4-yl-3,4-t_2)phenyl)-7-(4-(trifluoromethyl)phenyl)-2-naphthoic acid ([^{3}H]**1**).* HPLC purity, 97% (R_t = 13.67 min). To a solution of compound **94** in water/methanol (1 mL, 1:1) was added dropwise 1 N KOH (0.1 mL) and stirred for 18 h at room temperature. The reaction mixture was evaporated to dryness. The residue was purified by HPLC (0.1% TFA/acetonitrile = 100:0 to 0:100).

Pharmacological Assays. *Mammalian Cells Expressing the P2Y$_{14}$R.* We recently described the establishment and validation using fluorescent antagonist **36** of an HEK293 cell line stably expressing the mP2Y$_{14}$R.[39] The cloning vector contained an N-terminal human influenza hemagglutinin (HA)-TAG, which allowed the initial selection by flow cytometry detection of cell colonies highly expressing the receptor protein. A secondary selection process identified cell lines having high levels of **36** binding, as indicated by flow cytometry.[7] The growth medium consisted of Eagle's minimal essential medium (EMEM) supplemented with 10% fetal bovine serum, penicillin (100 units/mL), streptomycin (100 μg/mL), and G418 sulfate (0.555 mg/mL). Cells were maintained in a humidified atmosphere and sterile incubating conditions held at 37 °C and 5% CO_2(g). Fluorescence assays were performed using a BD FACSCalibur flow cytometer (BD Biosciences, San Jose, CA) in conjunction with the software packages BD Bioscience PlateManager and CellQuest. Fluorescence microscopy of the HEK293-mP2Y$_{14}$R cell line, after incubation of the cells with a fixed concentration of **36** (200 nM) for 45 min, in the presence and absence of competing nonfluorescent antagonist **1**, validated the presence of functional receptors.[39]

As in our previous studies,[7] the growth medium for Chinese hamster ovary (CHO) cells stably expressing hP2Y$_{14}$R (CHO-hP2Y$_{14}$R) consisted of Dulbecco's modified Eagle's medium/Ham's F12 (DMEM/F12) 1:1 supplemented with 10% fetal bovine serum, penicillin (100 units/mL), streptomycin (100 μg/mL), and G418 sulfate (0.500 mg/mL). Cells were maintained in a humidified atmosphere and sterile incubating conditions held at 37 °C and 5% CO_2(g).

Competitive Binding Assay of P2Y$_{14}$R. All competitive fluorescence assays were performed using a BD FACSCalibur flow cytometer in conjunction with the software packages BD Bioscience PlateManager and CellQuest. The assay of antagonist binding to the hP2Y$_{14}$R expressed in CHO cells using flat-bottom 96-well plates was performed as described.[9] For the binding assay at the mouse homologue, HEK293-mP2Y$_{14}$R cells were grown in a 24-well plate and used when 80−90% confluency was reached. Unlabeled ligands are stored as 5 mM stock solutions in dimethyl sulfoxide (DMSO). A serial dilution of each compound was prepared in EMEM supplemented with 10% fetal bovine serum, penicillin (100 units/mL), streptomycin (100 μg/mL), and G418 sulfate (0.555 mg/mL) to generate solutions with different concentrations of unlabeled antagonist ranging from 1 nM to 100 μM. Cells were initially incubated with unlabeled antagonists (prepared as described) for 30 min at 37 °C and 5% CO_2(g). Cells were then incubated with **36** for 30 min at a final concentration of 20 nM. At the end of the incubation, cells were washed three times with 500 μL of sterile 1× DPBS minus Ca^{2+}/Mg^{2+}. HEK293-mP2Y$_{14}$R cells were then detached from the plate using Corning Cellstripper. Cells were resuspended in sterile 1× DPBS minus Ca^{2+}/Mg^{2+} and transferred to a 96-well plate for flow cytometry. IC_{50} values were determined from the gathered data using Prism 8.0 (GraphPad, San Diego, CA).

Competitive Binding Assay of CHO-hP2Y$_{14}$R Cells at Different pH Levels. CHO-hP2Y$_{14}$R cells were grown to approximately 80−90% confluency prior to the assay in a flat-bottom 96-well plate in DMEM/F12 1:1 supplemented with 10% fetal bovine serum, penicillin (100 units/mL), streptomycin (100 μg/mL), and G418 sulfate (0.500 mg/mL). HCl solution (1 N) was added dropwise to DMEM/F12 1:1 supplemented with 10% fetal bovine serum, penicillin (100 units/mL), streptomycin (100 μg/mL), and G418 sulfate (0.500 mg/mL) to generate cell media with pH values of 7.0, 6.5, and 6.0. These cell media with different pH levels were then used to perform serial dilution and prepare solutions with different concentrations of the tested antagonist ranging from 100 μM to 1 nM. CHO-hP2Y$_{14}$R cells were initially incubated with tested antagonists (prepared in different pH level cell media as described) for 30 min at 37 °C and 5% CO_2(g). Cells were then incubated with **36** for 30 min at a final concentration of 20 nM. The pH level of sterile 1× DPBS minus Ca^{2+}/Mg^{2+} was also adjusted by adding 1 N HCl dropwise to prepare three different appropriate washing buffers for the cells with pH levels of 7.0, 6.5, and 6.0. After the incubation period, cells were washed three times with appropriate 1× DPBS minus Ca^{2+}/Mg^{2+}. Cells were then detached from the plate using Corning Cellstripper and were resuspended in 1× DPBS minus Ca^{2+}/Mg^{2+} with an appropriate pH level for flow cytometry. IC_{50} values were determined from the gathered data using Prism 8.0 (GraphPad, San Diego, CA).

Animal Model of Asthma and Chronic Neuropathic Pain. Selected antagonists were examined in the ovalbumin/*Aspergillus*

https://dx.doi.org/10.1021/acs.jmedchem.0c00745
J. Med. Chem. XXXX, XXX, XXX−XXX

protease model of murine asthma.[36,38] C57BL/6J wild-type mice from the Jackson Laboratory (Bar Harbor, ME) were sensitized twice, week apart, by oropharyngeal instillation (op) of 50 μg of LPS-free OVA (Worthington Biomedical, CA) and 20 μg of protease from *Aspergillus oryzae* (Sigma-Aldrich, St. Louis, MO) in a total volume of 50 μL of PBS. On day 14, mice were injected intraperitoneally with tested compounds at 10 mg/kg or with 10 mL/kg vehicle (10% DMSO, 30% PEG-400, 60% water); 30 min later, animals were subjected to inhalation of 1% OVA aerosol in PBS for 1 h. BALF cells were collected and counted 48 h after OVA challenge. These animal studies were reviewed and approved by the Institutional Animal Care and Use Committee at the National Institute of Environmental Health Sciences, Research Triangle Park, NC.

Behavioral testing of mechano-allodynia was measured as described[12] in the CCI model using Hsd:ICR (CD-1) outbred adult male (20−30 g, Envigo, Indianapolis, IN).[12] All procedures were conducted in accordance with the International Association for the Study of Pain, the National Institutes of Health guidelines on laboratory animal welfare guidelines, and the approval of Saint Louis University Institutional Animal Care and Use Committee.

Computational Methods. *Molecular Modeling. Protein Preparation.* We used a previously published[8] hP2Y$_{14}$R homology model, which was built using an agonist-bound X-ray structure (PDB ID: 4PXZ[17]) of hP2Y$_{12}$R as the template and subsequently refined through MD simulation. The Protein Preparation Wizard tool[40] of the Schrödinger suite (Maestro 2019-1)[41] was used to assign the histidine protonation and tautomeric states, with His184, His217, and His280 protonated at N$^{\delta}$ nitrogen (named HSD according to the CHARMM nomenclature) and with His264 doubly protonated (HSP).

Molecular Docking. The compounds were drawn using the Schrödinger suite (Maestro 2019-1)[41] and minimized using the OPLS3 force field.[42] The molecules were docked to the hP2Y$_{14}$R homology model with Glide SP[43] on a grid centered on the previously published pose of **1**, with an inner box of 10 Å and an outer box of 30 Å. Maximum 20 poses were generated for each compound. In the case of compound **17**, a post-docking minimization of the ligand was included in the docking protocol. Successively, a pose was selected for each compound by visual inspection: the capability to maintain interactions with Lys77$^{2.60}$, Tyr102$^{3.33}$, and Lys277$^{7.35}$, in analogy with the published **1** pose, was taken into consideration.

Molecular Dynamics. The complex between hP2Y$_{14}$R and compound **17** was prepared for MD simulations using the HTMD[44] module. A 90 Å × 90 Å 1-palmitoyl-2-oleoyl-*sn*-glycero-3-phosphocholine (POPC) lipid bilayer was generated through the VMD membrane plugin,[45] and the system was inserted into the membrane according to the orientation provided by the Positioning of Proteins in Membrane (PPM)[46] web server. TIP3P[47] water molecules (with a positive and negative padding of 15 Å on the *z* axis) and Na$^+$/Cl$^-$ counterions (0.154 M) were added to the system, reaching charge neutrality.

The simulations were run employing ACEMD[48] as a molecular dynamics engine and CHARMM36[49,50] force field for protein, lipids, water, and ions. The CGenFF[51,52] force field was used for the ligand, assigning the missing parameters by analogy through the ParamChem[53] web service.

The system was submitted to 5000 conjugate-gradient steps of minimization and then equilibrated for 40 ns of MD simulation in the NPT ensemble, applying positional harmonic restraints to ligand and protein atoms (0.8 kcal mol^{-1} Å^{-2} for ligand atoms, 0.85 kcal mol^{-1} Å^{-2} for Cα carbon atoms, and 0.4 kcal mol^{-1} Å^{-2} for the other protein atoms) that were linearly reduced after 20 ns. Five 50 ns replicates of MD simulations were run in the NVT ensemble, starting from the equilibrated system. A Berendsen barostat (relaxation time, 800 fs) was employed to maintain the pressure at around 1 atm during the equilibration, and a Langevin thermostat was used to keep the temperature at around 310 K (damping constants of 1 and 0.1 ps^{-1} for equilibration and production, respectively). The timestep was set to 2 fs in all the simulations, and the M-SHAKE[54] algorithm was used to constrain bonds containing hydrogen atoms. The nonbonded interaction cutoff and the switching distance were set respectively to 9 and 7.5 Å. The particle mesh Ewald (PME)[55] method (1 Å grid spacing) was used to compute the long-range electrostatic interactions beyond the cutoff. All the simulations were run on NVIDIA Tesla P100 GPUs of the NIH HPC Biowulf cluster.

Trajectory Analysis. The MD trajectories were analyzed with an in-house Tcl script employing VMD 1.9.3.[45] The system was aligned to the initial conformation by superposing the protein Cα carbon atoms. The VMD HBonds plugin was used to estimate hydrogen bonds, using a donor−acceptor distance of 3.5 Å and a donor−H−acceptor angle of 30°. Ligand−protein electrostatic and van der Waals interactions were computed with NAMD.[56] The data were plotted using the Gnuplot (version 5.0) software.[57]

■ ASSOCIATED CONTENT

Supporting Information

The Supporting Information is available free of charge at https://pubs.acs.org/doi/10.1021/acs.jmedchem.0c00745.

Synthesis of additional compounds (4-bromophenyl intermediates and carboxylate substitutions on the central phenyl ring of **2**); off-target binding inhibition curves; pharmacological data; molecular modeling data, including docking poses of selected compounds, number of contacts between the receptor residues and the ligand in each MD replicate, RMSD and ligand−receptor interaction pattern during MD replicate 3, RMSD and ligand-receptor interaction pattern during MD replicate 4, and analysis of MD replicates; predicted pharmacokinetic parameters; predicted log *D* and log *S*; and methods to measure solubility and lipohilicity (PDF)

NMR and mass spectra of final compounds (PDF)

3D coordinates of hP2Y$_{14}$R in complex with **17**, obtained through molecular docking (PDB)

MD trajectory (replicate 3) of the complex between compound **17** and hP2Y$_{14}$R, after alignment of the receptor Cα atoms to the initial frame (MP4)

MD trajectory (replicate 4) of the complex between compound **17** and hP2Y$_{14}$R, after alignment of the receptor Cα atoms to the initial frame (MP4)

Molecular formula strings of P2Y$_{14}$R antagonists (PDF)

■ AUTHOR INFORMATION

Corresponding Author

Kenneth A. Jacobson − *Molecular Recognition Section, Laboratory of Bioorganic Chemistry, National Institute of Diabetes and Digestive and Kidney Diseases, National Institutes of Health, Bethesda, Maryland 20892, United States;* orcid.org/0000-0001-8104-1493; Email: kennethj@niddk.nih.gov

Authors

Young-Hwan Jung − *Molecular Recognition Section, Laboratory of Bioorganic Chemistry, National Institute of Diabetes and Digestive and Kidney Diseases, National Institutes of Health, Bethesda, Maryland 20892, United States*

Jinha Yu − *Molecular Recognition Section, Laboratory of Bioorganic Chemistry, National Institute of Diabetes and Digestive and Kidney Diseases, National Institutes of Health, Bethesda, Maryland 20892, United States*

Zhiwei Wen − *Molecular Recognition Section, Laboratory of Bioorganic Chemistry, National Institute of Diabetes and Digestive and Kidney Diseases, National Institutes of Health, Bethesda, Maryland 20892, United States;* orcid.org/0000-0002-0821-1369

https://dx.doi.org/10.1021/acs.jmedchem.0c00745
J. Med. Chem. XXXX, XXX, XXX−XXX

Veronica Salmaso − *Molecular Recognition Section, Laboratory of Bioorganic Chemistry, National Institute of Diabetes and Digestive and Kidney Diseases, National Institutes of Health, Bethesda, Maryland 20892, United States*
Tadeusz P. Karcz − *Immunity, Inflammation, and Disease Laboratory, National Institute of Environmental Health Sciences, National Institutes of Health, Durham, North Carolina 27709, United States; Jagiellonian University, Kraków 31-007, Poland*
Ngan B. Phung − *Molecular Recognition Section, Laboratory of Bioorganic Chemistry, National Institute of Diabetes and Digestive and Kidney Diseases, National Institutes of Health, Bethesda, Maryland 20892, United States*
Zhoumou Chen − *Department of Pharmacology and Physiology and the Henry and Amelia Nasrallah Center for Neuroscience, Saint Louis University School of Medicine, Saint Louis, Missouri 63104, United States*
Sierra Duca − *Molecular Recognition Section, Laboratory of Bioorganic Chemistry, National Institute of Diabetes and Digestive and Kidney Diseases, National Institutes of Health, Bethesda, Maryland 20892, United States*
John M. Bennett − *Molecular Recognition Section, Laboratory of Bioorganic Chemistry, National Institute of Diabetes and Digestive and Kidney Diseases, National Institutes of Health, Bethesda, Maryland 20892, United States*
Steven Dudas − *Molecular Recognition Section, Laboratory of Bioorganic Chemistry, National Institute of Diabetes and Digestive and Kidney Diseases, National Institutes of Health, Bethesda, Maryland 20892, United States*
Daniela Salvemini − *Department of Pharmacology and Physiology and the Henry and Amelia Nasrallah Center for Neuroscience, Saint Louis University School of Medicine, Saint Louis, Missouri 63104, United States*
Zhan-Guo Gao − *Molecular Recognition Section, Laboratory of Bioorganic Chemistry, National Institute of Diabetes and Digestive and Kidney Diseases, National Institutes of Health, Bethesda, Maryland 20892, United States*
Donald N. Cook − *Immunity, Inflammation, and Disease Laboratory, National Institute of Environmental Health Sciences, National Institutes of Health, Durham, North Carolina 27709, United States*

Complete contact information is available at: https://pubs.acs.org/10.1021/acs.jmedchem.0c00745

Author Contributions

[⊥]Y.-H.J. and J.Y. contributed equally to this work.

Notes

The authors declare no competing financial interest.

■ ACKNOWLEDGMENTS

We acknowledge support from the NIDDK (ZIA DK031116) and NIEHS (ZIAES102025) Intramural Research Programs and from Kantum Diagnostics (Belmont, NH). We thank Bryan L. Roth, National Institute of Mental Health's Psychoactive Drug Screening Program (Univ. North Carolina at Chapel Hill, Contract #HHSN-271-2008-00025-C) for screening data. We thank Dr. John Lloyd (NIDDK) for MS spectra and Dr. Jeff Reece (NIDDK Advanced Light Microscopy and Imaging Analysis Core, ALMIAC). This work utilized the computational resources of the NIH HPC Biowulf cluster (http://hpc.nih.gov).

■ ABBREVIATIONS

ADME, absorption, distribution, metabolism, and excretion; AF488, Alexa Fluor 488; CHO, Chinese hamster ovary; DCM, dichloromethane; DIPEA, diisopropylethylamine; DMEM, Dulbecco's modified Eagle's medium; DMF, *N*,*N*-dimethylformamide; DPPF, 1,1′-bis(diphenylphosphino)ferrocene; EL, extracellular loop; HATU, 1-[bis(dimethylamino)methylene]-1*H*-1,2,3-triazolo[4,5-*b*]pyridinium 3-oxid hexafluorophosphate; IE, interaction energy; MD, molecular dynamics; PDSP, Psychoactive Drug Screening Program; PEG, polyethylene glycol; PPTN, 4-(4-(piperidin-4-yl)-phenyl)-7-(4-(trifluoromethyl)-phenyl)-2-naphthoic acid; RMSD, root-mean-square deviation; SAR, structure−activity relationship; UDPG, uridine-5′-diphosphoglucose; TBAF, tetrabutyl ammonium fluoride; TEA, triethylamine; TFA, trifluoroacetic acid; THF, tetrahydrofuran; TM, transmembrane helix; TMS, trimethylsilyl

■ REFERENCES

(1) Lazarowski, E. R.; Harden, T. K. UDP-sugars as extracellular signaling molecules: cellular and physiologic consequences of $P2Y_{14}$ receptor activation. *Mol. Pharmacol.* **2015**, *88*, 151−160.
(2) Giuliani, A. L.; Sarti, A. C.; Di Virgilio, F. Extracellular nucleotides and nucleosides as signalling molecules. *Immunol. Lett.* **2019**, *205*, 16−24.
(3) Gao, Z.-G.; Ding, Y.; Jacobson, K. A. UDP-glucose acting at $P2Y_{14}$ receptors is a mediator of mast cell degranulation. *Biochem. Pharmacol.* **2010**, *79*, 873−879.
(4) Azroyan, A.; Cortez-Retamozo, V.; Bouley, R.; Liberman, R.; Ruan, Y. C.; Kiselev, E.; Jacobson, K. A.; Pittet, M. J.; Brown, D.; Breton, S. Renal Intercalated Cells Sense and Mediate Inflammation via the $P2Y_{14}$ receptor. *PLoS One* **2015**, *10*, No. e0121419.
(5) Battistone, M. A.; Mendelsohn, A. C.; Spallanzani, R. G.; Allegretti, A. S.; Liberman, R. N.; Sesma, J.; Kalim, S.; Wall, S. M.; Bonventre, J. V.; Lazarowski, E. R.; Brown, D.; Breton, S. Pro-inflammatory $P2Y_{14}$ receptor inhibition protects against ischemic acute kidney injury in mice. *J. Clin. Invest.* **2020**, 3734.
(6) Ferreira, M. A.; Jansen, R.; Willemsen, G.; Penninx, B.; Bain, L. M.; Vicente, C. T.; Revez, J. A.; Matheson, M. C.; Hui, J.; Tung, J. Y.; Baltic, S.; Le Souëf, P.; Montgomery, G. W.; Martin, N. G.; Robertson, C. F.; James, A.; Thompson, P. J.; Boomsma, D. I.; Hopper, J. L.; Hinds, D. A.; Werder, R. B.; Phipps, S.; Australian Asthma Genetics Consortium Collaborators. Gene-based analysis of regulatory variants identifies 4 putative novel asthma risk genes related to nucleotide synthesis and signaling. *J. Allergy Clin. Immunol.* **2017**, *139*, 1148−1157.
(7) Meister, J.; Le Duc, D.; Ricken, A.; Burkhardt, R.; Thiery, J.; Pfannkuche, H.; Polte, T.; Grosse, J.; Schöneberg, T.; Schulz, A. The G protein-coupled receptor $P2Y_{14}$ influences insulin release and smooth muscle function in mice. *J. Biol. Chem.* **2014**, *289*, 23353−23366.
(8) Sesma, J. I.; Weitzer, C. D.; Livraghi-Butrico, A.; Dang, H.; Donaldson, S.; Alexis, N. E.; Jacobson, K. A.; Harden, T. K.; Lazarowski, E. R. UDP-glucose promotes neutrophil recruitment in the lung. *Purinergic Signalling* **2016**, *12*, 627−635.
(9) Xu, J.; Morinaga, H.; Oh, D.; Li, P.; Chen, A.; Talukdar, S.; Mamane, Y.; Mancini, J. A.; Nawrocki, A. R.; Lazarowski, E.; Olefsky, J. M.; Kim, J. J. GPR105 ablation prevents inflammation and improves insulin sensitivity in mice with diet-induced obesity. *J. Immunol.* **2012**, *189*, 1992−1999.
(10) Khalafalla, F. G.; Kayani, W.; Kassab, A.; Ilves, K.; Monsanto, M. M.; Alvarez, R., Jr.; Chavarria, M.; Norman, B.; Dembitsky, W. P.; Sussman, M. A. Empowering human cardiac progenitor cells by $P2Y_{14}$nucleotide receptor overexpression. *J. Physiol.* **2017**, *595*, 7135−7148.
(11) (a) Karcz, T.; Whitehead, G.; Nakano, H.; Jacobson, K. A.; Cook, D. N. Endogenous UDP-Glc acts through the purinergic

receptor P2RY$_{14}$ to exacerbate eosinophilia and airway hyperresponsiveness in a protease model of allergic asthma. *J. Immunol.* **2019**, *202*, 119−118. (b) Karcz, T.; Whitehead, G.; Nakano, H.; Jacobson, K. A.; Cook, D. N. The P2Y purinoceptor, P2Y$_{14}$R, promotes AHR in an animal model of asthma. *J. Immunol.* **2018**, *200*, 44−19.

(12) Mufti, F.; Jung, Y. H.; Giancotti, L. A.; Yu, J.; Chen, Z.; Phung, N. B.; Jacobson, K. A.; Salvemini, D. P2Y$_{14}$receptor antagonists reverse chronic neuropathic pain in a mouse model. *ACS Med. Chem. Lett.* **2020**, *11*, 1281−1286.

(13) Jacobson, K. A.; Civan, M. M. Ocular purine receptors as drug targets in the eye. *J. Ocul. Pharmacol. Ther.* **2016**, *32*, 534−547.

(14) Gauthier, J. Y.; Belley, M.; Deschênes, D.; Fournier, J. F.; Gagné, S.; Gareau, Y.; Hamel, M.; Hénault, M.; Hyjazie, H.; Kargman, S.; Lavallée, G.; Levesque, J. F.; Li, L.; Mamane, Y.; Mancini, J.; Morin, N.; Mulrooney, E.; Robichaud, J.; Thérien, M.; Tranmer, G.; Wang, Z.; Wu, J.; Black, W. C. The identification of 4,7-disubstituted naphthoic acid derivatives as UDP-competitive antagonists of P2Y$_{14}$. *Bioorg. Med. Chem. Lett.* **2011**, *21*, 2836−2839.

(15) Belley, M.; Deschenes, D.; Fortin, R.; Fournier, J. F.; Gagne, S.; Gareau, Y.; Gauthier, J. Y.; Li, L.; Robichaud, J.; Therien, M.; Tranmer, G. K.; Wang, Z. Substituted 2-naphthoic acids as antagonists of GFPR105 activity. WO2,009,070,873 A1, 2009.

(16) Robichaud, J.; Fournier, J.-F.; Gagné, S.; Gauthier, J. Y.; Hamel, M.; Han, Y.; Hénault, M.; Kargman, S.; Levesque, J. F.; Mamane, Y.; Mancini, J.; Morin, N.; Mulrooney, E.; Wu, J.; Black, W. C. Applying the pro-drug approach to afford highly bioavailable antagonists of P2Y$_{14}$. *Bioorg. Med. Chem. Lett.* **2011**, *21*, 4366−4368.

(17) Barrett, M. O.; Sesma, J. I.; Ball, C. B.; Jayasekara, P. S.; Jacobson, K. A.; Lazarowski, E. R.; Harden, T. K. A selective high-affinity antagonist of the P2Y$_{14}$receptor inhibits UDP-glucose-stimulated chemotaxis of human neutrophils. *Mol. Pharmacol.* **2013**, *84*, 41−49.

(18) Sesma, J. I.; Kreda, S. M.; Steinckwich-Besancon, N.; Dang, H.; García-Mata, R.; Harden, T. K.; Lazarowski, E. R. The UDP-sugar-sensing P2Y$_{14}$ receptor promotes Rho-mediated signaling and chemotaxis in human neutrophils. *Am. J. Physiol. Cell Physiol.* **2012**, *303*, C490−C498.

(19) Kiselev, E.; Barrett, M. O.; Katritch, V.; Paoletta, S.; Weitzer, C. D.; Hammes, E.; Yin, A. L.; Zhao, Q.; Stevens, R. C.; Kendal Harden, T.; Jacobson, K. A. Exploring a 2-naphthoic acid template for the structure-based design of P2Y$_{14}$ receptor antagonist molecular probes. *ACS Chem. Biol.* **2014**, *9*, 2833−2842.

(20) Zhang, J.; Zhang, K.; Gao, Z. G.; Paoletta, S.; Zhang, D.; Han, G. W.; Li, T.; Ma, L.; Zhang, W.; Müller, C. E.; Yang, H.; Jiang, H.; Cherezov, V.; Katritch, V.; Jacobson, K. A.; Stevens, R. C.; Wu, B.; Zhao, Q. Agonist-bound structure of the human P2Y$_{12}$ receptor. *Nature* **2014**, *509*, 119−122.

(21) Makar, S.; Saha, T.; Singh, S. K. Naphthalene, a versatile platform in medicinal chemistry: Sky-high perspective. *Eur. J. Med. Chem.* **2018**, *161*, 252−276.

(22) Junker, A.; Balasubramanian, R.; Ciancetta, A.; Uliassi, E.; Kiselev, E.; Martiriggiano, C.; Trujillo, K.; Mtchedlidze, G.; Birdwell, L.; Brown, K. A.; Harden, T. K.; Jacobson, K. A. Structure-based design of 3-(4-aryl-1H-1,2,3-triazol-1-yl)-biphenyl derivatives as P2Y$_{14}$ receptor antagonists. *J. Med. Chem.* **2016**, *59*, 6149−6168.

(23) Yu, J.; Ciancetta, A.; Dudas, S.; Duca, S.; Lottermoser, J.; Jacobson, K. A. Structure-guided modification of heterocyclic antagonists of the P2Y$_{14}$ receptor. *J. Med. Chem* **2018**, *61*, 4860−4882.

(24) Lassalas, P.; Gay, B.; Lasfargeas, C.; James, M. J.; Tran, V.; Vijayendran, K. G.; Brunden, K. R.; Kozlowski, M. C.; Thomas, C. J.; Smith, A. B., III; Huryn, D. M.; Ballatore, C. Structure property relationships of carboxylic acid isosteres. *J. Med. Chem.* **2016**, *59*, 3183−3203.

(25) Turecek, P. L.; Bossard, M. J.; Schoetens, F.; Ivens, I. A. PEGylation of biopharmaceuticals: A review of chemistry and nonclinical safety information of approved drugs. *J. Pharm. Sci.* **2016**, *105*, 460−475.

(26) Jacobson, K. A.; Tosh, D. K.; Toti, K. S.; Ciancetta, A. Polypharmacology of conformationally locked methanocarba nucleosides. *Drug Discovery Today* **2017**, *22*, 1782−1791.

(27) Degorce, S. L.; Bodnarchuk, M. S.; Cumming, I. A.; Scott, J. S. Lowering lipophilicity by adding carbon: One-carbon bridges of morpholines and piperazines. *J. Med. Chem.* **2018**, *61*, 8934−8943.

(28) Chalmers, B. A.; Xing, H.; Houston, S.; Clark, C.; Ghassabian, S.; Kuo, A.; Cao, B.; Reitsma, A.; Murray, C.-E. P.; Stok, J. E.; Boyle, G. M.; Pierce, C. J.; Littler, S. W.; Winkler, D. A.; Bernhardt, P. V.; Pasay, C.; De Voss, J. J.; McCarthy, J.; Parsons, P. G.; Walter, G. H.; Smith, M. T.; Cooper, H. M.; Nilsson, S. K.; Tsanaktsidis, J.; Savage, G. P.; Williams, C. M. Validating Eaton's hypothesis: Cubane as a benzene bioisostere. *Angew. Chem., Int. Ed.* **2016**, 3580−3585.

(29) Reekie, T. A.; Williams, C. M.; Rendina, L. M.; Kassiou, M. Cubanes in medicinal chemistry. *J. Med. Chem.* **2019**, *62*, 1078−1095.

(30) Wang, X.-M.; Xin, M.-H.; Xu, J.; Kang, B.-R.; Li, Y.; Lu, S.-M.; Zhang, S.-Q. Synthesis and antitumor activities evaluation of m-(4-morpholinoquinazolin-2-yl)benzamides in vitro and in vivo. *Eur. J. Med. Chem.* **2015**, *96*, 382−395.

(31) Gillies, R. J.; Pilot, C.; Marunaka, Y.; Fais, S. Targeting acidity in cancer and diabetes. *Biochim. Biophys. Acta, Rev. Cancer* **2019**, *1871*, 273−280.

(32) Wang, T. C.; Qiao, J. X.; Clark, C. G.; Jua, J.; Price, L. A.; Wu, Q.; Chang, M.; Zheng, J.; Huang, C. S.; Everlof, G.; Schumacher, W. A.; Wong, P. C.; Seiffert, D. A.; Stewart, A. B.; Bostwick, J. S.; Crain, E. J.; Watson, C. A.; Rehfuss, R.; Wexler, R. R.; Lam, P. Y. S. Discovery of diarylurea P2Y$_1$ antagonists with improved aqueous solubility. *Bioorg. Med. Chem. Lett.* **2013**, *23*, 3239−3243.

(33) Besnard, J.; Ruda, G. F.; Setola, V.; Abecassis, K.; Rodriguiz, R. M.; Huang, X.-P.; Norval, S.; Sassano, M. F.; Shin, A. I.; Webster, L. A.; Simeons, F. R.; Stojanovski, L.; Prat, A.; Seidah, N. G.; Constam, D. B.; Richard Bickerton, G.; Read, K. D.; Wetsel, W. C.; Gilbert, I. H.; Roth, B. L.; Hopkins, A. L. Automated design of ligands to polypharmacological profiles. *Nature* **2012**, *492*, 215−220.

(34) Baell, J. B.; Holloway, G. A. New substructure filters for removal of pan assay interference compounds (PAINS) from screening libraries and for their exclusion in bioassays. *J. Med. Chem.* **2010**, *53*, 2719−2740.

(35) Pires, D. E. V.; Blundell, T. L.; Ascher, D. B. pkCSM: Predicting small-molecule pharmacokinetic and toxicity properties using graph-based signatures. *J. Med. Chem.* **2015**, *58*, 4066−4072.

(36) Tetko, I. V.; Tanchuk, V. Y. Application of associative neural networks for prediction of lipophilicity in ALOGPS 2.1 program. *J. Chem. Inf. Comput. Sci.* **2002**, *42*, 1136−1145.

(37) Whitehead, G. S.; Thomas, S. Y.; Shalaby, K. H.; Nakano, K.; Moran, T. P.; Ward, J. M.; Flake, G. P.; Nakano, H.; Cook, D. N. TNF is required for TLR ligand−mediated but not protease-mediated allergic airway inflammation. *J. Clin. Invest.* **2017**, *127*, 3313−3326.

(38) Ballesteros, J. A.; Weinstein, H. [19] Integrated methods for the construction of three-dimensional models and computational probing of structure function relations in G protein-coupled receptors. *Methods Neurosci.* **1995**, *25*, 366−428.

(39) Cosyn, L.; Palaniappan, K. K.; Kim, S. K.; Duong, H. T.; Gao, Z. G.; Jacobson, K. A.; Van Calenbergh, S. 2-Triazole-substituted adenosines: A new class of selective A$_3$ adenosine receptor agonists, partial agonists, and antagonists. *J. Med. Chem.* **2006**, *49*, 7373−7383.

(40) Sastry, G. M.; Adzhigirey, M.; Day, T.; Annabhimoju, R.; Sherman, W. Protein and ligand preparation: Parameters, protocols, and influence on virtual screening enrichments. *J. Comput.-Aided Mol. Des.* **2013**, *27*, 221−234.

(41) *Schrödinger Release 2019−3: Maestro*; Schrödinger, LLC: New York, NY, 2019.

(42) Harder, E.; Damm, W.; Maple, J.; Wu, C.; Reboul, M.; Xiang, J. Y.; Wang, L.; Lupyan, D.; Dahlgren, M. K.; Knight, J. L.; Kaus, J. W.; Cerutti, D. S.; Krilov, G.; Jorgensen, W. L.; Abel, R.; Friesner, R. A. OPLS3: A force field providing broad coverage of drug-like small molecules and proteins. *J. Chem. Theory Comput.* **2016**, *12*, 281−296.

(43) Friesner, R. A.; Banks, J. L.; Murphy, R. B.; Halgren, T. A.; Klicic, J. J.; Mainz, D. T.; Repasky, M. P.; Knoll, E. H.; Shelley, M.;

https://dx.doi.org/10.1021/acs.jmedchem.0c00745
J. Med. Chem. XXXX, XXX, XXX−XXX

Perry, J. K.; Shaw, D. E.; Francis, P.; Shenkin, P. S. Glide: A new approach for rapid, accurate docking and scoring. 1. Method and assessment of docking accuracy. *J. Med. Chem.* **2004**, *47*, 1739−1749.
(44) Doerr, S.; Harvey, M. J.; Noé, F.; De Fabritiis, G. HTMD: High-throughput molecular dynamics for molecular discovery. *J. Chem. Theory Comput.* **2016**, *12*, 1845−1852.
(45) Humphrey, W.; Dalke, A.; Schulten, K. VMD: Visual molecular dynamics. *J. Mol. Graph.* **1996**, *14*, 33−38.
(46) Lomize, M. A.; Pogozheva, I. D.; Joo, H.; Mosberg, H. I.; Lomize, A. L. OPM database and PPM web server: Resources for positioning of proteins in membranes. *Nucleic Acids Res.* **2012**, *40*, D370−D376.
(47) Jorgensen, W. L.; Chandrasekhar, J.; Madura, J. D.; Impey, R. W.; Klein, M. L. Comparison of simple potential functions for simulating liquid water. *J. Chem. Phys.* **1983**, *79*, 926.
(48) Harvey, M. J.; Giupponi, G.; Fabritiis, G. D. ACEMD: Accelerating biomolecular dynamics in the microsecond time scale. *J. Chem. Theory Comput.* **2009**, *5*, 1632−1639.
(49) Best, R. B.; Zhu, X.; Shim, J.; Lopes, P. E. M.; Mittal, J.; Feig, M.; Mackerell, A. D., Jr. Optimization of the additive CHARMM all-atom protein force field targeting improved sampling of the backbone φ, ψ and side-chain $\chi(1)$ and $\chi(2)$ dihedral angles. *J. Chem. Theory Comput* **2012**, *8*, 3257−3273.
(50) Klauda, J. B.; Venable, R. M.; Alfredo Freites, J.; O'Connor, J. W.; Tobias, D. J.; Mondragon-Ramirez, C.; Vorobyov, I.; MacKerell, A. D., Jr.; Pastor, R. W. Update of the CHARMM all-atom additive force field for lipids: Validation on six lipid types. *J. Phys. Chem. B* **2010**, *114*, 7830−7843.
(51) Vanommeslaeghe, K.; MacKerell, A. D., Jr. Automation of the CHARMM general force field (CGenFF) I: Bond perception and atom typing. *J. Chem. Inf. Model.* **2012**, *52*, 3144−3154.
(52) Vanommeslaeghe, K.; Raman, E. P.; MacKerell, A. D., Jr. Automation of the CHARMM general force field (CGenFF) II: Assignment of bonded parameters and partial atomic charges. *J. Chem. Inf. Model.* **2012**, *52*, 3155−3168.
(53) CHARMM *General Force Field (CGenFF) program*, https://cgenff.umaryland.edu/
(54) Kräutler, V.; van Gunsteren, W. F.; Hünenberger, P. H. A fast SHAKE algorithm to solve distance constraint equations for small molecules in molecular dynamics simulations. *J. Comput. Chem.* **2001**, *22*, 501−508.
(55) Essmann, U.; Perera, L.; Berkowitz, M. L.; Darden, T.; Lee, H.; Pedersen, L. G. A smooth particle mesh Ewald method. *J. Chem. Phys.* **1995**, *103*, 8577.
(56) Phillips, J. C.; Braun, R.; Wang, W.; Gumbart, J.; Tajkhorshid, E.; Villa, E.; Chipot, C.; Skeel, R. D.; Kalé, L.; Schulten, K. Scalable molecular dynamics with NAMD. *J. Comput. Chem.* **2005**, *26*, 1781−1802.
(57) Williams, T.; Kelley, C. *Gnuplot 5.0*, http://www.gnuplot.info
(58) Massarotti, A.; Aprile, S.; Mercalli, V.; Del Grosso, E.; Grosa, G.; Sorba, G.; Tron, G. C. Are 1,4- and 1,5-disubstituted 1,2,3-triazoles good pharmacophoric groups? *ChemMedChem* **2014**, *9*, 2497−2508.

https://dx.doi.org/10.1021/acs.jmedchem.0c00745
J. Med. Chem. XXXX, XXX, XXX−XXX